

THE CANCER SPECIFIC UBIQUITIN LIGASE MAGE-A3/6-TRIM28 DRIVES
TUMORIGENESIS BY UBIQUITINATION AND PROTEASOMAL DEGRADATION OF
AMPK

APPROVED BY SUPERVISORY COMMITTEE

Ryan Potts, Ph.D. (Mentor)

Hongtao Yu, Ph.D. (Chair)

Beth Levine, M.D.

Michael White, Ph.D.

DEDICATION

I would like to dedicate this thesis to several people, all of whom have played key roles in my journey to reach this point. First, I would like to thank my parents Carlos and Nancy Pineda. From the time I was born until now my parents have always emphasized the extreme importance of education. My father has always been there to help with my homework, working out math, chemistry, or physics problems. Next, I would like to thank my high school AP Biology teacher Mr. Mark Schmidt. During my sophomore year of high school, his class was my first exposure to what could be called modern molecular biology. I would like to thank Dr. Amanda Baker at the University of Arizona for giving me my first chance in a laboratory. This first opportunity gave me the base of my laboratory skills that has carried me this far and provided me with invaluable experience that allowed me to attend UT Southwestern. I would like to thank my wife, Erin Pineda, for all the love and support that she has given me. She has been there every step of the way and without her I could have never finished this endeavor. She has been there through all of the long nights in the lab, bringing me Sonic and food from other various takeout restaurants. I would like to thank all of my lab mates. Over the past four years their help and advice has been indispensable. I would particularly like to thank Dr. Saumya Ramanathan. She has continually provided insights, into not only how to do good science, but also how to survive graduate school. I would like to thank my committee for their helpful input on my project. Finally, I would like to thank my mentor Dr. Ryan Potts. Any successes that I have or may achieve in the future will come from his lessons on how to perform high quality science.

THE CANCER SPECIFIC UBIQUITIN LIGASE MAGE-A3/6-TRIM28 DRIVES
TUMORIGENESIS BY UBIQUITINATION AND PROTEASOMAL DEGRADATION OF
AMPK

by

CARLOS TYLER PINEDA

DISSERTATION

Presented to the Faculty of the Graduate School of Biomedical Sciences

The University of Texas Southwestern Medical Center at Dallas

In Partial Fulfillment of the Requirements

For the Degree of

DOCTOR OF PHILOSOPHY

The University of Texas Southwestern Medical Center

Dallas, Texas

August, 2015

Copyright

by

CARLOS TYLER PINEDA, 2015

All Rights Reserved

THE CANCER SPECIFIC UBIQUITIN LIGASE MAGE-A3/6-TRIM28 DRIVES
TUMORIGENESIS BY UBIQUITINATION AND PROTEASOMAL DEGRADATION OF
AMPK

CARLOS TYLER PINEDA, Ph.D.

The University of Texas Southwestern Medical Center at Dallas, 2015

PATRICK RYAN POTTS, Ph.D.

Abstract:

The genes MAGE-A3 and MAGE-A6 (MAGE-A3/6) have a unique expression pattern in which they are normally expressed in the adult testis but are aberrantly expressed in cancer. It is known that when expressed in cancer, MAGE-A3/6 is a negative prognostic indicator and cancer cells are dependent on it for survival. Using the knowledge that MAGE-A3/6 binds and regulates the E3 ubiquitin ligase TRIM28, I investigated its biochemical role in cancer. I used unbiased methods to identify 19 novel substrates of MAGE-A3/6-TRIM28, including the known tumor suppressor AMPK. Ubiquitination of AMPK by MAGE-A3/6-TRIM28 induces its proteasomal degradation and, thereby enhancing mTOR signaling and inhibiting autophagy within cells. Through this modulation of AMPK, MAGE-A3/6 is also able to act as an oncogene, inducing evasion of anoikis and the growth of tumors *in vivo*. Understanding the mechanism by which

MAGE-A3/6 acts as an oncogene has revealed potential avenues of therapeutic intervention. Treatment of MAGE-A3/6 expressing cells with AMPK agonists reverses oncogenic properties *in vitro*. Ultimately, these studies have revealed how a germline protein functions in cancer and the potential points for therapeutic intervention.

TABLE OF CONTENTS

Dedication	ii
Abstract	v
Table of Contents	vii
Publications	x
List of Figures	xi
List of Tables	xiii
<u>Chapter I: Introduction</u>	1
I. Cancer	1
II. MAGEs	1
III. Cancer Testis Antigens	4
IV. Cancer Immunotherapy	5
V. Oncogenes	6
VI. Ubiquitin Signaling Cascade	9
VII. TRIM28	12
<u>Chapter II: Materials and Methods</u>	17
I. ProtoArray	17
II. Cell Culture	18
III. siRNA Sequences	18
IV. In Vitro Binding	18
V. Immunoprecipitation	19
VI. GFP/LC3 Staining	19
VII. GFP-LC3 Flow Cytometry	20
VIII. SDS-PAGE/Western Blot	20
IX. Drug Treatments	21
X. Soft Agar Colony Formation	21
XI. Mouse Xenograft Studies	21

<u>Chapter III: AMPK is a Substrate of MAGE-TRIM28</u>	22
I. ProtoArray Identifies MAGE-TRIM28 Targets	22
II. AMPK	25
III. Substrate Confirmation	26
IV. AMPK is targeted for proteasomal degradation	28
V. MAGE-A3/6 reduces active AMPK	30
VI. MAGE-A3/6 is a substrate adapter	30
VII. MAGE-A3/6 controls AMPK in clinical samples	37
<u>Chapter IV: MAGE-A-TRIM28 Regulates mTOR Signaling and Autophagy</u>	42
I. mTOR	42
II. MAGE-A3/6 control S6K signaling	43
III. MAGE-A3/6 promotes mTOR in clinical samples	47
IV. Autophagy	47
V. MAGE-A3/6 regulates autophagy	49
VI. MAGE-A3/6 inhibit autophagic flux	53
<u>Chapter V: MAGE-A Functions as an Oncogene Capable of Transforming Cells</u>	62
I. Cellular transformation and Anchorage Independent Growth	62
II. MAGE-A3/6 expression induces soft agar growth	62
III. MAGE-A3/6 is capable of inducing tumor formation in vivo	65
IV. MAGE-A3/6 targeted therapy	65
<u>Chapter VI: Discussion</u>	72
I. Summary of findings	72
II. Treatment strategies for MAGE-A3/6 tumors	74
III. Key pathways altered by MAGE-A3/6	75
IV. Timing of MAGE-A3/6 activation in cancer	75
V. TRIM28 in an autophagy switch	76
VI. Molecular drivers of MAGE-A3/6 expression	77
VII. Physiological role of MAGE-A3/6-TRIM28	78

VIII. TRIM/MAGE/AMPK crosstalk	79
<u>References</u>	81

Prior Publications

Pineda, C.T.*, Ramanathan, S.*, Fon Tacer, K, Weon, J.L., Potts, M.B., Ou, Y., White, M.A.,
Potts, P.R. Degradation of AMPK by a Cancer-Specific Ubiquitin Ligase. (2015) Cell 160, 715-
728 (* Denotes co-first author)

Pineda, C.T., Potts P.R. MAGE-A-TRIM28 Ubiquitin Ligase Downregulates Autophagy by
Ubiquitinating and Degrading AMPK in Cancer (2015) Autophagy 11(5): 844-6

LIST OF FIGURES

Figure 1-1	The Human MAGE Gene Family	3
Figure 1-2	MAGE-A3 Expression and Effect on Survival	8
Figure 1-3	Cells Exhibit Oncogene Addiction to MAGE-A3	16
Figure 3-1	ProtoArray Scheme	23
Figure 3-2	AMPK is a Substrate of MAGE-A3/6-TRIM28	27
Figure 3-3	MAGE-A3/6 Negatively Regulates AMPK Protein Levels	29
Figure 3-4	AMPK α 1 is Degraded by the Proteasome	31
Figure 3-5	MAGE-A3/6 Knockdown Increases Active AMPK	32
Figure 3-6	MAGE-A3/6 Knockdown Increases AMPK Activity	34
Figure 3-7	AMPK is not Regulated in MAGE (-) Cell Lines	35
Figure 3-8	MAGE-A3 Binds to AMPK α 1 in Cells	36
Figure 3-9	MAGE-A3/6 Binds Directly to AMPK	38
Figure 3-10	MAGE-A3/6 Correlates with Reduced AMPK Protein in Patients	39
Figure 3-11	MAGE-A3/6 Expression Anti-Correlates with LKB1 Mutation	41
Figure 4-1	MAGE-A3/6 is Required for mTOR Signaling	44
Figure 4-2	MAGE-A3/6 Controls mTOR via AMPK	46

Figure 4-3	MAGE-A3/6 Expression Correlates with mTOR Signaling in Tumors	48
Figure 4-4	Knockdown of MAGE-A3/6-TRIM28 Increases ULK1 Activity	50
Figure 4-5	Knockdown of MAGE-A3/6-TRIM28 Increases GFP-LC3 Puncta	52
Figure 4-6	Knockdown of MAGE-A3/6 Increases LC3 Puncta	54
Figure 4-7	Compound C Inhibits GFP-LC3 Puncta Formation	55
Figure 4-8	MAGE-A3/6 Knockdown Increases GFP-LC3 Consumption	57
Figure 4-9	Depletion of MAGE-A3/6-TRIM28 Increases Autophagic Flux	59
Figure 4-10	MAGE-A3/6 Inhibits Autophagy	61
Figure 5-1	MAGE-A6 Increases Soft Agar Growth	64
Figure 5-2	MAGE-A6 Induces Tumor Growth	66
Figure 5-3	HCEC-MAGE-A6 Tumors form Lung Metastasis	67
Figure 5-4	AMPK Agonists Block MAGE-A6 Induced Soft Agar Growth	69
Figure 5-5	AMPK Agonists Selectively Inhibit MAGE-A6 Induced Soft Agar Growth	70
Figure 6-1	Model of MAGE-A3/6's Role in Cancer Development	73

LIST OF TABLES

Table 3-1	List of Putative MAGE-TRIM28 Substrates Identified by ProtoArray	24
-----------	--	----

Chapter I: Introduction

Cancer

Cancer is a terrible disease that has approximately 1.5 million new cases each year and approximately half a million deaths each year are attributed to cancer (Society, 2015). In their lifetime, women and men have an approximately 33% and 50% chance, respectively of developing cancer. It has long been known that cancer is not a singular disease and one of the simplest ways that cancer is categorized is by the tissue in which the neoplasia originates (Society, 2015). In terms of deaths per year, the most deadly cancer is that of the lung and bronchus, accounting for more than 25% of cancer deaths. Following lung cancer, breast/prostate and colorectal cancer account for the bulk of cancer deaths (Society, 2015). In addition to the tissue of origin, tumors have traditionally been categorized by their histological features. For example, lung cancer is generally classified as small cell and non-small cell cancers, with non-small cell having additional subtypes such as squamous or adenocarcinoma. Current research seeks to define cancer not by histological features, but instead by the molecular mechanisms that drive the neoplastic phenotype.

In order to better understand cancer, the wide varieties of changes that occur have largely been categorized into groups that describe the common factors needed for cancer to initiate and progress. These groups have been termed the “Hallmarks of Cancer” (Hanahan and Weinberg, 2000, 2011). Some of these hallmarks include the ability to evade the immune system, changes in cellular metabolism, and an ability to evade apoptotic or other death signals (Hanahan and Weinberg, 2000, 2011).

MAGEs

Melanoma Antigen Genes (MAGEs) are a family of genes that were discovered more than two decades ago in the tumor of a patient with melanoma (Gaugler et al., 1994). Unlike most proteins in the human body, expression of these proteins was noted for their ability to provoke a response from host immune cells. These MAGEs and several other unrelated genes with similar properties were then termed Cancer-testis antigens and studied for their potential usage in cancer treatment (Simpson et al., 2005).

Since their initial discovery, several additional non-antigenic MAGEs have been discovered by sequence homology, and it is now understood that this family contains more than 50 unique genes in humans (Figure 1-1) (Chomez et al., 2001; Feng et al., 2011). In addition to some of these being expressed in various cancers, the type I MAGE gene family has other features that suggest their importance, such as rapid expansion in recent evolutionary history and an association with various diseases (Chomez et al., 2001). Despite their evident importance, relatively little insight has been gained on this enigmatic family of genes and a definitive cellular function has yet to be found for most of them. The majority of knowledge that has accumulated on MAGEs relates to their genomic arrangement and expression patterns throughout the body. When sequence similarity, genomic arrangement or expression pattern is compared, the MAGE family is clearly bifurcated into two groups (Figure 1-1) (De Plaen et al., 1994). These two groups have been termed type I or type II MAGEs and they represent a key distinction.

The type I MAGEs are comprised of the family members that were originally discovered in melanoma but with the MAGE family now being populated by dozens of members, the type I MAGEs have additionally been stratified into three subgroups, consisting of A, B and C branches. All three of these subgroups have a similar genetic arrangement; they are located on

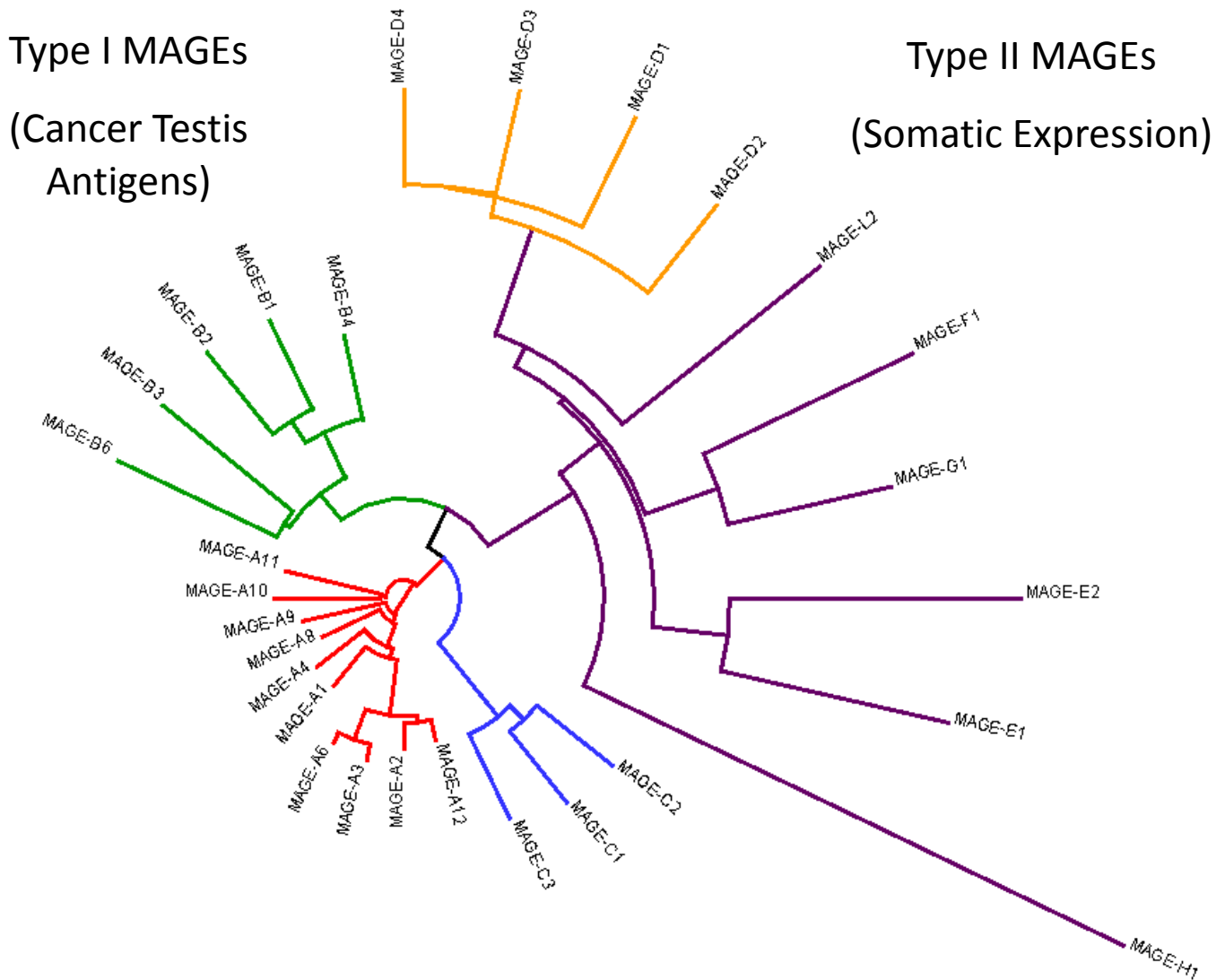


Figure 1-1 The Human MAGE Gene Family

Dendrogram of selected members of the human MAGE gene family. DNA sequences of MAGE homology domains were aligned and compared using a neighbor joining algorithm. Relationships were plotted as a phylogram using Dendroscope.

the X-chromosome, in clusters (De Plaen et al., 1994). These highly homologous and closely located clusters are indicative of the rapid evolution of the MAGE family, with type I MAGEs being duplicated with recent evolutionary pressure. For example, several of the type I MAGEs are only found in primates. Corresponding with their location on the chromosomes, type I MAGEs have a unique expression pattern in which they are primarily expressed in the adult testis (De Plaen et al., 1994). This expression pattern is intriguing and may potentially reveal the function of these proteins. One example of a type I MAGE that adheres to this pattern of genomic localization and testicular expression is MAGE-A1, the original MAGE family member.

Contrasting the genetic organization of the type I genes, the type II MAGEs are scattered in loci throughout the autosomes (De Plaen et al., 1994). Type II MAGEs have an expected expression profile in which they are expressed in various somatic tissues, and many of these have an enriched expression in central nervous system. Type II MAGEs most likely represent the older MAGE family members, with the ancestral MAGE found in early eukaryotes sharing the most homology and function with the type II MAGE-G1 (Hudson et al., 2011; Pebernard et al., 2004). Additionally, an example of a type II MAGE that conforms to this typical trend of genetic localization and expression pattern is MAGE-L2. MAGE-L2 is located on chromosome 15 and it is primarily expressed in the brain and spinal cord. Attesting to the importance of this gene, defects in MAGE-L2 are associated with a disorder known Prader-Willi syndrome, a disorder associated with cognitive and behavioral problems (Boccaccio et al., 1999; Devos et al., 2011).

Cancer-testis antigens

The expression of type I MAGEs in the testis and cancer is not unique and, in conjunction with their antigenic properties, they fall into the broader classification of genes known as cancer-testis antigens. The ability of type I MAGEs to generate immune responses when expressed in cancer is due to the structure and normal physiology of the adult testis (Simpson et al., 2005). The adult testis, like tissues such as brain and eye, have a privileged status with respect to the immune system (Zhao et al., 2014). In the testis, this immune privilege is owed to four factors. First, the complement of immune cells that surveils the testis is different from the rest of the body. For example, the macrophages that are present in the testis have low inflammatory properties and instead are specialized to regulate steroidogenic Leydig cells (Hedger, 2002; Yee and Hutson, 1985). Secondly, immune cells have reduced access to large sections of the testis. This is because, in the structure of the testis, germ cells are surrounded and supported by nurse cells known as Sertoli cells (Smith and Braun, 2012). These cells form much of the structure of the seminiferous tubules and they compartmentalize the testis using a specialized tight junction (Zhao et al., 2014). The tight junction of the testis, known as the “blood-testis barrier” restricts access to immune cells (Smith and Braun, 2012; Wong and Cheng, 2005). Third, cells within the testis secrete a set of immune modulatory cytokines, such as Fas ligand, which induces the death of lymphocytes (Zhao et al., 2014). Finally, male germ cells lack MHC class I molecules, and because they lack this complex, they are unable to present antigens to the immune system (Zhao et al., 2014). All of these factors contribute to a condition in which proteins that are only expressed in the testis have the potential to be antigenic when found in other regions of the body.

Cancer Immunotherapy

While several strategies have been pursued as methods to combat cancer, one idea that has seen multiple iterations is the ability to use the body’s immune system against the tumor. One

enduring version of cancer immuno-therapy has been the development of anti-cancer vaccines that target the immune system towards specific antigens within the cancer. Since their discovery, restricted tissue expression, high penetrance in tumors, and strong antigenicity has made the cancer-testis antigens, including several MAGE proteins ideal targets for cancer vaccine development (Sang et al., 2011). One of the most commonly tested family members is MAGE-A3 (Sang et al., 2011). Studies in vitro and in mice have demonstrated that MAGE-A3 vaccination is able to induce an immune response toward the tumor (Gerard et al., 2014; Liu et al., 2015). Despite these early successes MAGE-A3 vaccines have not performed well in clinical trials. In most cases anti-MAGE-A3 therapy was tolerated but use of MAGE-A3 vaccines as a therapy has failed to generate a statistically significant increase in patient survival (Ramlogan-Steel et al., 2014). Contrasting with the relatively weak results of MAGE-A3 vaccines has been the breakthrough successes of PD-1/PD-L1 and CTLA4 inhibitors (Homet Moreno et al., 2015; Swaika et al., 2015). It is interesting to note that some of the greatest successes in this field have come in the treatment of melanoma, where highly immunogenic cancer-testis antigens are extremely prevalent (Di Giacomo and Margolin, 2015; Homet Moreno et al., 2015). Going forward, one strategy may be the combination usage of PD-1/L1 or CTLA4 with anti-MAGE-A3-directed immunotherapy (Homet Moreno et al., 2015).

Oncogenes

For a significant amount of time people have sought to classify various genes in cancer cells as either “oncogenes” or “tumor suppressors”. While it continues to evolve, the definition of these labels has revolved around if the mutation, amplification, or over-expression of a particular gene is associated with an increased or decreased incidence of cancer. While some genes have been well documented as oncogenes or tumor suppressors using this system, accumulating genetic

data on cancer have shown that this classification is inadequate. Because of the complexity of changes in a cancer's genome and the relative genomic instability of cancer, the field has determined that several changes that occur in cancer are innocuous and play no role in the development of cancer (Pon and Marra, 2015). These changes have been termed "passenger" mutations because they are carried along by the true "driver" mutations that actually effect the changes in cancer (Pon and Marra, 2015). In order to properly determine if a gene is a true driver oncogene, the ability of the gene to induce the various hallmarks of cancer is assayed.

Due to their expression in cancer, all three groups of type I MAGEs (A, B, C), have been implicated in cancer to various degrees. Several studies have shown that MAGE expression is commonly found in cancers such a lung, breast, and colon (Cancer Genome Atlas Research, 2014; Shantha Kumara et al., 2012). In each of these cases, the expression of the MAGE generally correlates with reduced overall survival. Our lab has compared MAGE expression frequency in various cancers and one the most commonly expressed MAGE is MAGE-A3, and its identical copy MAGE-A6. They are expressed in approximately 75% of melanomas and lung squamous carcinomas, 50% of colorectal and lung adenocarcinomas, and 25% of breast cancers (Figure 1-2A). When MAGE-A3 is expressed in cancer, patients have a significantly reduced survival time (Figure 1-2B). In addition, there is some evidence that MAGE-A3 plays an active role in cancer. Others have found that when MAGE-A3 is expressed in an orthotopic xenograft model of thyroid cancer, where it is normally never found, it dramatically increases the size and aggressiveness of the tumors (Liu et al., 2008). In this thyroid cancer model, expression of MAGE-A3 increases cell cycle progression, likely through reduced expression of p21 (Liu et al., 2008) Studies have also shown that MAGE-A3 expression may be able to increase metastatic potential of cancer cells and it is often found enriched in metastatic populations of cells

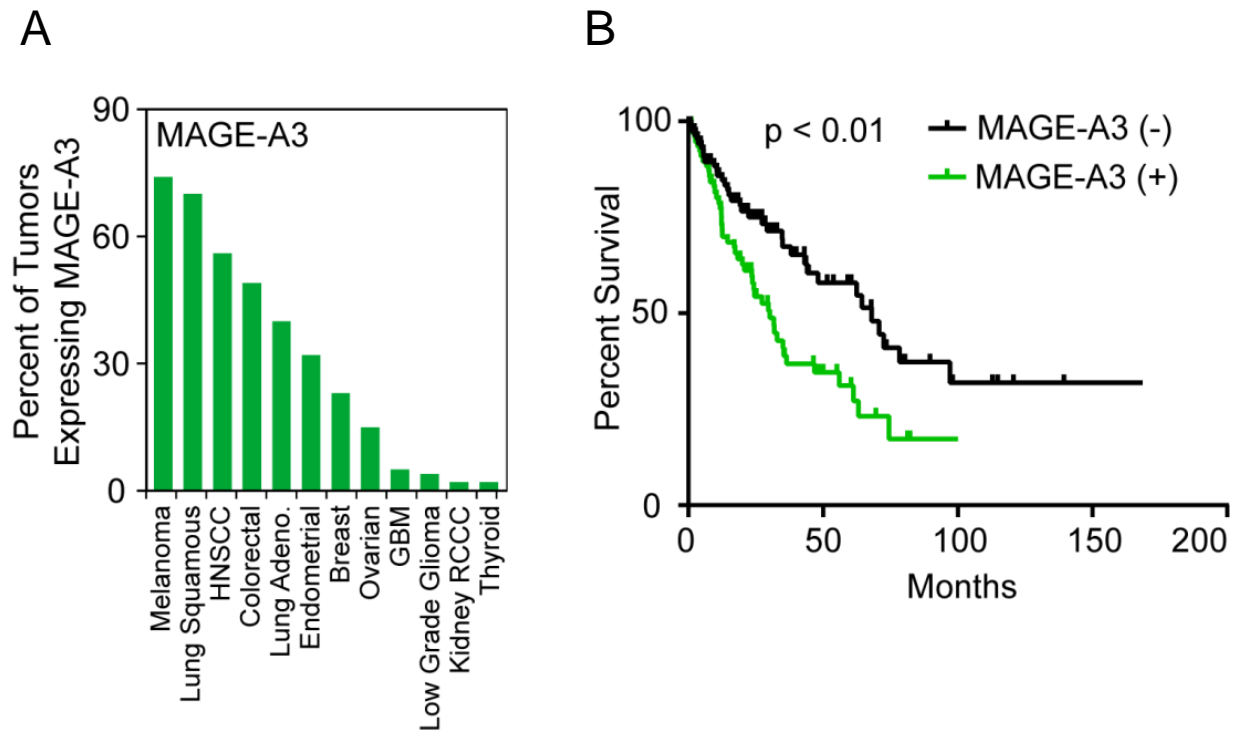


Figure 1-2 MAGE-A3 Expression and Effect on Survival

- A. Expression data from was stratified into MAGE-positive and MAGE-negative groups. Percentage of patient tumors expressing MAGE-A3 in various cancer types.
- B. Kaplan-Meier curve comparing survival of patients with MAGE-positive or MAGE-negative lung squamous cell carcinoma. Expression of MAGE- correlates with poor overall survival

(Dango et al., 2010; Liu et al., 2008; SieneI et al., 2007)Also, loss of MAGE-A in cancer cell lines leads to increased apoptosis through increased Bax expression (Nardiello et al., 2011). Even though some evidence suggests that MAGEs may play an active role in the development or progression of cancer, the importance of MAGE expression and the mechanism through which MAGEs function remains to be established.

Recently, a general mechanism has been found for MAGE family members. Multiple studies have determined that MAGEs, through a conserved MAGE homology domain (MHD), bind to and stimulate RING type E3 ubiquitin ligases (Doyle et al., 2010; Feng et al., 2011; Hao et al., 2013). This ultimately leads to changes in ubiquitin signaling within the cells.

Ubiquitin Signaling Cascade

The ubiquitin system is a method of cellular signaling that utilizes the post translational addition of a small protein, ubiquitin, onto an acceptor lysine present on proteins. In order to accomplish this task, the ubiquitin system utilizes a multi-step enzymatic cascade, which is comprised of a series of enzymes known as E1, E2 and E3 (Clague et al., 2015). Additionally, this enzymatic system is used in numerous other systems that conjugate the closely related homologues of ubiquitin that are present in mammals (Clague et al., 2015).

Ubiquitin is encoded in 4 distinct genetic loci UbB, UbC, UBA62, and UBA80. In the first two gene copies, UbB and UbC, ubiquitin is fused in a head to tail orientation into 3x or 9x copies. Similarly, in UBA52 and UBA80 a single ubiquitin is fused to a ribosomal subunit. In each of these cases ubiquitin is translated fused to the other proteins. After translation, free ubiquitin is generated by proteolytic processing, creating a C-terminus that ends with two glycine residues. The terminal glycine serves as the attachment point for conjugation onto targets.

After it has been processed into its free form, ubiquitin monomers are then charged by one of two E1 enzymes, UBA1 or UBA6, that are present in humans (Clague et al., 2015). These enzymes utilize ATP to charge ubiquitin via a process termed trans-esterification and form a high energy thioester bond with the catalytic cysteine present in one of the 35 different E2 enzymes in the human genome. After charging, the E2-Ub enzyme adducts binds to an E3 ubiquitin ligase. The E3 ubiquitin ligase, which confers substrate specificity, then stimulates the discharge of ubiquitin onto the target protein, and the energy from the thioester bond is utilized to generate a stable iso-peptide between the terminal glycine on ubiquitin and the sidechain of the target lysine (Clague et al., 2015).

In addition to being attached to the lysine of target proteins, ubiquitin can also be attached onto its own internal lysine moieties or its own N-terminus. This allows ubiquitin to form long chains on proteins and each of the internal lysine residues form different chains, which have differential activities within cells (Komander and Rape, 2012). The most studied chain type is formed by ubiquitin K48 linkages and it has the well described effect of targeting proteins for degradation by the 26S proteasome. Other chain linkages have various signaling functions throughout the cells and can affect regulatory events such as protein localization and kinase activation (Komander and Rape, 2012).

Given the number of ubiquitinated proteins in the cells and their multiple modification forms, it is unsurprising that there are several hundred E3 ubiquitin ligases and they fall into three distinct classes HECT (Homologous to the E6-AP Carboxyl Terminus), RING (Really Interesting New Gene), and RBR (RING Between RING) ligases (Komander and Rape, 2012). Besides their structures, the major distinguishing factor between these families is that HECT and RBR ligases form a covalent intermediate with the ubiquitin transfer to substrate. In contrast, RING ligases

never form a covalent link with ubiquitin and instead they only stimulate transfer to substrate, without an intermediate step (Komander and Rape, 2012).

Given their large number, there are also several commonly studied subclasses of RING type ubiquitin ligases. Two of the most extensively studied RING subclasses are the Cullin type and Tripartite Motif (TRIM) type ubiquitin ligases. The Cullin ligase family is a group multi-subunit complexes comprised of three primary subunits (Vittal et al., 2015). At their core each ligase contains one of two catalytic RING proteins, either RBX1 or RBX2. Each core is then associated with one of seven Cullin proteins and one of dozens of substrate recognition proteins such as the F-box or BTB proteins (Vittal et al., 2015). Together, the combinatorial effects are that unique complexes play distinct roles within the cell. In contrast to the multi-subunit Cullin ligase are the largely independently functioning TRIM ubiquitin ligases. Members of this family are defined by the presence of their N-terminal tripartite motif (TRIM) (Hatakeyama, 2011). This motif contains a RING domain, one or two b-boxes, and a coiled-coil domain (RBCC). While this family shares a similar N-terminal arrangement, they have divergent C-terminal domains, and the family is grouped accordingly into eleven sets based on their C-terminus (Hatakeyama, 2011). These C-termini often contain other accessory domains that allow regulation, protein-protein interaction or additional catalytic activities (Hatakeyama, 2011).

Several different mechanisms that govern the activity of TRIM type ubiquitin ligases have been investigated. One mechanism that has been shown to regulate this family of ligases is the formation of higher order homo and heterotypic oligomers. For example, the ligase TRIM28 has been demonstrated to function in higher order oligomers with its two closest family members TRIM24 and TRIM33 (Herquel et al., 2011). Recent data from our laboratory has started to reveal a second method of regulation of TRIM type ligases. Previous and ongoing studies have

demonstrated that several MAGE proteins bind to the TRIM family of ligases and enhance their activity through unknown mechanisms. For example the type II MAGE, MAGE-L2 binds specifically to the ligase TRIM27 (Hao et al., 2013). This interaction is specific, with TRIM27 binding to no other MAGE proteins and MAGE-L2 binding no additional ligases. Type I MAGEs are also found binding to TRIM ligases and at least MAGE-C2, -A2, -A3 and -A6 bind to the TRIM28 E3 ligase (Doyle et al., 2010).

TRIM28

TRIM28 has already been studied in both the context of normal physiology and disease states. In normal physiology the majority of TRIM28's previous functions have been attributed to its control of chromatin regulation and how it effects transcription and the DNA repair pathway.

In normal chromatin function, TRIM28 is recruited to DNA via two mechanisms; binding between KRAB zinc finger transcription factors and its RBCC domain and binding of its PHD and bromo domains to chromatin (Iyengar and Farnham, 2011; Iyengar et al., 2011). Once localized to chromatin, TRIM28 utilizes its adjacent PHD and bromo domains as an E3 SUMO ligase and autosumoylates (Ivanov et al., 2007). Next TRIM28 acts as a scaffold for other factors such as HP1, Mi2 α , and the methyl transferase SETDB1 (Iyengar and Farnham, 2011). This promotes the formation of histone 3 lysine 9 trimethylation marks and suppression of the genetic locus (Barde et al., 2009). TRIM28 has been extensively studied for its role in DNA repair (Hu et al., 2012). Upon DNA damage, TRIM28 is localized to the DNA break and the kinase ATM phosphorylates near the bromo domain; inhibiting autosumoylation (Hu et al., 2012; Iyengar and Farnham, 2011; White et al., 2012). Because of this, repressive proteins such as SETDB1 are lost and the chromatin de-condenses, allowing the DNA repair machinery to fix the break.

Subsequently, the phosphatase PP1 β removes the phosphorylation from TRIM28, returning it to its original chromatin condensing state (Iyengar and Farnham, 2011; Li et al., 2010; White et al., 2012).

Another feature of TRIM28 is its ability to repress viruses. For example, TRIM28 has been shown to suppress the transcription of endogenous retroviruses, a type of transposon (Fasching et al., 2015; Iyengar and Farnham, 2011; Rowe et al., 2013a; Rowe et al., 2010; Rowe et al., 2013b). Through another mechanism, TRIM28 inhibits the integration of HIV into the genome (Allouch et al., 2011). This is accomplished by the compliment of binding proteins that are normally associated with TRIM28 on the chromatin. In this case, HDAC1 deacetylates the viral integrase protein and suppresses integration (Allouch et al., 2011).

In addition to molecular roles, the potential importance of TRIM28 on the entire organism has been studied. Whole body knockouts of TRIM28 are embryonically lethal, with embryos dying between E8.5 and E9.5 (Herzog et al., 2011). When TRIM28 is knocked out in specific tissues, several additional phenotypes are observed. For example, liver specific deletion of TRIM28 causes the deregulation of several genes and ultimately leads to hepatosteatosis and adenoma of the liver (Bojkowska et al., 2012). Perhaps the most interesting due to its association with testis specific proteins, TRIM28 is required for maintenance of spermatogenesis and its loss results in failure of spermatogonia to form (Weber et al., 2002).

While there are studies defining the role of TRIM28 in normal physiology, there has also been significant research into the role of TRIM28 in cancer. It appears that increased expression of TRIM28 may enhance the aggression and metastasis of cancers in which it is over expressed (Ho et al., 2009). Generally, more aggressive tumors have been found in both cervical and ovarian

cancers when TRIM28 is expressed (Cui et al., 2015; Lin et al., 2013). When breast cancer metastases are compared to the original tumor they have significantly higher levels of TRIM28, possibly indicating enrichment for this population during metastasis, and high levels of TRIM28 are an independent predictor of peritoneal carcinomatosis in gastric cancer (Yokoe et al., 2010). Some mechanisms have been proposed for TRIM28's role in metastasis. In lung cancer, TRIM28 has been shown to transcriptionally regulate EMT, though regulation of E-cadherin and N-cadherin (Chen et al., 2014).

Other possible mechanisms have been investigated for TRIM28's role in cancer aggressiveness. Significant research has focused on the connection between TRIM28 and the degradation of the tumor suppressor p53 (Monte et al., 2006; Yang et al., 2007). It is well known that p53 can be degraded by E3 ubiquitin ligase MDM2 and early reports looked at the role that TRIM28 may play in this process. These studies determined that TRIM28 is able to enhance the ubiquitination of p53 by bringing it to MDM2 (Wang et al., 2005) While this may be the case for some cell lines, it has recently been determined that when bound by MAGEs such as MAGE-C2, TRIM28 is able to directly ubiquitinate p53 and targets it for degradation (Doyle et al., 2010). While this finding was groundbreaking, it was not sufficient to explain all of the phenotypes that were associated with TRIM28 binding MAGEs in cancer. Previous data in our lab has determined that when MAGEs are expressed in cancer, they exhibit a phenomenon known as oncogene addiction, a condition where loss of an oncogene is toxic to cancer cells (Weinstein, 2002). This is indeed the case for MAGE-As, were knockdown of MAGE-A3/6 is able to robustly decrease the viability of all MAGE-A3/6 expressing cell lines, regardless of genetic background, but not those which are MAGE-A negative (Figure 1-3). This is significant because several of the cell lines that exhibit addiction to MAGE-A3/6 are indeed p53 mutated. If the exclusive function of

MAGE-TRIM28 were to prevent p53 function, its activity should not be required in p53 mutant cell lines, where p53's activity is abrogated. Therefore, while the data clearly indicated that MAGE-A3/6 could be playing a role in cancer, I wanted to expand this knowledge by solving two distinct problems. First, I wanted to determine what molecular role, outside of p53 regulation, the complex of MAGE-A3/6-TRIM28 played within the cell. Second, I wanted to clearly demonstrate that MAGE-A3/6 is an oncogene and identify a way to combat its effects in cancer.

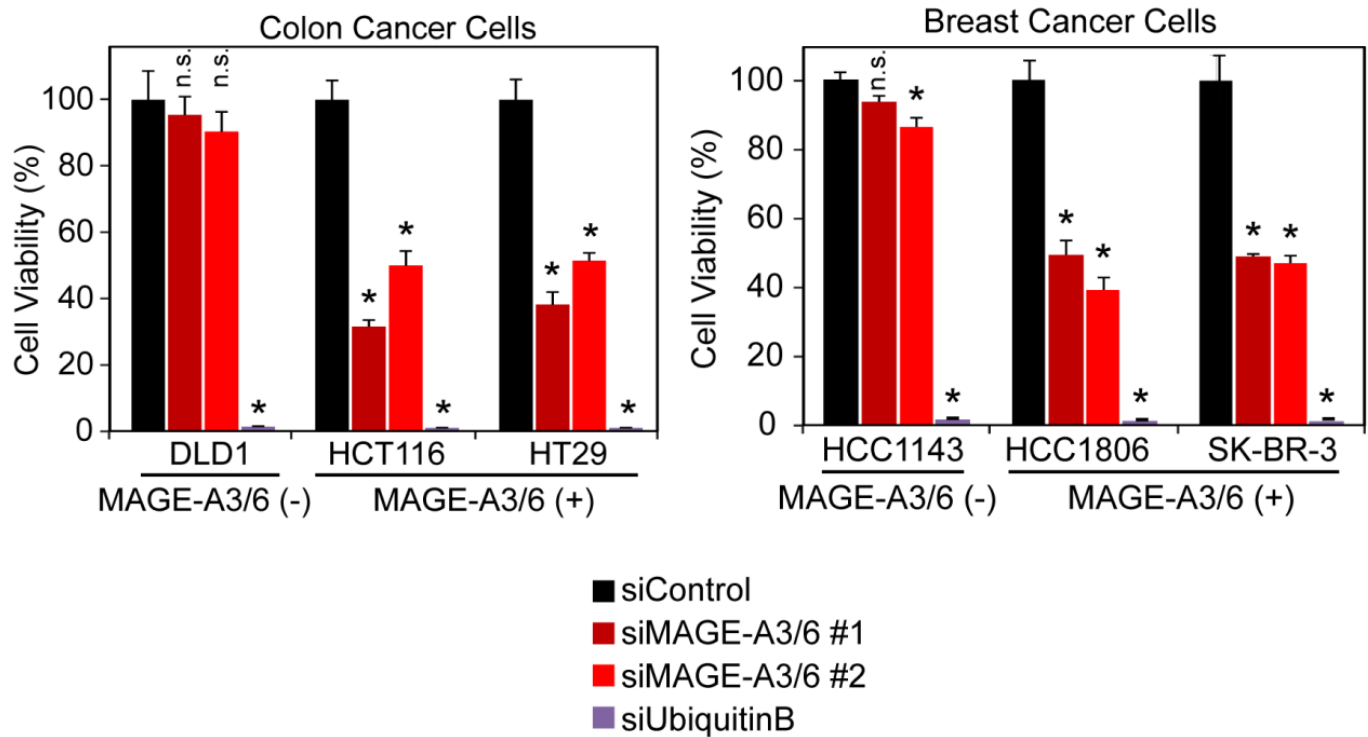


Figure 1-3 Cells Exhibit Oncogene Addiction to MAGE-A3

MAGE-A3/6 depletion reduces viability of MAGE-A3/6 expressing colon cancer and breast cancer cell lines. Cells lines were plated in triplicate in 96 well plates. 24 hours later cells were transfected with indicated siRNAs and 48 hours post transfection cells were assayed for viability by MTT. Bars represent mean survival \pm SD. Asterisks indicate $p \leq .05$ as determined by Student t-test.

Chapter II: Materials and Methods

Proto Array

ProtoArray containing > 9,000 GST-tagged recombinant proteins purified from SF9 insect cells was purchased from Invitrogen. Slides were allowed to equilibrate to 4 °C and blocked for 60 min at 4 °C shaking in 50 mM HEPES, pH 7.5, 200 mM NaCl, 0.08% (v/v) Triton X-100, 25% (v/v) Glycerol, 20 mM reduced glutathione, 1 mM DTT, and 1% (w/v) BSA. Slides were then washed for 3 min at 4 °C shaking in assay buffer (50 mM Tris-HCl, pH 7.5, 50 mM NaCl, 5 mM MgSO₄, 0.1% (v/v) Tween 20, 1 mM DTT, and 1% (w/v) BSA). In vitro ubiquitination on the slide was performed with 100 mg/ml N-terminal labeled biotinylated-Ubiquitin (Boston Biochem), 100 nM UBE1 (Boston Biochem), 500 nM UbcH2 E2 (Boston Biochem), Energy Regeneration Solution (a mixture that contains MgCl₂, ATP, and ATP-regenerating enzymes to recycle hydrolyzed ATP, Boston Biochem), and with or without 100 mg/mL recombinant MAGE-TRIM28 (22-418). Reaction mixture was incubated on array slide for 90 min at 30 °C. Slides were washed in 0.5% (w/v) SDS three times shaking for 5 min each to remove non-covalent ubiquitin interactions, followed by washing in assay buffer two times shaking for 5 min. Ubiquitinated proteins were then labeled by incubation with 1 mg/ml streptavidin conjugated-Alexa-647 at 4 °C for 45 min shaking. Slides were then washed five times for 5 min shaking in assay buffer, followed by briefly dipping into dH₂O three times. Slides were dried by centrifugation for 1 min at 200 xg. Dried slides were then scanned with a GenePix400B microarray slide scanner (Molecular Devices). Spots were identified and quantitated using GenePix Pro microarray analysis software and statistical analysis was performed using ProtoArray Prospector (Invitrogen).

Cell Culture

DLD1, HCC1143, HCC1806, HCT116, HeLa, HT29, NIH 3T3, SK-BR-3, and U2OS cells were grown in DMEM supplemented with 10% FBS, 2 mM L-Glutamine, 100 units/mL penicillin, 100 mg/mL streptomycin, and 0.25 mg/mL amphotericin B. HTB126, H1648, H1693, H2126, and HCC193 were grown in RPMI supplemented with 5% heat inactivated serum. HeLa GFP-LC3 cells were grown in Opti-MEM supplemented with 5% FBS. Human colonic epithelial cells (HCECs) were maintained in media (3:1 ratio of Dulbecco's modified Eagle's Medium and Medium 199) containing 2% FBS and supplemented with 10 mg/mL insulin, 2 mg/mL transferrin, 20 ng/mL EGF, 5 nM sodium selenite, and 1 mg/mL hydrocortisone (Roig et al., 2010). Human bronchial epithelial cells (HBEC) were grown in keratinocyte serum free media (KSFM) supplemented with 5 ng/mL EGF and 50 mg/mL bovine pituitary extract (Ramirez et al., 2004; Sato et al., 2006).

siRNA Sequences

siControl (targeted against LonRF1), siRagC, simTOR, and siULK1 were purchased as SmartPools from Thermo Scientific. Sequences for other siRNAs are as follows: siMAGE-A3/6 #1 (5'-GAUGGUUGAAUGAGCGUCAdTdT-3'), siMAGE-A3/6 #2 (5'-GGUAAAGAUCAGUGGAGGAdTdT-3'), siTRIM28 (5'-GCAUGAACCCCUUGUGCUGdTdT-3'), and siAMPK α 1 (5'-CAAAGUCGACCAAUGAUA-3').

In Vitro Binding

15 mg of purified GST-tagged proteins were bound to glutathione Sepharose beads (Amersham) in binding buffer (25 mM Tris pH 8.0, 2.7 mM KCl, 137 mM NaCl, 0.05% (v/v) Tween-20, and

10 mM β - mercaptoethanol) for 1 hr and then blocked for 1 hr in binding buffer containing 5% (w/v) milk powder. In vitro translated proteins (Promega SP6-TNT Quick rabbit reticulocyte lysate system) were then incubated with the bound beads for 1 hr, extensively washed in binding buffer, eluted with 2X SDS-sample buffer, boiled, subjected to SDS-PAGE, and immunoblotting.

Immunoprecipitation

HeLa cells were plated in 6 well plates. 16 hr after plating cells were transfected with plasmids of interest using Effectine. Scrapped in ice cold PBS and pelleted. Cells were then resuspended in 300 μ l of ice cold NP-40 lysis buffer and incubated on ice for 45 min. Cells were then cleared by spinning at max speed for 15 min. Samples were then transferred to a new tube and 30 μ l were taken as whole cell lysate. 10 μ l of SDS sample buffer was added to whole cell lysate. 700 μ l of lysis buffer was then added to the remaining lysate. 10 μ l of washed myc beads were then added to lysate and rotated at 4 °C for 2 hr. Beads were then washed 5x with lysis buffer and eluted with 40 μ l of SDS sample buffer. Samples were then analyzed by western blot.

GFP/LC3 Staining

Cells were washed in 1X PBS, fixed in 3% paraformaldehyde for 15 min at room temperature (LC3 staining), washed twice in 1X PBS, and permeabilized for 20 min at 4 °C in 1X PBS containing 100 mg/mL digitonin (LC3 staining) and 3% (w/v) BSA. After permeabilization, cells were incubated for 60 min in primary antibodies diluted in 1X PBS containing 100 mg/mL digitonin (LC3) and 3% (w/v) BSA. Cells were then washed in PBS containing 100 mg/mL digitonin (LC3 staining) three times and incubated for 30 min in 4 mg/mL Alexa-488 secondary antibody (Invitrogen Molecular Probes) diluted in PBS containing 100 mg/mL digitonin (LC3)

and 3% (w/v) BSA. Cells were then washed three times in PBS containing 100 mg/mL digitonin (LC3 staining), DNA stained with 1 mg/mL DAPI for 2 min, washed in PBS, and mounted. Cells were imaged with a 63X or 100X objective on Nikon-TiU or DeltaVision inverted fluorescence microscopes. Image stacks (0.3 μ m intervals) were acquired with a CoolSnap HQ2 charge-coupled device camera (Photometrics), deconvolved using the nearest neighbor algorithm, and stacked to better resolve GFP-LC3 puncta. At least 50-100 cells were counted for each condition in each experiment.

GFP-LC3 Flow Cytometry

U2OS GFP-LC3 (150,000 cells) or HeLa GFP-LC3 (125,000 cells) were plated in 6 well plates in 2 mL media. 24 hr after plating cells were treated with siRNAs. 72 hr after siRNA treatment cells were trypsinized with minimal trypsin. Cells were then spun down and re-suspended in FACs buffer (3% Serum in PBS). Samples were then analyzed using a BD FACS Scan. Data was then analyzed using FlowJo 7.6.5.

SDS-PAGE/Western Blot

Cells were lysed on the plate with 100 μ l of SDS sample loading buffer and scraped. Cell lysates were then sonicated to break open cells. Cell lysates were then heated at 60 °C. Samples were then spun at max speed for 10 min.

7.5%, 10%, 12.5% Tris-acrylamide gels were run at 80 V for 20 min followed by 100 V for 90 min. Gels were transferred to nitrocellulose membranes at 150 mA for 1 hr per gel. Membranes were blocked in 5% milk/TBST. Blots were then incubated overnight at 4 °C with antibody (1:1000 dilution).

Drug Treatment

Cells were treated with 10 μ M compound C for 4 hr. Cells were then processed according to assay protocol. Cells were plated and treated with siRNA as in previous experiments. Cells were treated with 50 nm Bafilomycin A1 for 4 hr. After 4 hr cells were processed by standard western blot protocols.

Soft Agar Colony Formation

A base layer of 0.5% Noble agar was plated in a 6 well plate. Once solidified, cells were suspended in 0.375% Noble agar supplemented with regular growth medium. Cells were grown for 2-4 weeks. The number of colonies that were greater than 100 μ m was counted.

Mouse Xenograft Studies

4-6 week old female NOD-SCID Il2 gamma knockout mice were used in mouse experiments. 24 hr prior to injection mice were shaved on the right flank. Mice were injected in the right flank with 200 μ L of a mixture containing 50% PBS, 50% matrigel and 5×10^6 cells. 8 mice in each group were injected with either HCEC-CTR vector or HCEC-CTR MAGE-A6 cells. 4 days post injection mice were examined for the presence of tumors. Tumors were measured using digital calipers on two axes. Tumor volume was calculated using the formula Long x Short x Short x .52= Volume. Tumor volume was then plotted in relationship to number of days post injection. Error bars represent SEM. Mice were sacrificed when tumors reached 20 mm in any axis. At time of sacrifice tumors and lungs were fixed in formalin and send for histopathological analysis.

Chapter III: AMPK is a Substrate of MAGE-TRIM28

ProtoArray Identifies MAGE-TRIM28 Substrates

The single known substrate of MAGE-TRIM28, p53, is insufficient to explain all of the effects of this complex in cancer; therefore, I set out to identify additional substrates that could account for the oncogenic properties of this complex. After considering alternative strategies that are capable of revealing ubiquitin ligase substrates, such as SILAC mass spectrometry, I elected to use the commercially available ProtoArray, because of its relative cost, short optimization time and availability of reagents (Meierhofer et al., 2008; Persaud et al., 2009; Persaud and Rotin, 2011). This technology utilizes approximately 9000 baculovirus produced GST-tagged proteins which are then spotted onto a nitrocellulose coated array chip and any desired biochemical reaction that is capable of being performed in vitro may be used in conjunction with this array.

In order to test the substrates of MAGE-TRIM28, I purified MAGE and the soluble RBCC domain of TRIM28. I then used commercially available E1 enzyme, E2 enzyme UbcH2, and biotinylated ubiquitin in conjunction with purified MAGE-TRIM28 complex to run the ubiquitination reaction directly on the chip. Potential substrates were conjugated with biotinylated ubiquitin and subsequently detected with fluorescent streptavidin (Figure 3-1). This experiment identified 19 putative substrates (Table 3-1). I found several of these hits to be very interesting for various reasons. For example, one hit that was interesting was EP300 interacting inhibitor of differentiation 3 (EID3) because other MAGEs have been identified as binding to related EID proteins (Guerineau et al., 2012; Hudson et al., 2011). While binding to these proteins has been established, they have not been investigated for their potential to be substrates for modification by MAGE-RING ligase complexes. Another protein that was identified as a

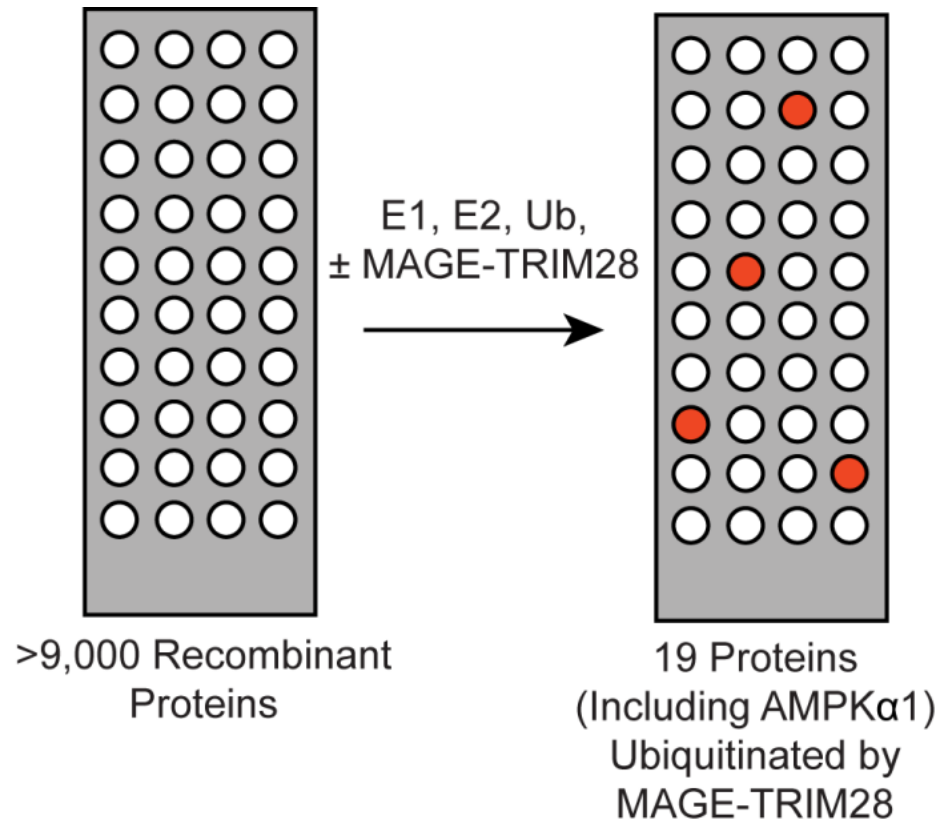


Figure 3-1 ProtoArray Scheme

Schematic of in vitro screen for MAGE-TRIM28 ubiquitination substrates using protein arrays. Slides were blocked in 1% BSA for 45 min. Ubiquitin reaction was performed with UBE1, Ubc H2, MAGE-TRIM28 for 90 minutes. Slides were then rinsed and incubated with Strep-647. Slides were then washed with 1% SDS and read using microarray reader.

Table 3-1 MAGE-TRIM28 targets identified by *in vitro* ubiquitination screening.

Protein	UniProt ID	Description	GO - Biological Process(es)
AMPK α 1	AAPK1_HUMAN	AMP-activated protein kinase (AMPK), alpha 1 catalytic subunit PRKAA1	autophagy, cellular response to glucose starvation, fatty acid homeostasis, cholesterol biosynthetic process, glycolysis, negative regulation of TOR signaling cascade, glucose homeostasis, regulation of energy homeostasis, protein phosphorylation
RSRP	RSRP1_HUMAN	arginine/serine-rich protein 1	-
GBGT1	GBGT1_HUMAN	globoside alpha-1,3-N-acetylgalactosaminyltransferase 1	glycolipid biosynthetic process, glycosylation
HMGB1	HMGB1_HUMAN	high-mobility group box 1	DNA repair, DNA recombination, apoptosis, innate immune response, chemotaxis,
RAPGEF4	RPGF4_HUMAN	Rap guanine nucleotide exchange factor 4	guanyl-nucleotide exchange factor activity, exocytosis, cAMP-mediated signaling
TIGD1	TIGD1_HUMAN	Tigger transposable element-derived protein 1	-
LPAL2	LPAL2_HUMAN	apolipoprotein(a)-like protein 2	-
LUC7L2	LC7L2_HUMAN	LUC7-like 2	mRNA splice site selection
ARID3A	ARI3A_HUMAN	AT rich interactive domain 3A	transcription
EID3	EID3_HUMAN	EP300-interacting inhibitor of differentiation 3	transcription, DNA recombination, DNA repair
BUD31	BUD31_HUMAN	BUD31 homolog	cell cycle, mRNA splicing and processing
HSPB7	HSPB7_HUMAN	heat shock 27kDa protein family, member 7	unfolded protein response
REEP5	REEP5_HUMAN	Receptor expression-enhancing protein 5	-
TMPRSS3	TMPS3_HUMAN	transmembrane protease serine 3	cellular sodium ion homeostasis
PPP2R5C	2A5G_HUMAN	protein phosphatase 2, regulatory subunit B', gamma isoform	protein phosphatase type 2A regulator activity
FTL	FRIL_HUMAN	ferritin, light polypeptide	cellular iron ion homeostasis
METTL5	METL5_HUMAN	methyltransferase like 5	methylation
NR1D1	NR1D1_HUMAN	nuclear receptor subfamily 1, group D, member 1	transcription, gluconeogenesis, circadian rhythm, bile acid biosynthetic process, TLR4 signaling pathway, glycogen biosynthetic process, steroid hormone mediated signaling pathway, cholesterol homeostasis
CAND1	CAND1_HUMAN	Cullin-associated NEDD8-dissociated protein 1	SCF complex assembly, protein ubiquitination

strong hit in the screen was the transmembrane protease serine type 3 (TMPRSS3). While little is known about this protein, it has been shown to be associated with the progression of pancreatic cancer (Wallrapp et al., 2000). Ultimately, I decided to follow up the putative substrate AMPK α 1 because it is well documented to play multiple roles as a tumor suppressor.

AMPK

AMPK is a hetero-trimeric kinase that is involved in energy regulation within the cell, specifically responding to ATP/ADP/AMP levels (Hardie et al., 2012b). The response of AMPK to high ADP/AMP is mediated through two different mechanisms. First, the α catalytic subunit is regulated by β and γ subunits, and when ADP/AMP is high, they replace ATP in the γ subunit (Suter et al., 2006). This causes allosteric changes within the complex that bias the kinase towards its active conformation. The second mechanism that generates AMPK's response to ADP/AMP is mediated through phosphorylation of the α subunit by multiple upstream kinases (Hawley et al., 2003; Hawley et al., 2005). This modification of T172 is found in the kinase activation loop, and is added by the kinase LKB1 (STK11) in low energy conditions when the activation loop is exposed by conformational change (Hawley et al., 2003). This phosphorylation of T172 can also be added by CAMKK β , tying AMPK activation to processes which release Ca²⁺ (Hardie, 2015). When the AMPK holoenzyme is active, it generally acts to oppose anabolic energy consuming pathways and promotes catabolic ATP generating pathways (Hardie et al., 2012b). For example, AMPK directly phosphorylates and inhibits the enzyme ACC1, the committed step in fatty acid synthesis. It also inhibits cholesterol biogenesis through HMG-CoA reductase and inhibits protein synthesis through phosphorylation of TSC2 and mTOR (Carling et al., 1989; Clarke and Hardie, 1990). At the same time AMPK increases glucose uptake and utilization, and autophagy through several mechanisms (Barnes et al., 2002; Meley et al., 2006).

While the role of AMPK in normal physiology has been studied extensively, the role of AMPK in the inhibition of cancer is also well established. In general it has been determined AMPK acts as a tumor suppressor in both animal models and in humans (Hardie and Alessi, 2013; Shackelford and Shaw, 2009). AMPK plays multiple tumor suppressive roles through its multifaceted regulation of metabolism. In tumors, AMPK restrains growth by inhibiting mTOR and synthesis of cellular macromolecules, and promotes cell cycle arrest through activation of cyclin dependent kinase inhibitors and stabilization of p53 (Imamura et al., 2001; Jones et al., 2005; Liang et al., 2007). Additionally, AMPK can oppose the process of epithelial to mesenchymal transition, by opposition to the Akt-MDM2-Foxo3a signaling axis (Chou et al., 2014). Unsurprisingly, because of its importance, the AMPK signaling axis is deregulated in disease states and 20% of lung adenocarcinomas and cervical cancers have a mutation in LKB1 (Matsumoto et al., 2007; Sanchez-Cespedes et al., 2002; Wingo et al., 2009). Additionally, B-RAF^{V600E} can erroneously phosphorylate and inhibit LKB1 (Esteve-Puig et al., 2009; Zheng et al., 2009; Zheng et al., 2013). Finally, loss of LKB1 is associated with Peutz-Jeghers syndrome, a disease whose patients who are prone to develop intestinal polyps and colorectal cancer (Shackelford et al., 2009).

Substrate Confirmation

The first action that I took after identifying AMPK α 1 as a substrate by ProtoArray was determining if this ubiquitination occurs in cells. I began by taking the MAGE expressing cell line, HeLa, and assaying AMPK α ubiquitination. I immunoprecipitated myc-ubiquitin and blotted for AMPK α 1 in order to reduce the possibility that any ubiquitin chain signals found were due to proteins in complex with AMPK α 1. When this was done in the presence of MAGE-A3/6-TRIM28 complex there was a smear indicating ubiquitinated AMPK α 1 (Figure 3-2A) but

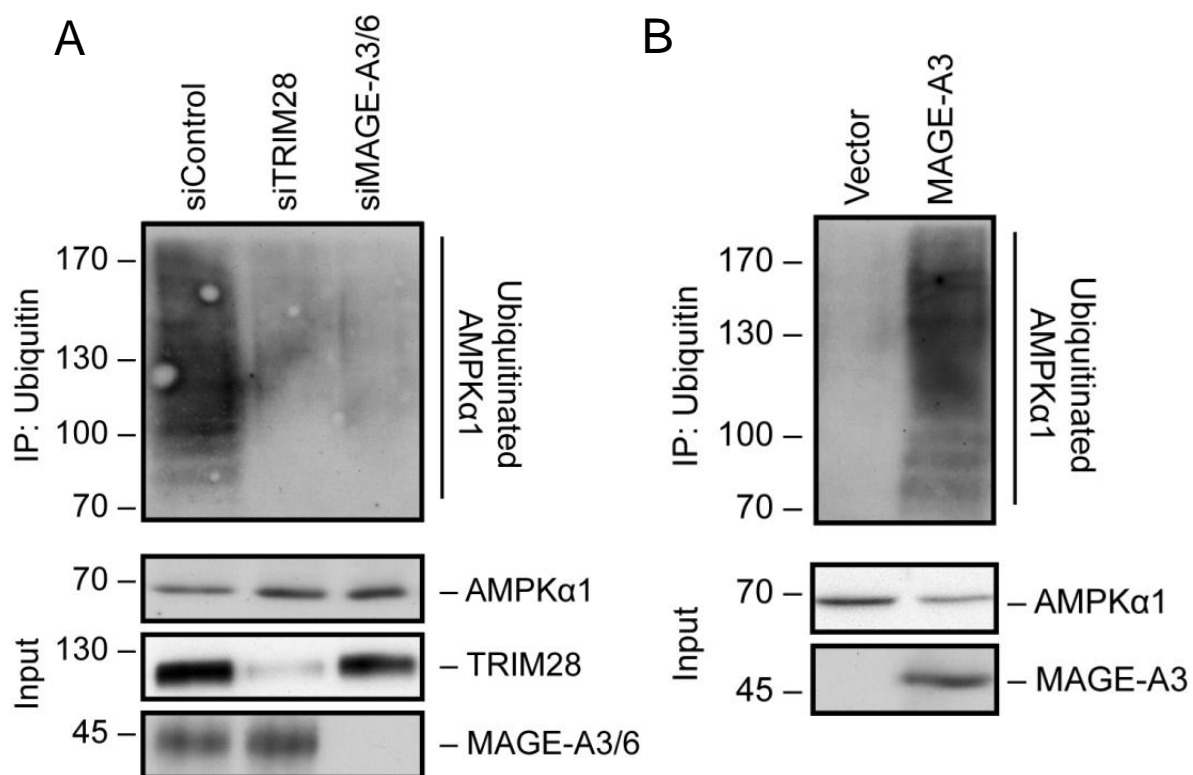


Figure 3-2 AMPK is a Substrate of MAGE-A3/6-TRIM28

- A. AMPK α 1 ubiquitination requires MAGE-A3/6-TRIM28. HeLa (MAGE-A3/6-positive) were treated with the indicated siRNAs for 24 hr before transfection with myc-tagged ubiquitin for 48 hr before anti-myc IP and western blot was performed
- B. Expression of MAGE-A3 promotes AMPK α 1 ubiquitination. MAGE-A3/6-negative HEK293 cells stably expressing FLAG-MAGE-A3 were transfected with myc-ubiquitin before IP and western blotting.

when TRIM28 or MAGE-A3/6 was depleted by siRNA, Ub-AMPK was dramatically reduced. The ability of both siRNAs to block AMPK ubiquitination was critical because it supported the conclusion that this phenotype was not due off-target siRNA effects and depletion of either complex component was capable of effecting AMPK. These results suggested that MAGE-A3/6-TRIM28 is required for AMPK ubiquitylation. I next wanted to test if expression of MAGE-A3 was sufficient to induce ubiquitination of AMPK in MAGE-negative cell lines. I did this by stably expressing a 3X FLAG tagged MAGE-A3 in HEK293. I again used myc-ubiquitin to pulldown modified protein and probed for AMPK α 1. While there was no signal detected in the control condition, the Ub-AMPK α 1 smear observed with MAGE-A3 expression indicated that it alone was sufficient to induce ubiquitination of AMPK α 1 (Figure 3-2B). Not only did these data demonstrate that that MAGE-A3/6 expression alone was sufficient to induce ubiquitination of AMPK, they also further confirmed the validity of the previous siRNA based experiments. This is because it is highly unlikely that an off target effect of siRNA would have a specific yet opposite effect to the overexpression of the target gene.

AMPK is targeted by MAGE-A3/6-TRIM28 for ubiquitin/proteasome-dependent degradaton

Once I had confirmed that AMPK α 1 was ubiquitinated by MAGE-A3/6-TRIM28, I next wanted to understand what effect that modification had on AMPK. With the understanding that the canonical role of ubiquitin is in regulating protein degradation, I set out to test if ubiquitination of AMPK α 1 affected its abundance or stability. I first tested this by using the MAGE-positive cancer cell line U2OS. I knocked down MAGE-A3/6 or TRIM28 and I looked at the total levels of AMPK α 1 in the cells. Confirming earlier suspicions, knockdown of the ubiquitin ligase components increased the protein levels of AMPK α 1 (Figure 3-3A). In addition to the α subunit,

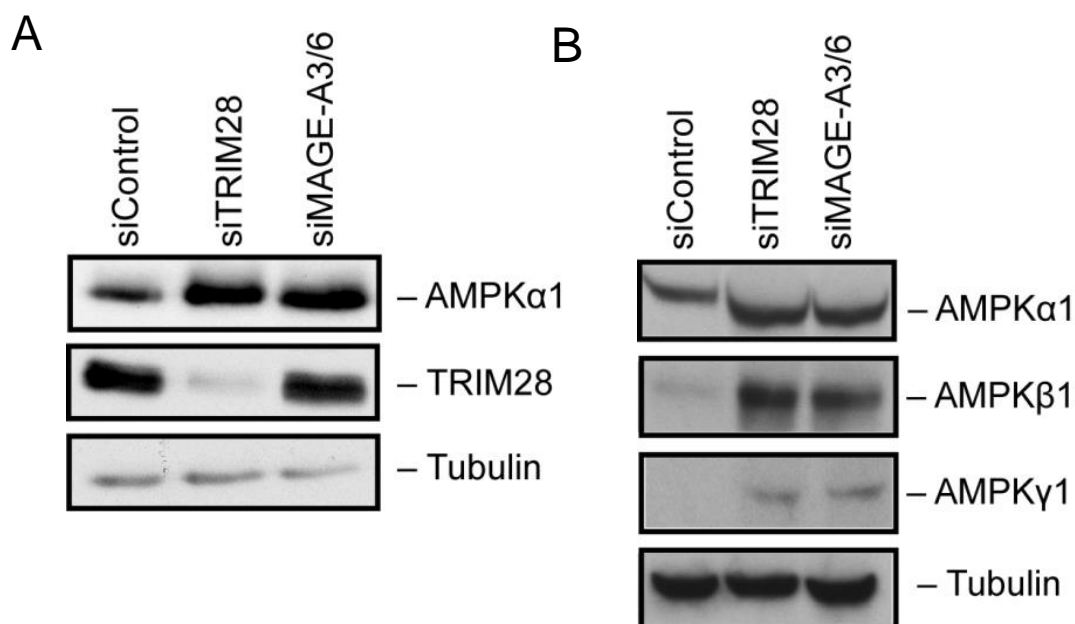


Figure 3-3 MAGE-A3/6 Negatively Regulates AMPK Protein Levels

- A. Knockdown of MAGE-A3/6-TRIM28 increases AMPKα1 protein levels
- B. Decreased ubiquitination and degradation of AMPKα1 by MAGE-A3/6-TRIM28 knockdown elevates other AMPK holoenzyme complex subunits

U2OS cells were plated and transfected with indicated siRNA 24 hrs later. 72 hrs post transfection cells were collected in sample loading buffer at 65 °C and analyzed by western blot.

other components of the AMPK complex also changed in their abundance (Figure 3-3B). This was encouraging because levels of the AMPK complex are known to be co-regulated and increase of one subunit can lead to gains in other components (Dyck et al., 1996).

The converse experiment, in which MAGE-A3 was overexpressed in a MAGE-negative cell line, was also able to reduce the overall levels of AMPK (Figure 3-2B). Once I determined that AMPK stability was being affected by MAGE-A3, I wanted to confirm that this was a consequence of proteasomal degradation. I treated the HEK293 MAGE-A3 cells with the proteasome inhibitor MG132. Inhibition of the proteasome was able to robustly rescue the levels of AMPK equal to that of control cells (Figure 3-4). These findings together suggested that expression of MAGE-A3/6 is necessary and sufficient to drive the ubiquitylation of AMPK α 1 by TRIM28 and target it for proteasomal degradation.

MAGE-A3/6 Inhibits AMPK Activity

While the increases observed in AMPK protein levels with MAGE-A3/6-TRIM28 knockdown were dramatic, the possibility remained that a change in abundance may not translate to an increase in AMPK activity, and thus negate the importance of this finding. In order to address this problem I first probed the levels of phosphorylated AMPK in both HeLa and U2OS following knockdown of my ligase complex. When this was done, a dramatic increase in P-AMPK was found, suggesting more active complex (Figure 3-5). I next confirmed the presence of increased AMPK signaling by assaying the phosphorylation of the direct substrate ACC1. As expected, when MAGE-A3/6-TRIM28 was knocked down, phosphorylation of ACC1 was augmented (Figure 3-6).

MAGE-A3/6 Is a Substrate Adapter

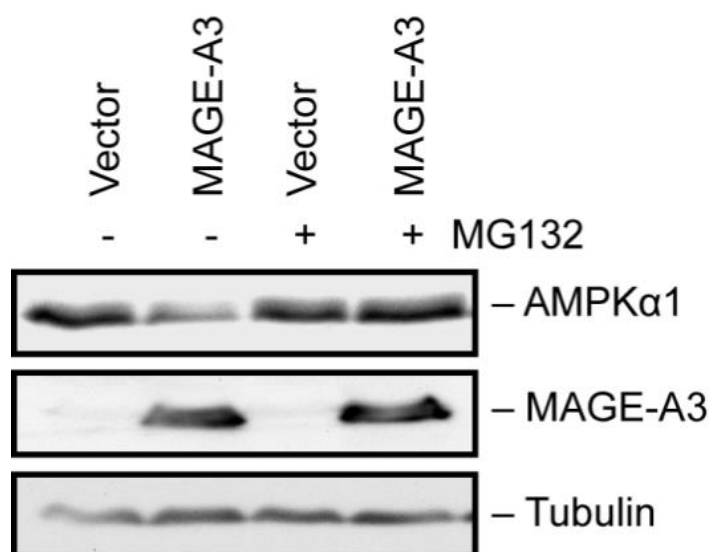


Figure 3-4 AMPK α 1 is Degraded by the Proteasome

MAGE-A3 promotes proteasome-dependent AMPK α 1 degradation. HEK293 MAGE-A3 cells were plated and 72 hr later treated with either 5 μ M MG132 or DMSO. 4 hr post treatment cells were collected in sample loading buffer and analyzed by western blot

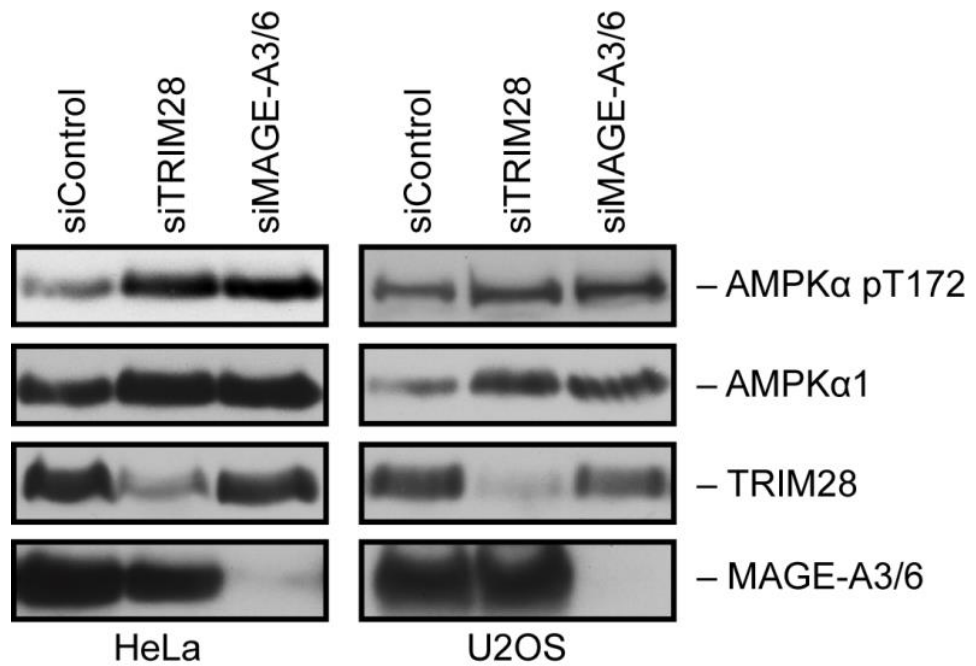


Figure 3-5 MAGE-A3/6 Knockdown Increases Active AMPK

MAGE-A3/6-TRIM28 knockdown increases total and phospho-AMPK in both HeLa and U2OS. Cells were plated and transfected with the indicated siRNA 24 hrs later. 72 hrs post transfection cells were collected in sample loading buffer at 65 °C and analyzed by western blot.

After I had determined that AMPK abundance and activity was being controlled by TRIM28, I next wanted to determine how MAGE-A3/6 was able to induce the ubiquitination of AMPK. I had several hypotheses explaining how MAGE-A3/6 may function with TRIM28 and studies of other MAGEs have suggested that MAGEs may affect E2/E3 binding, enhance the discharge of ubiquitin onto target proteins, or that MAGEs may act as substrate adapters.

In order to test if MAGE-A3/6 is simply enhancing an already existing MAGE-independent activity of TRIM28, I knocked down TRIM28 in MAGE-negative cell lines. I did not observe any change in AMPK α 1 protein levels, likely ruling out an existing TRIM28 activity (Figure 3-7). Next, I elected to test the hypothesis that MAGE-A3/6 is acting as a substrate adapter for TRIM28 and bringing AMPK as a novel substrate. My first experiment was to test if AMPK was able to pull down MAGE-A3 in cells. Indeed, when myc-AMPK α 1 was immunoprecipitated, it was able to bring down FLAG-MAGE-A3 (Figure 3-8A). In a more stringent reciprocal experiment, FLAG-MAGE-A3 was able to pull down endogenous AMPK α 1 (Figure 3-8B). These experiments in cells demonstrate that MAGE-A3/6 and AMPK α 1 are able to bind within the same complex.

Once I had confirmed that MAGE-A3 and AMPK were binding in the same complex, I was interested in determining if MAGE-A3/6 may be directly binding to AMPK. In order to do this, I purified GST-TRIM28 RBCC, GST-MAGE-A3, GST-MAGE-A6 and in vitro translated the AMPK α 1 subunit. When I test AMPK α 1's ability to bind TRIM28 or MAGEs independently, in

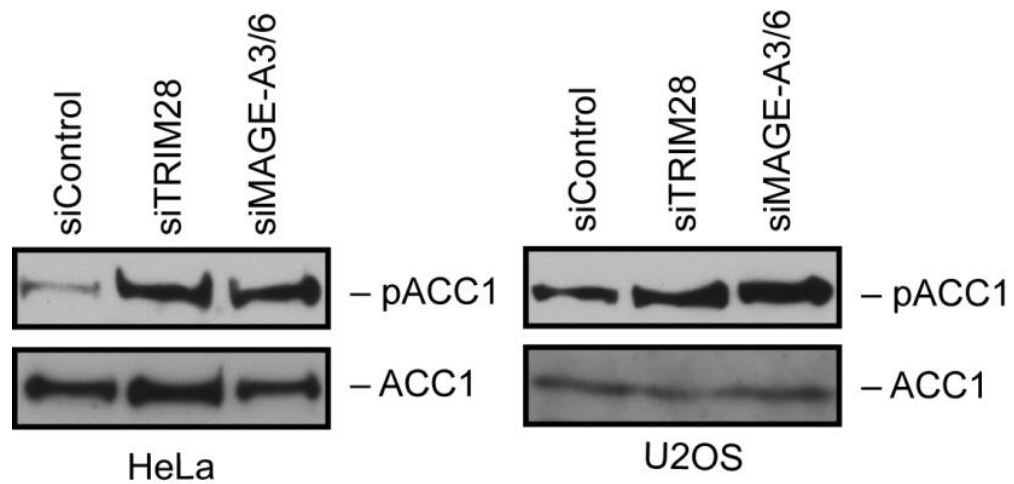


Figure 3-6 MAGE-A3/6 Increases AMPK Activity

MAGE-A3/6-TRIM28 knockdown increases phospho-ACC1 signaling in both HeLa and U2OS cells. Cells were plated and transfected with indicated siRNA 24 hrs later. 72 hrs post transfection cells were collected in sample loading buffer at 65 °C and analyzed by western blot.

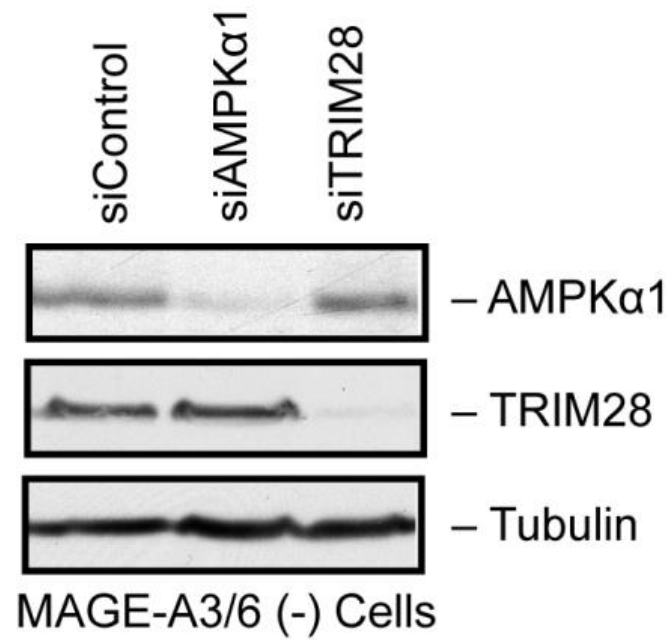


Figure 3-7 AMPKα1 is not Regulated in MAGE (-) Cell Lines

Depletion of TRIM28 has no effect in MAGE negative HEK293 cells. HEK293 cells were plated and transfected with indicated siRNA 24 hrs later. 72 hrs post transfection cells were collected in sample loading buffer at 65 °C and analyzed by western blot.

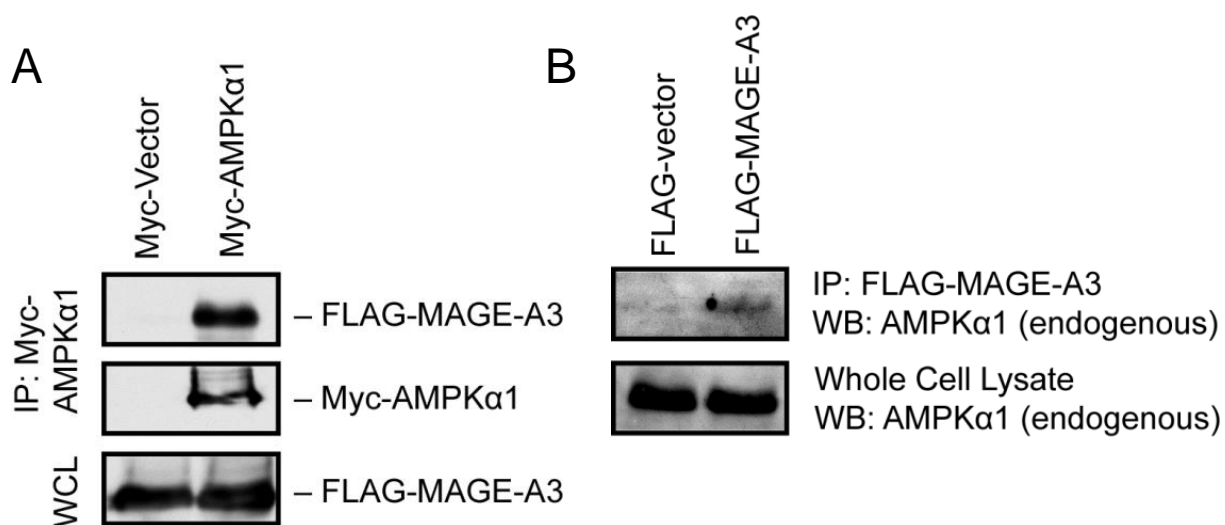


Figure 3-8 MAGE-A3 Binds to AMPK α 1 in Cells

- A. AMPK binds MAGE-A3 in cells.
 B. MAGE-A3 binds endogenous AMPK α 1 in cells.

HeLa cells were plated and 24 hrs later double (A) or single (B) transfected using Effectine. 48 hrs post transfection cells were myc (A) or FLAG (B) immunoprecipitated. IPs were eluted in sample loading buffer and analyzed by western blot

vitro, I found that TRIM28 was completely unable to bind to the catalytic subunit of AMPK (Figure 3-9A). Contrasting this result, both of the closely related MAGE-A3 and MAGE-A6 were able to bind to AMPK α 1 alone or in trimeric complex (Figure 3-9B).

These findings were particularly interesting because previous experiments looking at the ability of MAGE-C2-TRIM28 to degrade p53 demonstrated that MAGE-C2 does not bind p53 and instead enhances activity of the ligase, possibly through E2 recruitment. This finding therefore uncovers a new mechanism by which MAGEs are able to alter E3 specificity for a given substrate.

MAGE-A3/6 Controls AMPK in Clinical Samples

While the changes in AMPK level due to MAGE-A3/6 expression were easily observed in cell lines, I wanted to determine if these changes were applicable to patients in the clinic. In order to test this I utilized The Cancer Genome Atlas (TCGA) data set. In addition to the genomic information available with this database, subsets of samples have been analyzed using a reverse phase protein array (RPPA). This method of array protein analysis works in much the same way as a dot blot, and has been used to measure a variety of common signaling pathways in TCGA tumors (Li et al., 2013). When the TCGA expression data was segregated based on MAGE-A3/6 expression, a striking pattern was observed. Tumors in which MAGE-A3/6 was expressed had a significant reduction in the levels of both AMPK α 1 and phospho-AMPK (Figure 3-10). At the same time there was not any appreciable difference in the mRNA levels of AMPK α 1. This change was observed in patients with colorectal carcinoma, lung adenocarcinoma, and breast invasive carcinoma and it greatly supported the notion that the regulation of AMPK by MAGE-A3/6-TRIM28 could play a crucial role in the development and progression of cancer.

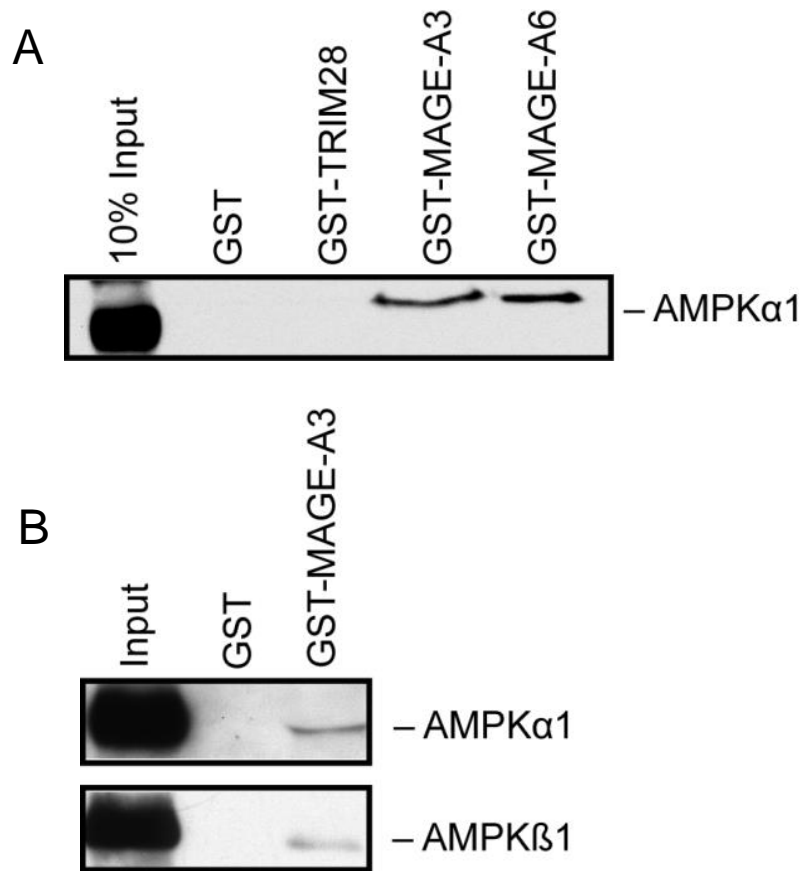


Figure 3-9 MAGE-A3/6 Binds Directly to AMPK

- A. GST pull-down assay reveals AMPK α 1 binds directly to MAGE-A3 and MAGE-A6 but not TRIM28.
- B. GST pulldown assay reveal purified, recombinant AMPK α 1 β 1 γ 1 holoenzyme binds to GST-MAGE-A3 but not GST alone.

GST tagged proteins were bound to glutathione sepharose beads in TBST and then blocked in 5% milk/TBST. In vitro translated myc-AMPK α 1 or recombinant AMPK complex were then incubated for 2hrs, washed and eluted with sample loading buffer.

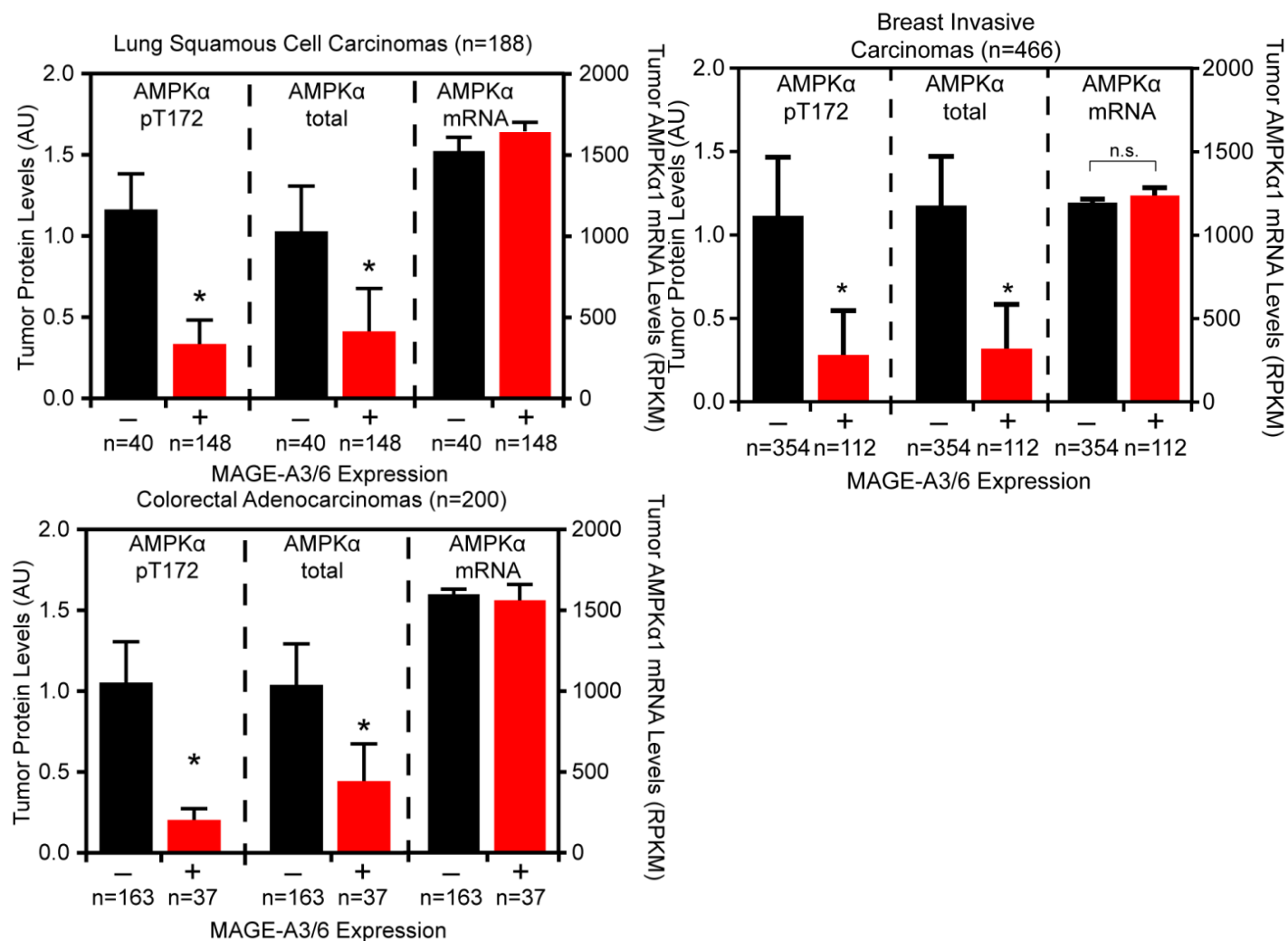


Figure 3-10 MAGE-A3/6 Correlates with reduced AMPK Protein in Patients

TCGA data were analyzed for MAGE-A3/6 mRNA levels and total and active (pT172) AMPK protein levels. Data are mean \pm SE with (n) of tumors indicated. Asterix indicate p < 0.01 determined by Students t-test. A) Lung Squamous Cell Carcinoma B) Breast Invasive Carcinoma C) Colorectal Adenocarcinoma

The TCGA data set provided genetic evidence that AMPK regulation may be the key role of MAGE-A3/6 in cancer. While p53 mutation status does not segregate based on MAGE-A3/6 expression status, when STK11 (LKB1) and MAGE-A3/6 expression were compared, it was clear that its mutation was enriched in MAGE-negative tumors (Figure 3-11). This suggested that STK11 mutation and MAGE expression may be redundant and dual mutation/expression does not confer an advantage onto tumor cells.

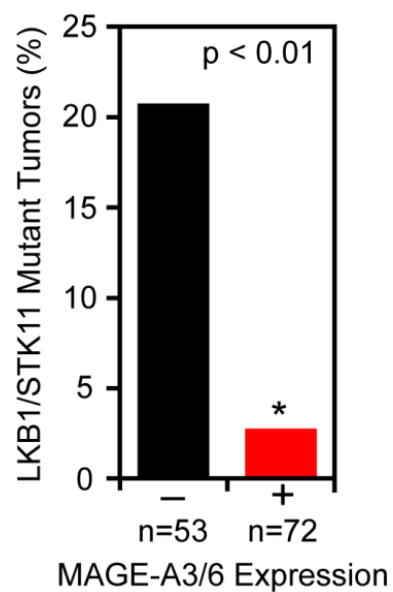


Figure 3-11 MAGE-A3/6 Expression Anti-Correlates with LKB1 Mutation

LKB1/STK11 mutation and MAGE-A3/6 expression are infrequently found in the same tumor. Mutational and RNA-seq data from TCGA were analyzed for MAGE-A3/6 expression and LKB1/STK11 mutation correlation. Number (n) of tumors analyzed is shown. Asterisks indicates $p < 0.01$ determined by students t-test.

Chapter IV: MAGE-A-TRIM28 Regulates mTOR Signaling and Autophagy

mTOR

Once I had found that MAGE-A3/6 was having a critical impact on AMPK signaling, I wanted to investigate what effects MAGE-A3/6 was having downstream of AMPK signaling. One key signaling pathway that is regulated by AMPK and has been implicated in cancer is the mechanistic target of rapamycin (mTOR). mTOR is a kinase that belongs to the PI3K related kinase family and interacts with large protein complexes, mTORC1 and mTORC2, in order to determine its function (Laplante and Sabatini, 2012b). mTORC1 is responsible for many of the functions attributed to mTOR and this complex is defined by the presence of Raptor, which is a scaffolding protein that regulates the binding of substrates. This protein also defines mTORC1 sensitivity to the inhibitors rapamycin and its analogues (Laplante and Sabatini, 2012b). Phosphorylation of Raptor is one way that AMPK is able to inhibit mTORC1 activity (Gwinn et al., 2008).

In addition to being part of a multi protein complex, mTOR is regulated by the interplay of multiple G proteins and their associated GEFs and GAPs (Laplante and Sabatini, 2012a). One of these G proteins is Rheb, which when bound by GTP, activates mTORC1. In order to turn this signaling off, the GAPs for Rheb are TSC1 and TSC2 (Laplante and Sabatini, 2012b). These two GAPs are also another point at which AMPK is able to regulate mTOR activity. When AMPK phosphorylates TSC1/2, it has the net effect of increasing GAP activity and reducing mTOR signaling within the cell (Inoki et al., 2003).

Much like the role of AMPK within the cell, mTOR functions to sense nutrients and adjust cellular processes accordingly, but in contrast to AMPK, mTOR functions to promote energy

usage and synthesis of new cellular components (Laplante and Sabatini, 2012b). For example, a key role of mTOR is to monitor amino acid levels within the cell. This is accomplished by a complex interplay of proteins, such as the G proteins RAG A/B, Rag C/D and the GEF, Ragulator, which reside on the surface of the lysosome (Bar-Peled et al., 2012; Sancak et al., 2010). When amino acids are released from the lysosome surface, mTORC1 is recruited to the lysosome by RAGs and this increases its ability to associate with Rheb (Bar-Peled et al., 2012; Sancak et al., 2010).

After mTORC1 has been activated by its complicated interplay of GTPases, it signals several downstream pathways, which have the ability to promote cell growth, cell cycle progression, translation of proteins, and synthesis of lipids. Many of the effects of mTOR, such as protein and lipid synthesis are transmitted through the phosphorylation and activation of the downstream enzyme S6 kinase (Laplante and Sabatini, 2012b). In protein translation, S6K activates the ribosomal protein S6, promoting translation.

MAGE-A Controls S6K Signaling

Because S6K is one of the most well characterized substrates of mTORC1, I first set out to determine if MAGE-A3/6 had an effect on S6K signaling. I first knocked down either MAGE-A3/6 or TRIM28 in two different MAGE-positive cell lines, HeLa and U2OS and after 72 hours lysates were collected and analyzed for the activation of S6K. Upon MAGE-A or TRIM28 knockdown, the static levels of phosphorylated S6K within the cell were greatly reduced, and there was no change in the total protein levels (Figure 4-1A). I next checked the downstream target of S6K, ribosomal protein S6. Again, in a dramatic fashion, the phosphorylated form of S6 was greatly reduced without any corresponding change to S6 protein levels. (Figure 4-1A) Both

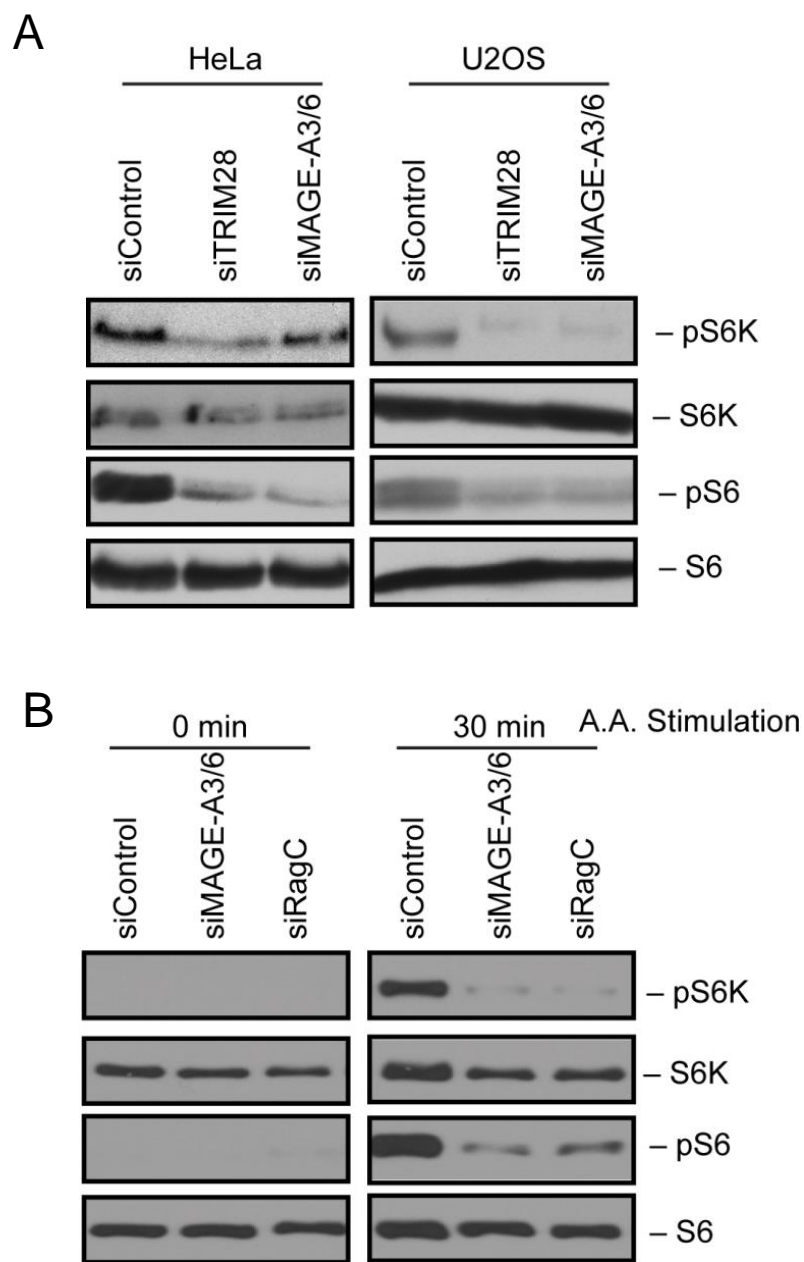


Figure 4-1 MAGE-A3/6 Is Required for mTOR Signaling

- A. MAGE-A3/6-TRIM28 depletion abrogates mTOR signaling.
- B. MAGE-A3/6 is required for mTOR response to amino acid stimulation.

Cells were plated and transfected with indicated siRNA 24 hr later. 72 hr post transfection cells were collected in sample loading buffer at 65 °C and analyzed by western blot (A). Additionally, cells in B were starved in EBSS and then refed with amino acids for 30 min.

of these results gave clear evidence that MAGE-A3/6-TRIM28 promotes mTOR signaling and I next wanted to investigate how MAGE-A3/6 could be impacting the mTOR response to amino acid stimulation. In this experiment, I used HeLa cells to test amino acid response. Samples collected at time 0 had been starved of amino acids, while another group was re-fed with amino acids for 30 minutes. I observed that knockdown of MAGE-A3/6 completely blocked the cells' ability to dynamically respond to amino acid stimulation (Figure 4-1B). In the cases of both S6K and S6, phosphorylation was blocked by the depletion of MAGE-A3/6. While I suspected that MAGE-A3/6 may have an effect on this process, the level of response was surprising because the defect in signaling was equivalent to depletion of Rag C, one of the G proteins required for amino acid sensing (Figure 4-1B). This study suggested that when expressed in cancer, MAGE-A3/6 is required for mTOR signaling and response to amino acid stimulation.

While the changes induced by knockdown of MAGE-A3/6 were consistent with an AMPK based effect, I sought concrete evidence that changes in mTOR signaling were a consequence of MAGE-A3/6-induced degradation of AMPK. In order to investigate if AMPK was involved, I performed two experiments in which AMPK activity is reduced after MAGE-A3/6 knockdown. First, I used the small molecule AMPK inhibitor, compound C, to block AMPK activity. This block in AMPK activity was demonstrated by the abolishment of phosphorylated AMPK and restored S6 phosphorylation baseline (Figure 4-2A). Because of the high chance of off-target effects with a small molecule, I also blocked AMPK by addition of a second siRNA directed towards AMPK α 1. Exactly like the previous experiment, this returned S6 phosphorylation to normal (Figure 4-2B). Overall these data suggest that, when MAGE-A3/6 is expressed, the resulting reduction in AMPK has the dramatic effect of causing a robust activation of mTOR.

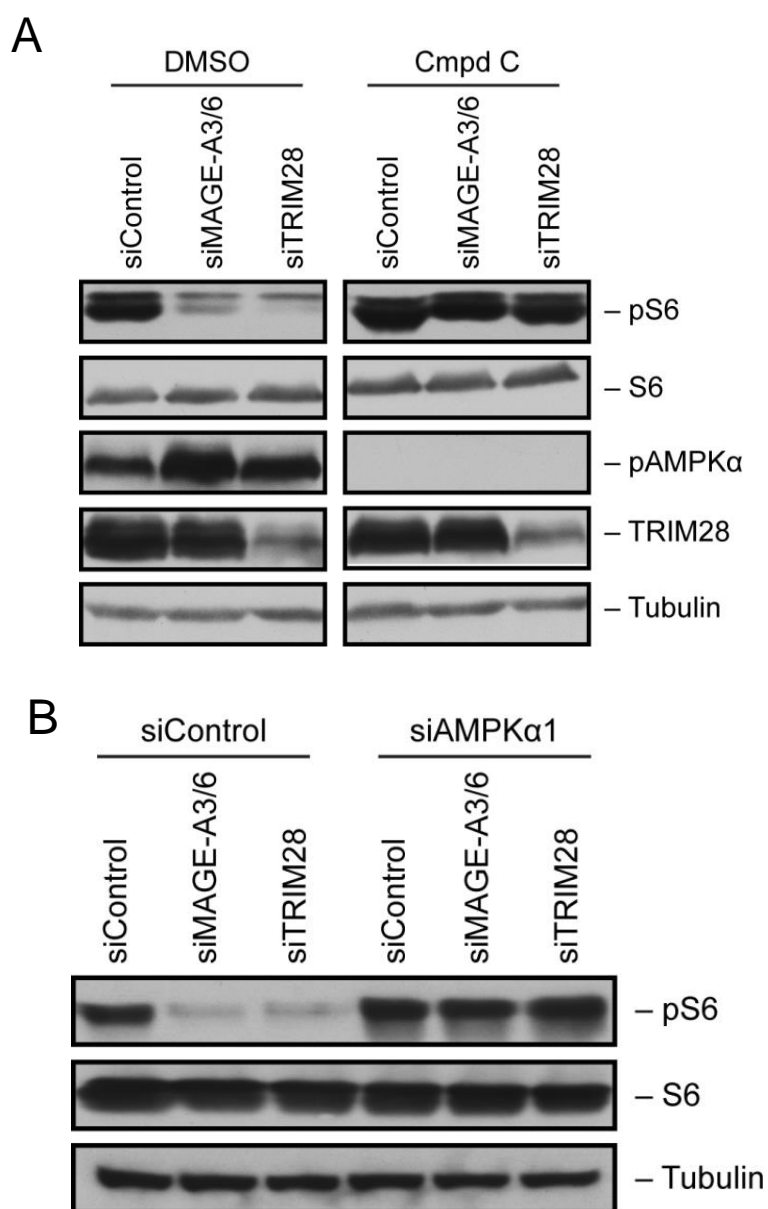


Figure 4-2 MAGE-A3/6 Controls mTOR via AMPK

- Inhibition of AMPK removes the requirement of MAGE-A3/6-TRIM28 for mTOR signaling.
- Co-depletion of AMPK α 1 rescues mTOR signaling with MAGE-A3/6-TRIM28 knockdown.

HeLa were plated and transfected with indicated siRNA 24 hrs later. 72 hrs post transfection cells were collected in sample loading buffer at 65 °C and analyzed by western blot. Cells were treated with compound C for 4 hrs prior to collection.

MAGE-A3/6 Promotes mTOR In Clinical Samples

Aware of the potential implications of my findings that MAGE-A3/6 regulates mTOR signaling *in vitro*, I wanted to determine if these findings would translate to the context of signaling within actual human tumors. When the RPPA data was again analyzed, I observed that in lung squamous cell carcinoma, MAGE-A3/6 expression correlated with a dramatic increase in phosphorylated S6 levels. At the same time there was no appreciable difference between total S6 protein levels in these two groups and these data suggest that MAGE-A3/6-dependent enhancement of mTOR signaling is relevant clinically (Figure 4-3).

Autophagy

After I had determined that MAGE-A3/6-TRIM28 has a dramatic effect on both AMPK and mTOR signaling, I next wanted to look at a pathway which integrates these two signals and one process that fits this description is the cellular process of autophagy. Autophagy, which literally means “self-eating”, is a dynamic process in which cellular components are packaged into double membrane vesicles known as autophagosomes (Klionsky et al., 2011). Autophagosomes are then trafficked to the lysosome where the contents are degraded and recycled. This process serves several different functions within the cell. The classical role of autophagy is to aid in the cells’ adaptation to nutrient stress (Choi et al., 2013). When cells are depleted of nutrients such as amino acids, old proteins or organelles are broken down and their building blocks are recycled back into the cell. This allows the cell to survive in conditions in which nutrients are suboptimal. In other contexts, autophagy can protect a cell from viral or bacterial infections (Choi et al., 2013). When a cell is infected, it may upregulate autophagy as a method of destroying the foreign object. Finally, this process is known to have a complicated interplay

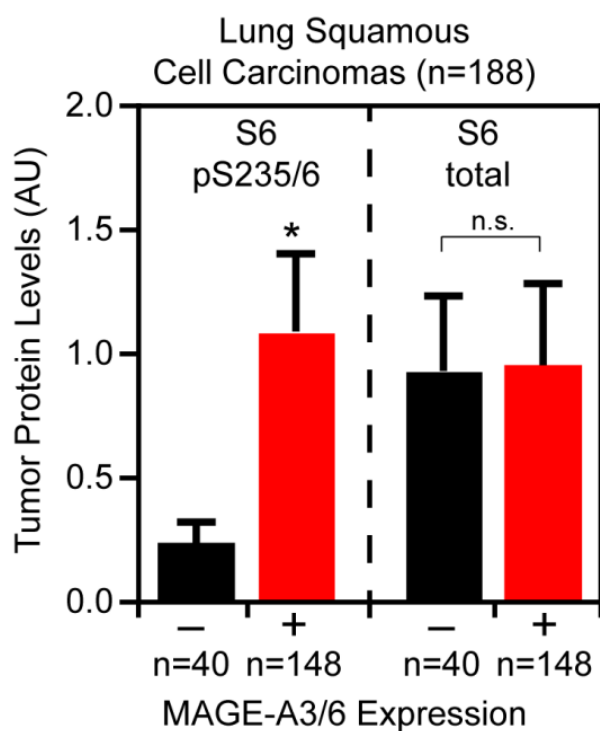


Figure 4-3 MAGE-A3/6 Expression Correlates with Increased mTOR Signaling in Tumors

RPPA analysis of human lung squamous cell carcinoma tumors expressing MAGE-A3/6 shows increased phosphorylated ribosomal S6 (pS235/S236) protein levels, consistent with increased mTOR activity. Data are mean + SE with number (n) of tumors. Asterisks indicate $p < 0.01$ determined by students t-test.

with the development and progression of cancer (White, 2012). Studies, such as autophagy gene knockouts, have shown that autophagy is tumor suppressive in the early stages of neoplastic development (Qu et al., 2003; Yue et al., 2003). It is believed, that in these early stages of cancer development autophagy is used to clear accumulating cellular damage, such as old proteins or damaged mitochondria (White, 2012). This housekeeping mechanism prevents the expansion of errors within a cell and supports normal tissue homeostasis. If this mechanism is lost, the gradual accrual of damage increases pro-tumorigenic factors such as DNA damage and increased inflammatory signaling within a tissue. There are also several contexts in which autophagy acts as a tumor promoter. For example, tumors often maintain an increase autophagy in order to cope with increased energy demands and survive in hypoxic conditions (Degenhardt et al., 2006; Rabinowitz and White, 2010)

MAGE-A3/6-TRIM28 Regulates Autophagy

While there are several nodes where AMPK and mTOR intersect with autophagy, the first protein that I examined was the upstream kinase that controls autophagy, Unc 51 like kinase 1 (ULK1) (Klionsky et al., 2011). AMPK and mTOR both phosphorylate ULK1 on serine residues, and these modifications have opposing effects (Kim et al., 2011). AMPK activates ULK1 with modification of serine 555 while mTOR blocks its function with a phosphorylation at serine 757 (Kim et al., 2011). In order to test if changes in MAGE-A3/6-TRIM28 would have an effect on ULK1 activation, I again used the cancer cell lines HeLa and U2OS.

When MAGE-A3/6 or TRIM28 were knocked down, I found that there was an increase in phosphorylation of ULK1 S555, the activating AMPK modification, and this was consistent with the previously found increase in AMPK (Figure 4-4). Additionally, corresponding with reduced

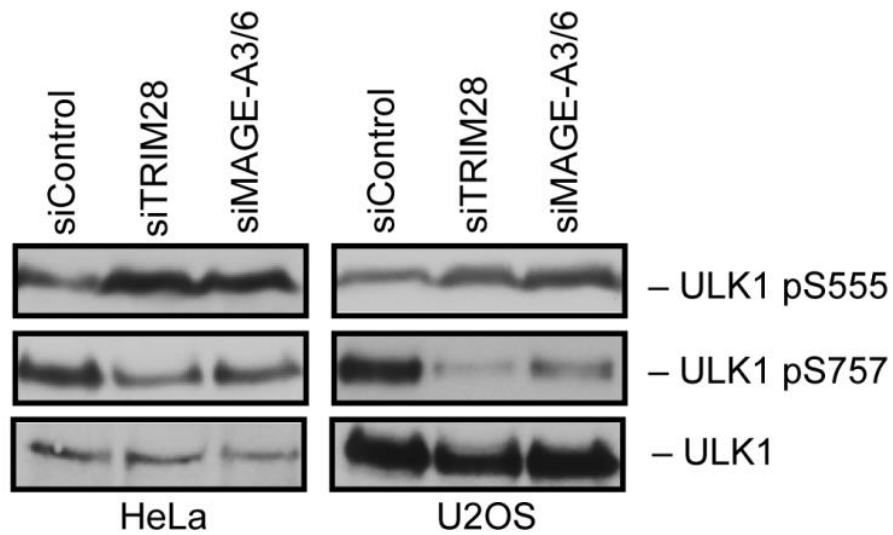


Figure 4-4 Knockdown of MAGE-A3/6-TRIM28 Increases ULK1 Activity

HeLa or U2OS show altered ULK1 phosphorylation with MAGE-A3/6-TRIM28 depletion. Cells were plated and transfected with indicated siRNA 24 hrs later. 72 hrs post transfection cells were collected in sample loading buffer at 65 °C and analyzed by western blot.

mTOR activity, ULK1 S757 exhibited reduced phosphorylation in the absence of MAGE-A3/6 (Figure 4-4). These results were exciting because the observed changes in ULK1 S555 and S757 phosphorylation would both suggest that ULK1 would be more active and that there may be an increase in autophagy when MAGE-A3/6 was depleted.

Once I had evidence that signaling changes caused by MAGE-A3/6 knockdown could alter ULK1 signaling, I wanted to directly assay the level and progression of autophagy. In order to do this, I acquired both HeLa and U2OS cells that stably express the transgene of GFP fused to the protein LC3 (Mizushima et al., 2010). During the process of autophagy, cytoplasmic LC3 (LC3-I) becomes conjugated to phosphatidylethanolamine (PE), and the product (LC3-II) resides on the nascent autophagosome membrane (Klionsky et al., 2011). When this process is tracked by the GFP-LC3 fusion product, a diffuse cytoplasmic GFP signal converts into distinct puncta that can be visualized by microscopy, the number of which indicates the level of autophagy (Mizushima et al., 2010).

The first set of experiments that I performed was to count the number of GFP-LC3 puncta in both the HeLa and U2OS cell lines. When I knocked down MAGE-A3/6 or TRIM28 there was a dramatic increase in the number of puncta in both HeLa and U2OS cells. In U2OS cells, when mTOR was knocked down, the resulting increase in puncta was about equal to MAGE-A3/6-TRIM28 knockdown (Figure 4-5A). This was striking because mTOR depletion is a classical method to induce autophagy and our results indicated that induction of autophagy was robust with knockdown of MAGE-A3/6-TRIM28. In order to help confirm that the puncta I observed were indeed autophagosomes, I co-depleted ULK1 in U2OS and again looked at puncta number. When ULK1 was depleted, the puncta formation was completely abrogated, consistent with autophagosomes (Figure 4-5B). While the general trend between the two cell lines was

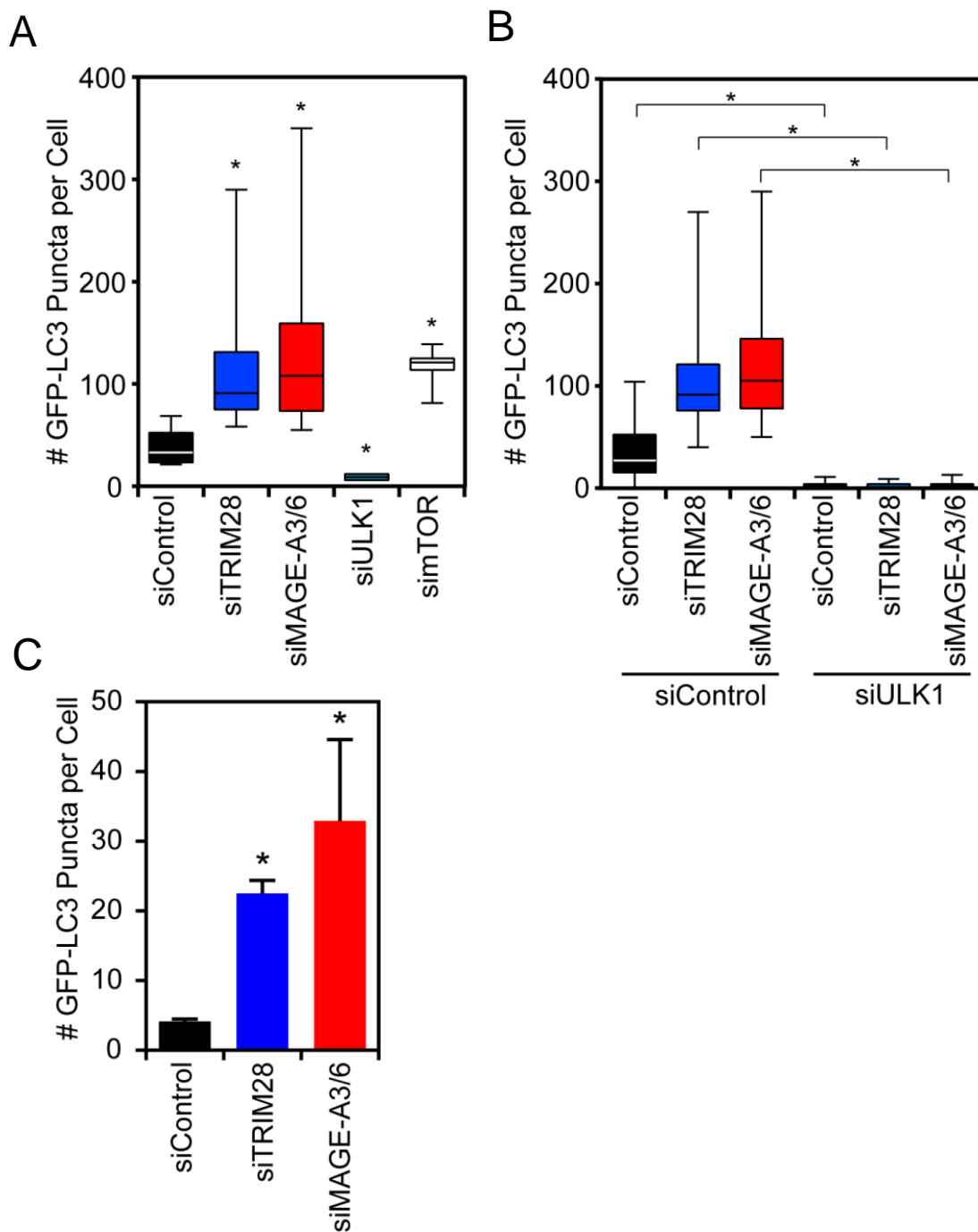


Figure 4-5 Knockdown of MAGE-A3/6-TRIM28 Increases GFP-LC3 Puncta

- A. MAGE-A3/6-TRIM28 knockdown increases GFP-LC3 puncta in U2OS
- B. ULK1 depletion blocks GFP-LC3 puncta formation
- C. MAGE-A3/6-TRIM28 knockdown increases GFP-LC3 puncta in HeLa.

Cells were plated and transfected with indicated siRNA 24 hrs later. 72 hrs post transfection cells were fixed in 4% PFA and permeabilized with saponin. Samples were then imaged and 100 cells counted per condition. Asterisks indicate $p \leq .05$ determined by students t-test.

consistent, there was an interesting dichotomy between the numbers of puncta the cells produced. In U2OS, there was several dozen puncta and upon knockdown this number increased to several hundred. In contrast, HeLa cells had on average less than ten puncta, which increased to 40-50 puncta (Figure 4-5C).

After I had assayed puncta using the GFP-LC3 transgene, I decided to investigate the number of endogenous LC3 puncta in other cell lines. In both MAGE-positive cell lines, HTB126 and HCT116, knockdown of MAGE-A3/6 increased the number of LC3 puncta, confirming our results with GFP-LC3 (Figure 4-6). In contrast, the non-cancer MAGE-negative cell line HBEC had no change in puncta number when treated with MAGE-A3/6 siRNA, indicating that the effects of my siRNA were on target. Additionally, all cell lines had a decrease in puncta number when ULK1 was depleted (Figure 4-6).

Next, I wanted to again confirm that the changes in autophagy seen were due to the increased AMPK signaling when MAGE-A3/6-TRIM28 was knocked down. As I had previously done, I knocked down MAGE-A3/6 and I treated cells with compound C to block the activity of AMPK. When I did this, the dramatic increase in the number of GFP-LC3 puncta that were observed was reduced back to baseline (Figure 4-7). These results indicated that MAGE-A3/6-TRIM28 was regulating autophagy through the modulation of AMPK.

MAGE-A3/6-TRIM28 Inhibits Autophagic Flux

While the changes that I observed in both ULK1 signaling and LC3 puncta number suggested that there was an increase in autophagy when MAGE-A3/6-TRIM28 was knocked down, there are instances in which an increase in the number of LC3 puncta could indicate a reduction in autophagy. This is because, if there is a block in the final steps of autophagy, such

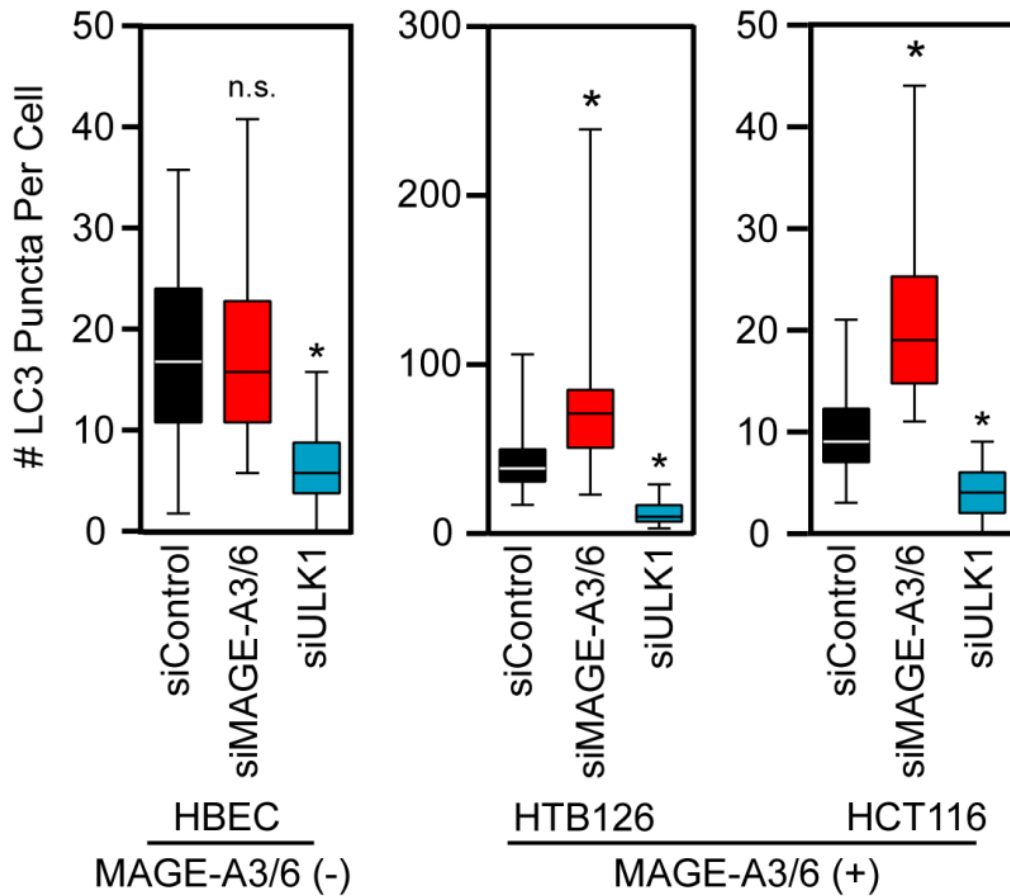


Figure 4-6 Knockdown of MAGE-A3/6 Increases LC3 Puncta

Cells were plated and transfected with indicated siRNA 24 hrs later. 72 hrs post transfection cells were fixed in 4% PFA and permeabilized with digitonin and stained with α -LC3. Cells were then imaged and 100 cells counted per condition.

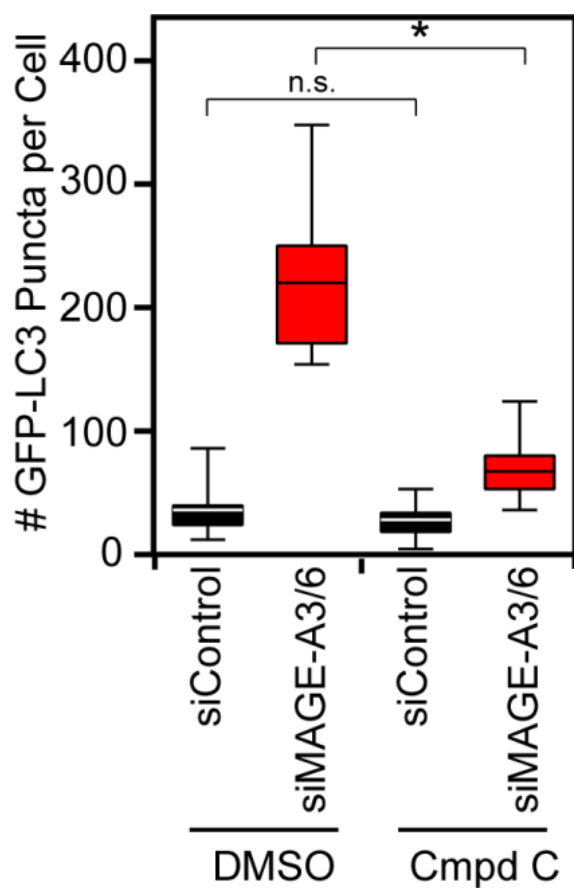


Figure 4-7 Compound C Inhibits GFP-LC3 Puncta Formation

U2OS GFP-LC3 cells were plated and transfected with indicated siRNA 24 hrs later. 72 hrs post transfection cells treated with compound C for 4 hrs. Samples were then fixed in 4% PFA and permeabilized with saponin. Samples were then imaged and 100 cells counted per condition. Data plotted with box-plots indicating mean and quartiles. Asterisks indicate $p \leq .05$ determined by students t-test.

as in lysosomal fusion or degradation, the outcome would also appear to generate more LC3 puncta. In order to address this, I used several methods to measure the consumption of GFP-LC3 in both U2OS and HeLa cell lines. The first method that I employed was flow cytometry. In this experiment, as autophagy progresses GFP-LC3 protein will be consumed when the autophagosome fuses with the lysosome and the resulting loss of fluorescence can be measured by a flow cytometer (Potts et al., 2013).

First, I investigated if measuring the GFP-LC3 transgenic protein expression by flow cytometry was robustly reporting autophagy. When mTOR was knocked down in U2OS cells, there was a clear decrease in fluorescence intensity, indicating the expected increase in autophagy. Conversely, when ULK1 was depleted, there was an accumulation of GFP signaling indicative of a block in autophagy (Figure 4-8B). When MAGE-A3/6 or TRIM28 was knocked down, in U2OS or HeLa cells, there was a decrease in GFP-LC3 signal, similar what was observed with mTOR (Figure 4-8B). This suggested that it was very likely that depletion of MAGE-A3/6-TRIM28 complex results in increased autophagy.

While the overall interpretation of the data from both U2OS and HeLa cells suggested that there was an increase in autophagy when MAGE-A3/6-TRIM28 was removed, the flow cytometry data varied considerably between these two cell lines and merits discussion. When the GFP intensity was measured in U2OS, there was a unimodal distribution of intensities within the population that shifted up or down with treatment (Figure 4-8A). While this finding was not surprising, it stood in stark contrast to the fluorescence signature that was exhibited by the HeLa GFP-LC3 cell line. In HeLa, the GFP intensity followed a bi-modal distribution. In this instance, there was a high intensity population and a population with almost no GFP detectable. When these cells were perturbed, the median of these peaks did not move and instead a large portion of

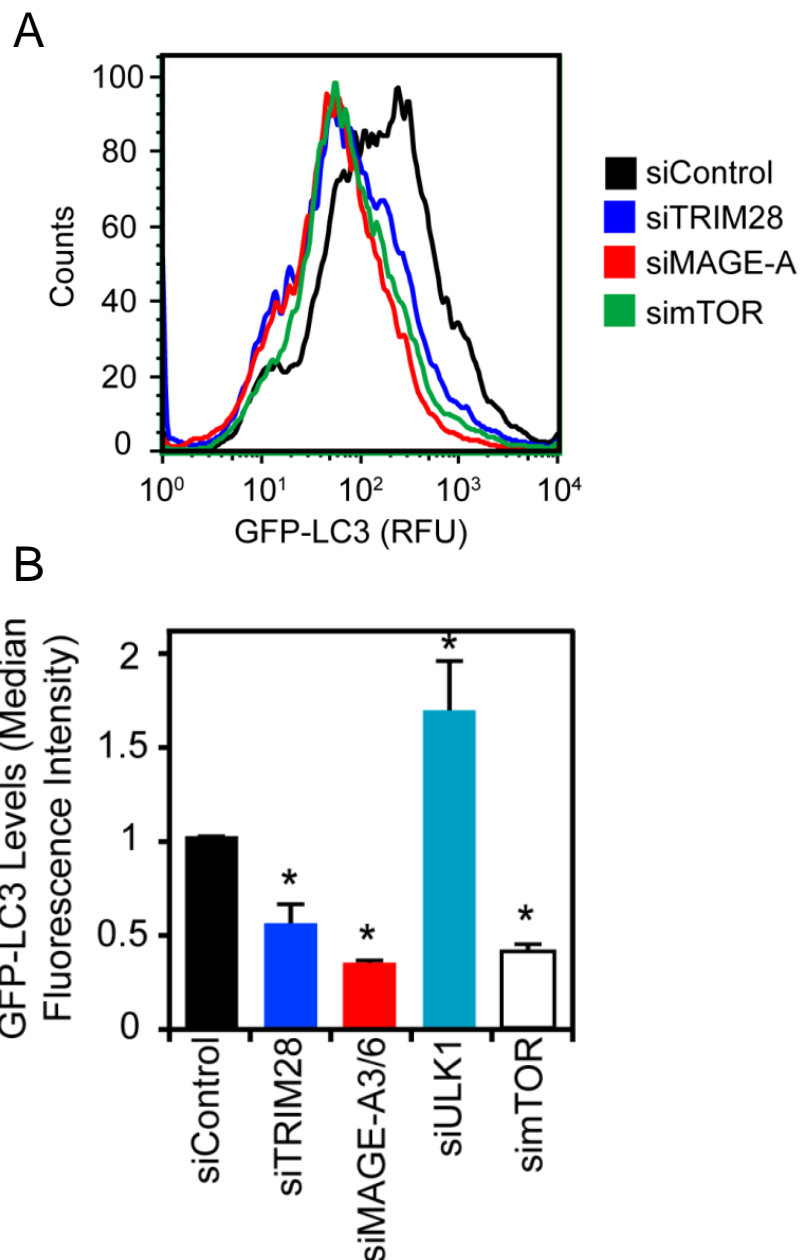


Figure 4-8 MAGE-A3/6 Knockdown Increases GFP-LC3 Consumption

- A. Representative flow cytometry data
 B. Quantification of flow cytometry data. Data is average of median values from 3 experiments. Asterisks indicate $p \leq .05$ determined students t-test.

U2OS GFP-LC3 were plated and transfected as previous experiments. At time of collection cells were trypsinized and resuspended in 2 mL of FACS buffer. 20,000 cells were analyzed for GFP intensity using FACS-SCAN.

the population passed from the high to the low intensity peak. While the data in each cell line showed the same trends, the analysis required was very different between data sets. In U2OS cells, the changes in autophagy were plotted as the shift in median intensity, while in HeLa cells, the changes were plotted as the percentage of the population found in the GFP consumed peak.

While I had strong evidence that knockdown of MAGE-A3/6-TRIM28 increased autophagy, there were caveats to the flow cytometry and puncta data. For example, even the apparent consumption of GFP-LC3, as measured by flow cytometry, is insufficient to definitively show that flux through the autophagy pathway is increased. This is because GFP-LC3 will lose its fluorescence as the autophagosome is acidified and this loss of fluorescence may occur before it is fully degraded by the lysosome. If this was indeed the case, it would constitute a block in autophagy and not an increase. In order to address this problem I turned to western blot analysis of GFP-LC3.

When MAGE-A3/6 or TRIM28 were knocked down, I observed a near complete consumption of GFP-LC3-II (lipidated form) by western blot (Figure 4-9A). Again, the GFP-LC3 reporter was functioning properly because inhibition of autophagy via ULK1 knockdown blocked the formation of LC3-II and there was an accumulation of the unlipidated LC3-I. In order to confirm that the increase in autophagy is full flux, I inhibited the final step in autophagy with the lysosomal inhibitor bafilomycin A1 (Mizushima et al., 2010). When HeLa cells were treated with Baf A1 the consumption of LC3 II was blocked, suggesting that knockdown of MAGE-A3/6 or TRIM28 increases autophagic flux (Figure 4-9B).

Finally, I sought to confirm these data without the use of the GFP-LC3 transgene, and I repeated these experiments, instead monitoring the protein p62 (SQSTM1). This protein is located on the

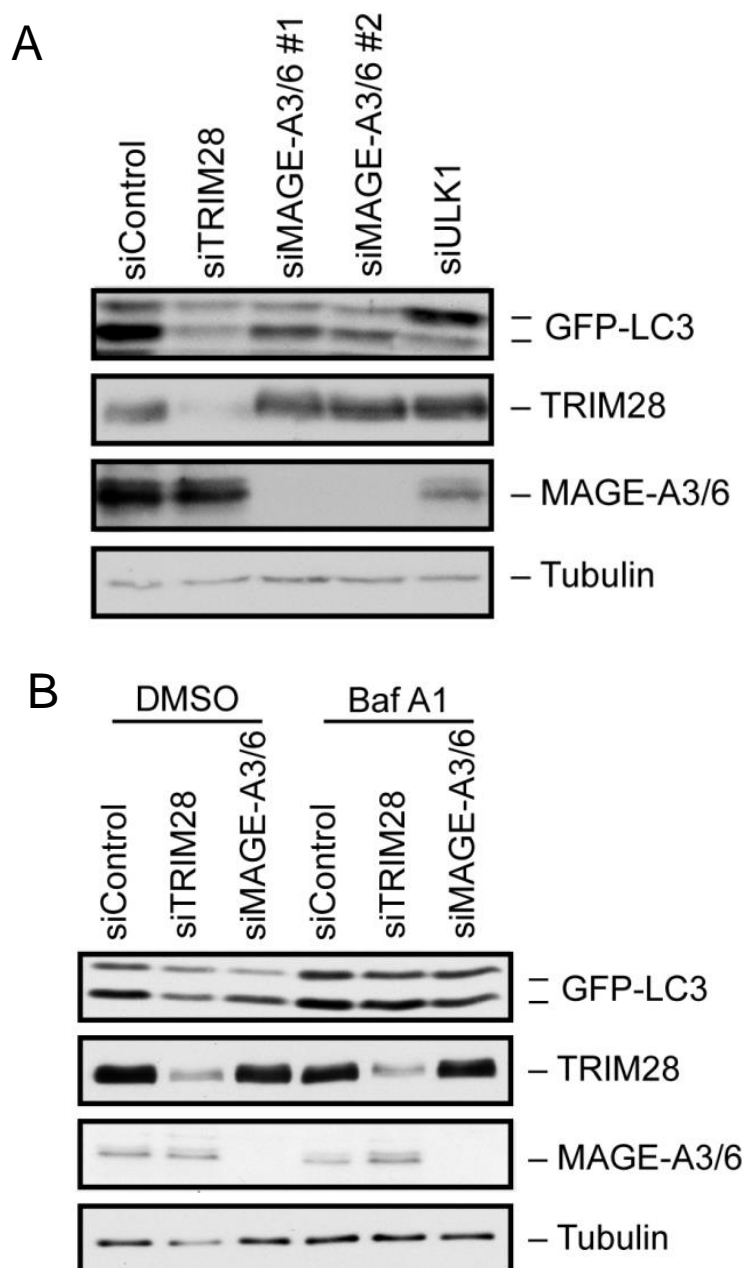


Figure 4-9 Depletion of MAGE-A3/6-TRIM28 Increases Autophagic Flux

- A. Knockdown of MAGE-A3/6-TRIM28 increases GFP-LC3 consumption.
- B. 4 hour treatment of HeLa GFP-LC3 with baf A1 rescues GFP-LC3 consumption.

Cells were plated and transfected with indicated siRNA 24 hrs later. 72 hrs post transfection cells were collected in sample loading buffer at 65 °C and analyzed by western blot.

autophagosomal membrane, is consumed during the process of autophagy, and is used analogously to LC3 (Klionsky et al., 2011). Again, in both HeLa and U2OS cells, the depletion of MAGE-A3/6 or TRIM28 decreased the levels of p62, implying increased consumption (Figure 4-10A). To confirm consumption, I treated cells with Baf A1 to block the final step of autophagy. This rescued the levels of p62, and definitively showed that knockdown of MAGE-A3/6 increases autophagic flux (Figure 4-10C). In order to show that expression of MAGE-A3/6 alone is sufficient to inhibit autophagy, I overexpressed MAGE-A3 in the previously used, MAGE-negative cell line, HBEC. In this cell line expression of MAGE-A3 decreased AMPK α 1 levels and increased p62, and these data solidified the conclusion that MAGE-A3/6-TRIM28 is a potent inhibitor of autophagy (Figure 4-10B).

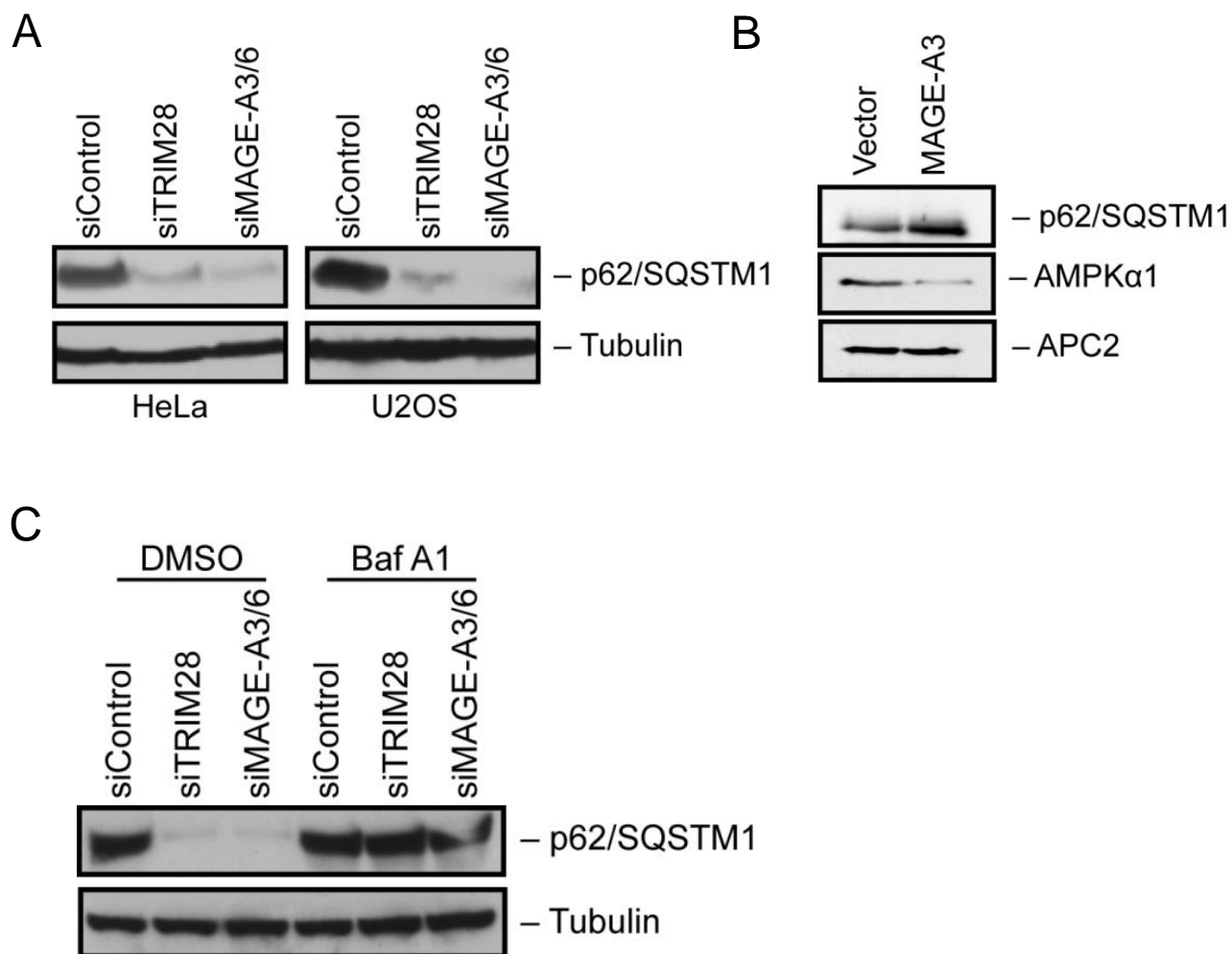


Figure 4-10 MAGE-A3/6 Inhibits Autophagy

- A. Knockdown of MAGE-A3/6-TRIM28 decreases endogenous p62.
 - B. Overexpression of MAGE-A3 in MAGE (-) HBEC cells increases p62 levels.
 - C. Depletion of p62 with MAGE-A3/6-TRIM28 knockdown is rescued by the addition of Baf A1.
- Cells were plated and transfected with indicated siRNA 24 hrs later. 72 hrs post transfection cells were collected in sample loading buffer at 65 °C and analyzed by western blot.

Chapter V: MAGE-A3/6 Functions as an Oncogene Capable of Transforming Normal Cells

Cellular Transformation and Anchorage Independent Growth

Given that MAGE-A3/6 clearly alters cellular signaling of AMPK and mTOR, and the role that autophagy may play in tumorigenesis, I wanted to investigate the idea that MAGE-A3/6 functions as an oncogene through degradation of a tumor suppressor. In order to test this hypothesis, I first wanted to test the ability of MAGE-A3/6 to induce the hallmarks of cancer *in vitro*. The hallmark of cancer that I tested was the ability of cells to avoid programmed death.

Normal cells require attachment to an extracellular matrix in order to generate tension and activate survival signaling through integrins and other pathways. When they are not attached to the extracellular matrix, normal cells will die (Buchheit et al., 2014). During the progression of cancer, including the process of metastasis, neoplastic cells generally acquire the ability to survive independently of substrate attachment. The increased ability of a cancer cell to grow without a substrate can be measured using a technique known as a soft agar assay. In this assay cells are plated onto an agar substrate and they are unable to generate the required attachment.. When cells have acquired increased anchorage independent growth, they are able to form colonies in the soft agar and the number of colonies formed is indicative of a cell's level of transformation.

MAGE-A3/6 Expression Induces Soft Agar Growth

I tested the ability of cells to achieve anchorage independent growth using a soft agar assay. The least stringent condition that I tested began with the established colon cancer cell line DLD1.

DLD1 is MAGE-A-negative and when I stably expressed MAGE-A6 there was increased soft agar growth when compared to vector (Figure 5-1A). While this was interesting, DLD1 is already a cancer cell line, and it is possible that the barrier to inducing anchorage independent growth could be lower due to the complexity of genetic changes and signaling deregulation that could have potentially occurred. In order to increase the stringency of this experiment I changed to a non-cancer cell line. I began using the human colon epithelial cell (HCEC) line. These cells were generated using cells from normal colon biopsies and the cell line was then immortalized in cell culture using the expression of CDK4 and telomerase (hTERT) to bypass senescence checkpoints that would normally be reached in culture. Without modification, these cells will form a very small number of colonies in soft agar, indicating that they have a poor ability to survive without a solid substrate.

I began by using HCEC in which oncogenic K-Ras^{G12V} had been expressed in the background. I did this because while still a more refined system than DLD1 derived cell lines, I feared that MAGE-A6 may not be sufficient to induce soft agar growth without K-Ras^{G12V}. I then assayed the ability of MAGE-A6 to increase soft agar growth and compared these effects to the expression of vector or the known oncogene APC^{min}. When MAGE-A6 was expressed in this background, it again robustly increased soft agar growth and it out performed APC^{min} (Figure 5-1B).

Given MAGE-A3/6's impressive ability to outperform a known oncogene, I again wanted to increase the stringency of my assay. I then decided to directly compare the effect of MAGE-A6 to K-Ras^{G12V} without the aid of another oncogene in the background. Again, expression of MAGE-A6 alone was sufficient to dramatically increase the number of soft agar colonies and

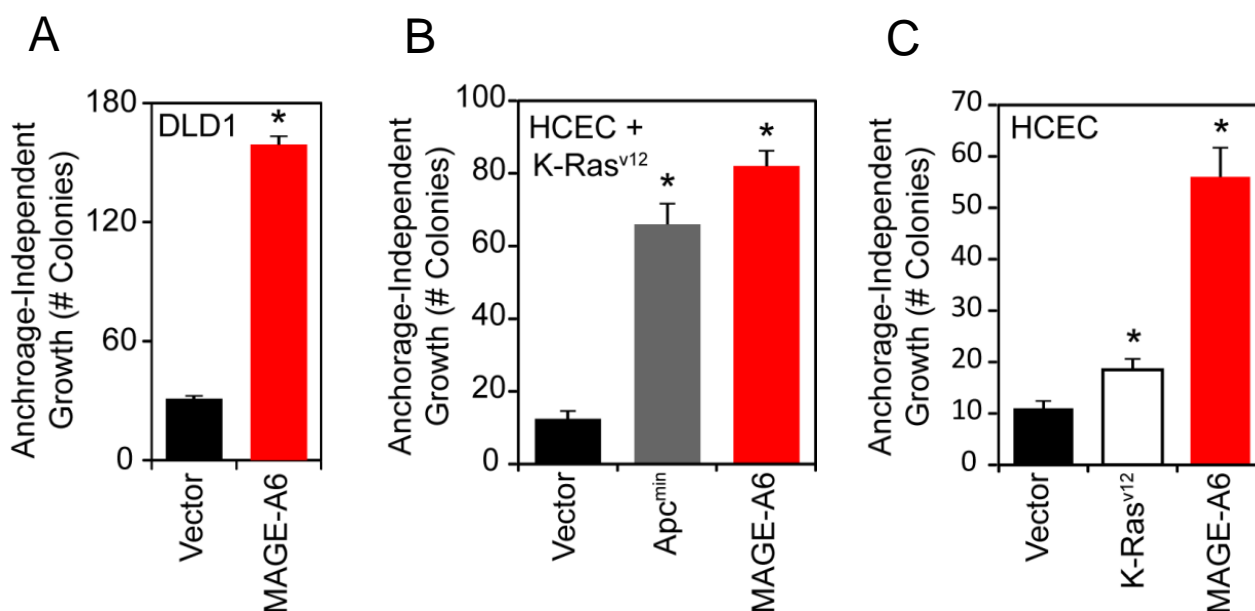


Figure 5-1 MAGE-A6 Increases Soft Agar Growth

- MAGE-A6 promotes anchorage independent growth of DLD1 colon cancer cell lines.
- MAGE-A6 promotes anchorage independent growth of HCEC cells containing K-Ras in the background.
- MAGE-A6 promotes anchorage independent growth of HCEC cells without additional oncogene support.

DLD1 and HCEC were plated in soft agar assay for 2 or 4 weeks. Cells were fed with fresh media 3x weekly. At completion wells were imaged and colonies were counted. Graphs represent mean + SD. Asterisks indicate $p \leq .05$ as determined by students t-test.

this phenotype was strong enough to outperform the well characterized and classical oncogene K-Ras (Figure 5-1C).

MAGE-A6 Is Capable of Inducing Tumor Formation *In Vivo*

Given the striking results that were obtained in soft agar, I wanted to test the ability of MAGE-A6 to act as an oncogene *in vivo*. I again used the HCEC system to test if MAGE-A6 could meet this rigorous definition. Previous data from other labs indicated formation of HCEC tumors is not an easy task and all past attempts at establishing tumors with this cell line have failed, including attempts with simultaneous knockdown of the tumor suppressor p53 and expression of both oncogenes c-Myc, and K-Ras^{G12V} (Eskiocak et al., 2011).

The injection of HCEC-MAGE-A6 into the flank of NOD-SCID IL2R γ immune compromised mice was able to yield palpable tumors in approximately one week and the study endpoint size of 20 mm was reached in four weeks (Figure 5-2A). Having achieved tumor growth, I harvested tumor tissue for histology at the time of sacrifice. When the tumors were analyzed by H&E staining, they appear to have a very de-differentiated and highly vascularized appearance (Figure 5-2B). Additionally, when stained for cytokeratin expression, these tumors exhibited a pattern indicative of colorectal cancer (Figure 5-2B) (Witek et al., 2005). Given the strength of the tumor formation phenotype, I also decided to analyze the mice for metastasis by harvesting the lungs at the time of sacrifice. When analyzed by histology, it was evident that there was a significant number of HCEC metastasis to lung (Figure 5-3B) and about 70% of mice had metastasis (Figure 5-3A).

MAGE-A3/6 Targeted Therapy

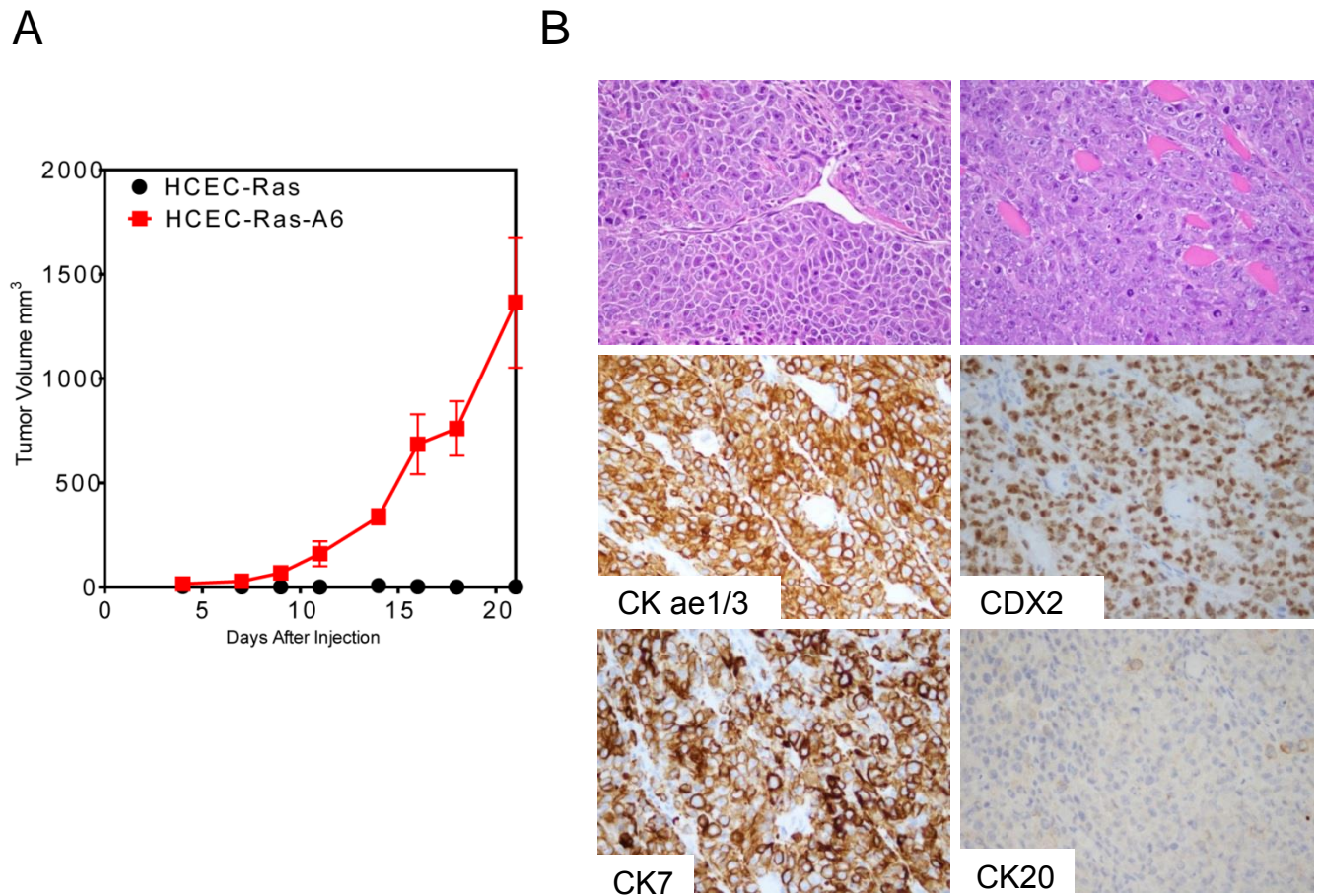


Figure 5-2 MAGE-A6 Induces Tumor Growth

- A. MAGE-A6 induces tumor growth of HCEC- K-Ras cells in flank xenograft models. N = 8 mice per condition.
- B. H&E and IHC indicate the HCEC-MAGE-A6 tumors are poorly differentiated and show cytokeratin staining indicative of colorectal tumors.
- NOD-SCID γ mice were injected with 5×10^6 HCEC cells. Tumors were measured on two axes and mice were sacrificed when tumors reached 20 mm. Tumors were harvested at time of sacrifice and analyzed by pathologist.

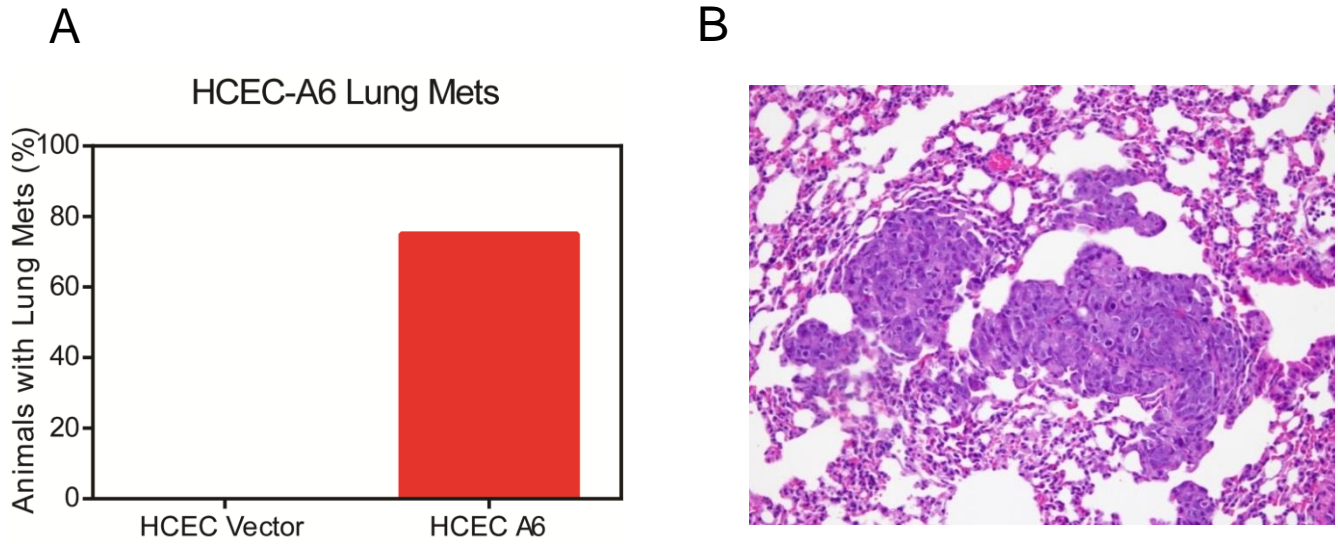


Figure 5-3 HCEC-MAGE-A6 Tumors Form Lung Metastasis.

- A. Quantification of mice bearing HCEC-MAGE-A6 tumor metastasis
- B. H&E staining of mouse lungs identifies HCEC tumor metastasis

Lungs were taken from mice (n=8) bearing HCEC tumors and were analyzed for metastasis by pathologist

Because MAGE-A3/6 is a potent oncogene that is normally only expressed in the testis and again in cancer, it is an extremely attractive target for therapy. While current immunotherapy only utilizes MAGE-A3/6 expression as a marker for the cancer cell, I set out to conceive of a therapy that would directly target the signaling induced by MAGE-A3/6. Having the knowledge that MAGE-A3/6 degrades AMPK and reduces its signaling, my strategy was to use pharmacological methods to increase the activity of the remaining AMPK within the cell. Reduction of AMPK signaling has been observed in multiple cancers and there are several ongoing studies investigating the potential usage of AMPK activating compounds, in cancer (Hadad et al., 2011; Niraula et al., 2012; Pernicova and Korbonits, 2014). I therefore decided to utilize three different AMPK activating compounds: metformin, AICAR, and A769662, with all three of these compounds working through slightly different mechanisms. Metformin is commonly used as an anti-diabetic drug and is the parent compound in a now larger class known as biguanides. While the mechanism of this class of drugs is still debated, it is generally accepted that metformin acts by inhibiting mitochondrial respiration (Hardie et al., 2012a). This has the net effect of reducing ATP generation and activating AMPK. 5-aminoimidazol-4-carboxamide ribonucleotide (AICAR) is an analogue AMP, that when added to cells, stimulates AMPK activity through activation of the γ subunit (Hardie et al., 2012b). Finally, A769662 is a small molecule in development by Abbott, which binds directly to the β subunit of AMPK and results in kinase activation (Landgraf et al., 2013).

When the DLD1 cancer cell line was assayed, metformin had a dose dependent ability to reduce the soft agar growth of MAGE-A6 cell lines, while growth of vector cells was only affected at very high concentrations (Figure 5-4A). These results were closely mirrored by the dose dependent decrease of DLD1-MAGE-A6 soft agar growth caused by treatment with A769662

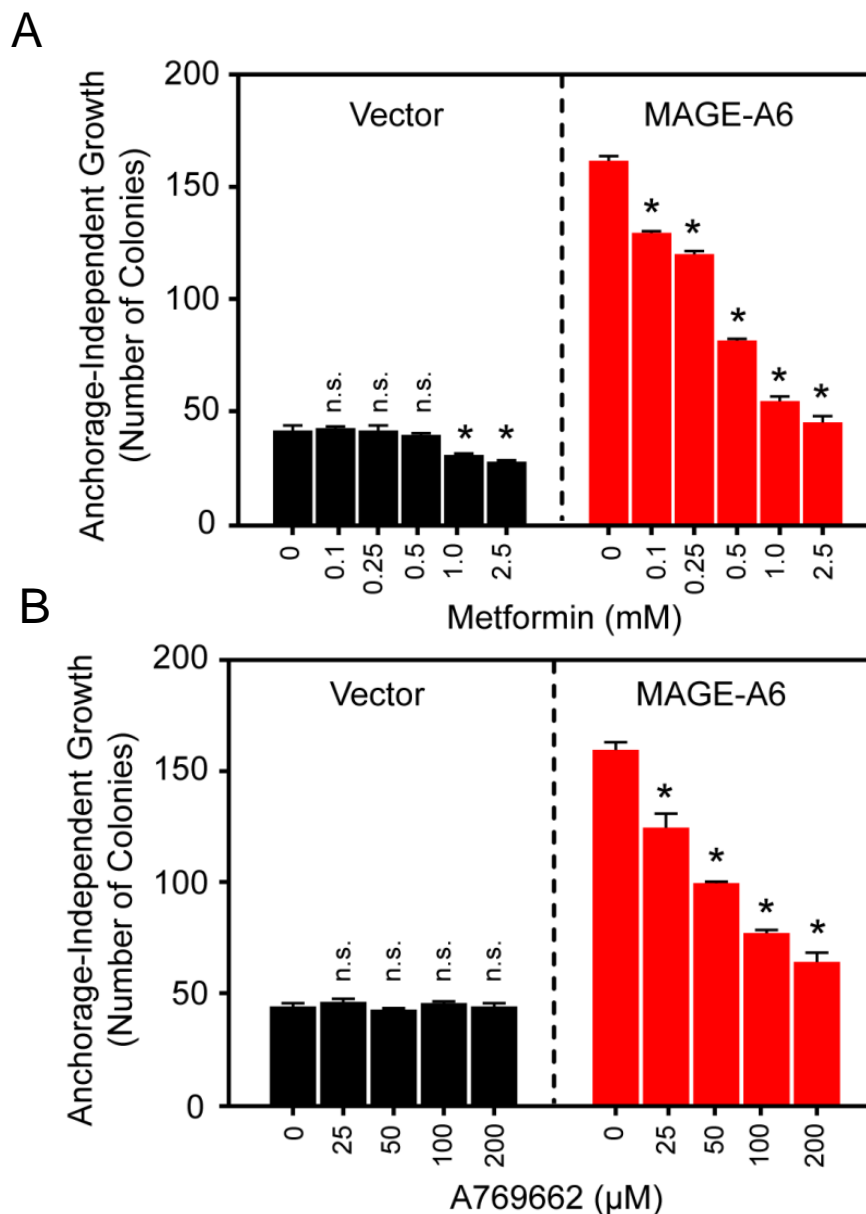


Figure 5-4 AMPK Agonists Block MAGE-A6 Induced Soft Agar Growth

- A. Metformin reduces soft agar growth of DLD1-MAGE-A6 but not DLD1 vector.
- B. A769662 reduces soft agar growth of DLD1-MAGE-A6 but not DLD1 vector.

DLD1 were plated in soft agar assay for 2 weeks. Cells were fed with fresh media containing drugs 3x weekly. At completion wells were imaged and colonies were counted. Bars represent mean + SD (n=3). Asterisks indicate $p \leq .05$ as determined by Student t-test.

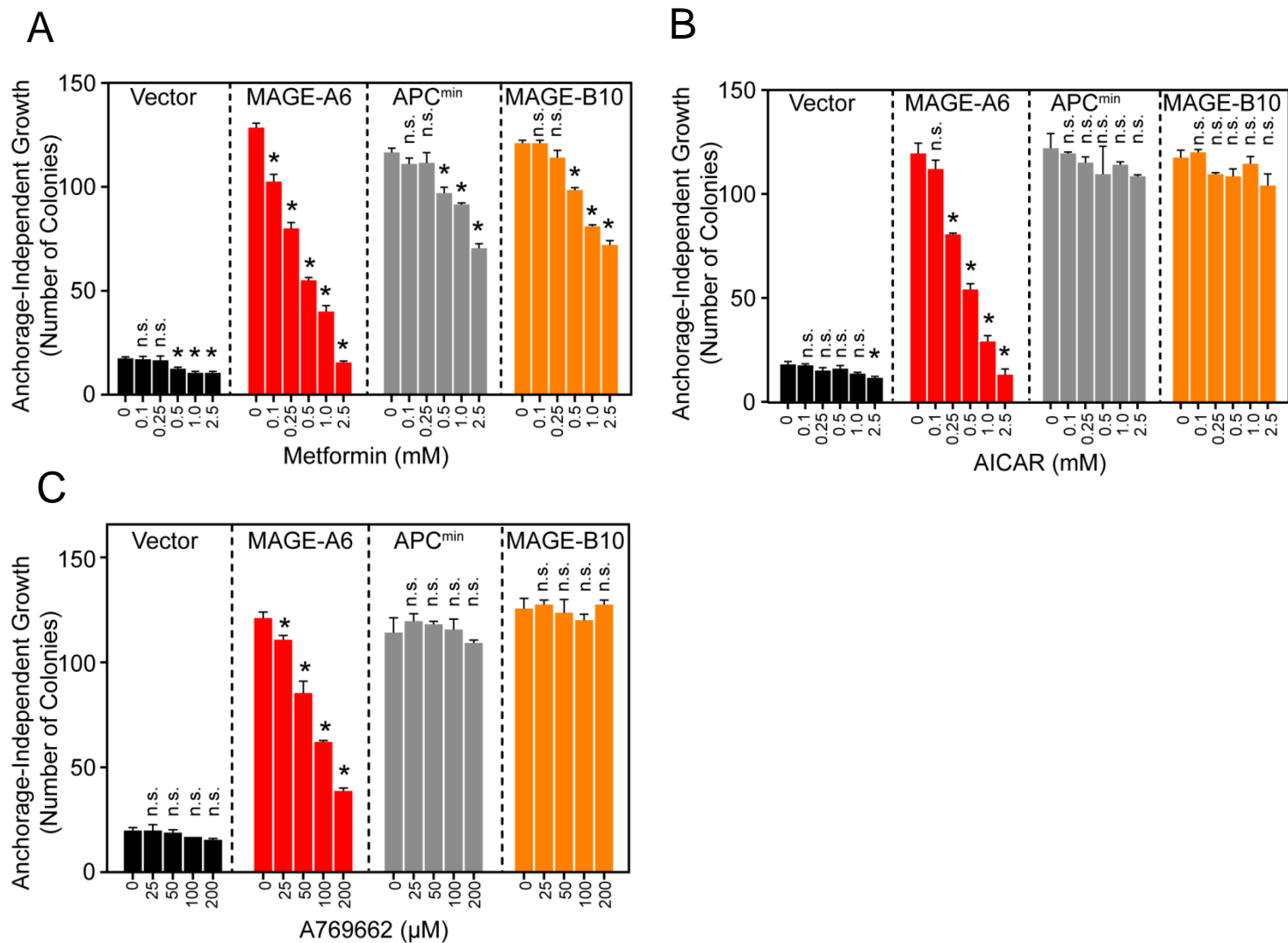


Figure 5-5 AMPK Agonists Selectively Inhibit MAGE-A6 Induced Soft Agar Growth

A-C. Treatment with metformin, AICAR, or A769662 blocks soft agar growth induced by MAGE-A6 but not by APC^{min} or MAGE-B10

HCEC were plated in soft agar assay for 4 weeks. Cells were fed with fresh media containing drugs 3x weekly. At completion wells were imaged and colonies were counted. Bars represent mean + SD (n=3). Asterisks indicate $p \leq .05$ as determined by Student t-test.

(Figure 5-4). These data were very encouraging, and I next wanted to test the effect of AMPK stimulation in the context of the HCEC cell line. When performing this experiment, I added two additional controls to further demonstrate the specificity of the AMPK agonists for MAGE-A6 induced soft agar growth. First, I also included a condition in which soft agar growth was stimulated by the expression of APC^{min}. This condition allowed me to control for the possibility that AMPK agonist treatment was affecting any increase in cell growth driven by an oncogene. Second, I included soft agar growth driven by MAGE-B2. Our lab has determined that MAGE-B2 is also a potent oncogene that acts through a mechanism completely independent of AMPK, and by including it as a control I was able to eliminate the possibility that these drugs are somehow affecting MAGE protein function generally. When I repeated the experiment with the described controls and the additional drug AICAR, the results were very promising. All three compounds had a dose dependent ability to robustly reduce soft agar growth induced by MAGE-A6 expression to baseline (Figure 5-5). This was in contrast with the other oncogenes which were completely resistant to the compounds tested, with only metformin showing potential off target effects at very high dosages. These results demonstrate a clear proof of principle that AMPK agonists may have clinical utility in cases where tumors are driven by the presence of MAGE-A3/6.

Chapter VI: Discussion

Summary of Findings

My studies have made key advancements in our understanding of the biochemical function of the cancer specific gene MAGE-A3/6 and determined that the role that it plays in the induction of cancer is through degradation of the tumor suppressor AMPK.

At the outset of this project I was equipped with the knowledge that several MAGEs have a very specific and high level of expression in cancer, which correlated with a poor patient prognosis. Among the MAGEs, I decided to follow MAGE-A3/6 because it showed the highest penetrance in cancer and published data explicitly demonstrated that it made tumors more aggressive (Liu et al., 2008). Additionally, I possessed the knowledge that MAGE-A3/6 bound to the ubiquitin ligase TRIM28, but I was unaware of a substrate of this complex that could explain the oncogene addiction phenotype that it displayed (Doyle et al., 2010). I then used an unbiased method to identify possible substrates of my ubiquitin ligase complex. Of the 19 substrates identified by this experiment, I decided to follow the kinase and known tumor suppressor AMPK. Further investigation revealed that MAGE-A3/6 acts as a substrate adapter for TRIM28, allowing it to ubiquitinate AMPK and target it for proteasomal degradation. Degradation of AMPK by MAGE-A3/6-TRIM28 consequently reduces AMPK signaling, leading to an increase in mTOR signaling and a robust block in autophagy (Figure 6-1).

Additionally, this study demonstrates that MAGE-A3/6 is a potent oncogene able to induce the hallmark features of cancer. For example, when MAGE-A3/6 is expressed in tumor or non-tumor derived cell lines they acquire anchorage independent growth, as demonstrated by their increased ability to grow in soft agar. Even more surprising, MAGE-A3/6 confers upon untransformed cell

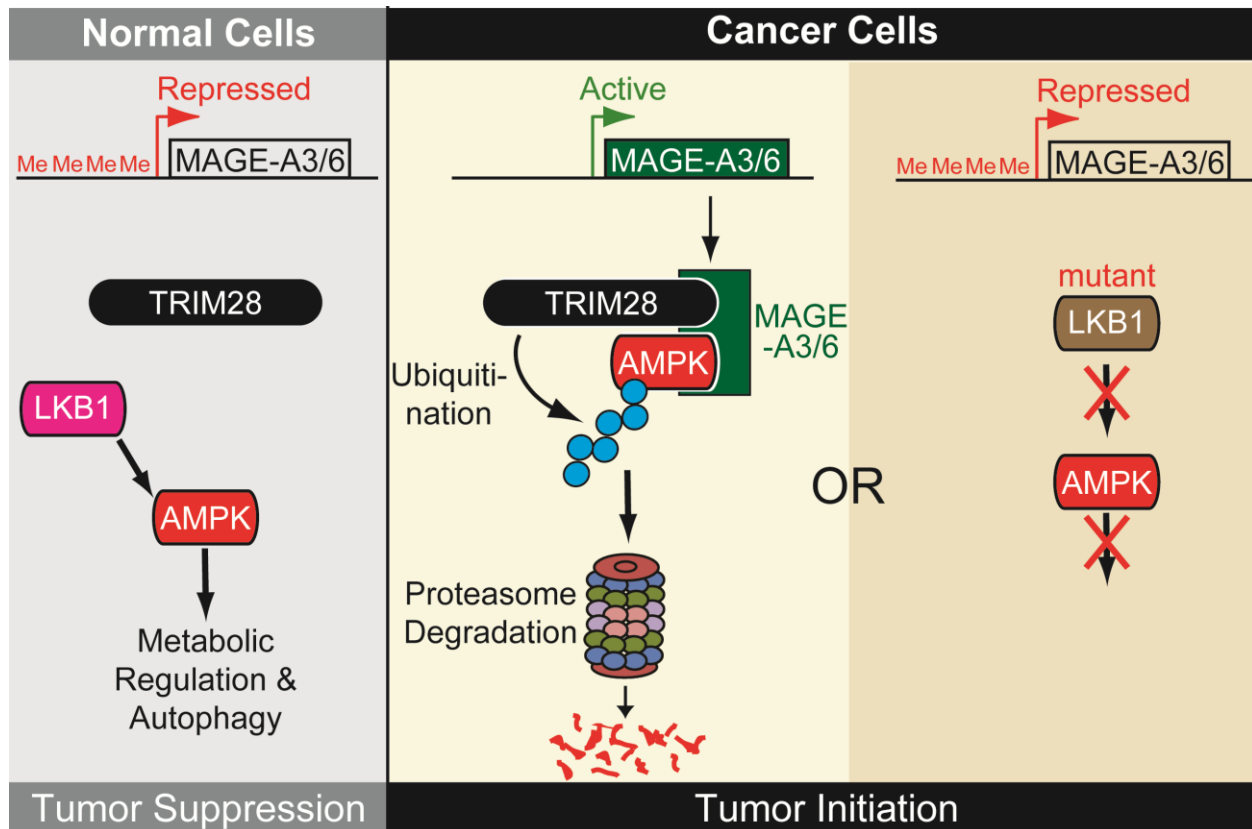


Figure 6-1 Model of MAGE-A3/6's Role in Cancer Development

MAGE-A3/6 expression in tumors acts to target AMPK for degradation and leads to pleiotropic changes that induce tumor formation.

lines the ability to form tumors in mice. Using my newly acquired knowledge of MAGE-A3/6's activity within cells I devised a strategy to counteract its effects and potentially treat tumors driven by it. I tested the hypothesis that increasing AMPK signaling within MAGE-A3/6 driven cell lines would be sufficient to abrogate tumor phenotypes. I did this by treating cells in soft agar with several different AMPK agonists, including the anti-diabetic drug metformin. Treatment was able to inhibit the increase in soft growth driven by MAGE-A3/6 but not by other oncogenes and suggests that metformin may aid patients with deregulated AMPK signaling.

Treatment Strategies for MAGE-A3/6 Tumors

Given the success that was found with metformin and other AMPK agonists being able to block soft agar growth, future experiments should investigate potential treatments for MAGE-A3/6 driven tumors. Currently, experiments are looking at the ability of metformin to block the formation or metastasis of MAGE-A3/6 driven HCEC tumors. Unfortunately, these experiments have not experienced a dramatic response to metformin treatment, as was seen repeatedly in the soft agar assay. Luckily, this failure appears to be result of technical problem with either drug administration or dosage schedule. This appears to be the case because the livers of treated mice show no increase in phosphorylated AMPK. It is well known that metformin accumulates and acts strongly in the liver and it is unlikely that metformin is acting elsewhere if liver effects are not observed. Ongoing efforts seek to optimize the delivery and dosage of metformin such that the AMPK response is verifiable in both liver and tumor tissues. Should the effect of metformin in xenograft tumors eventually copy that of its effects in vitro soft agar assays, MAGE-A3/6 may be considered for usage as an enrollment biomarker, dictating which subset of patients might benefit from metformin inclusion in their treatment regimen.

In addition to AMPK agonists, there are other potential treatment strategies that could be used against MAGE-A3/6 driven cancers. My data have shown that a consequence of MAGE-A3/6 expression in tumors is an increase in mTOR signaling and because of this, the application of clinically approved mTOR inhibitors, such as Everolimus could have a dramatic effect. Also, several potential treatments in development could also be useful. One example of these is the development of drugs that have the ability to activate autophagy within the cell. If MAGE-A3/6's ability to inhibit autophagy is critical to functioning as an oncogene, then bypassing this regulation and increasing autophagic flux could potentially slow or kill these tumors.

Key AMPK Pathways Altered by MAGE-A3/6

While there are several treatment strategies with the potential to yield effects in MAGE-A3/6 driven cancers, deeper mechanistic study may offer insight into which regimen will prove most advantageous. Future studies must determine which of AMPKs pleiotropic signaling modes is crucially altered when MAGE-A3/6 expression is induced. In order to determine which AMPK pathways are critical, I propose that future experiments should selectively reverse the changes induced by MAGE-A3/6 expression in a MAGE (-) cell line and assay either soft agar growth or tumor formation. For example, given that MAGE-A3/6 expression should increase mTOR signaling, the consequence of secondary mTOR knockdown should be tested. Another potential experiment would be to activate autophagy downstream of AMPK's interaction with the pathway. This could be accomplished by treatment of MAGE-A3/6 overexpressing cells with the autophagy inducing Tat-Beclin1 peptide (Shoji-Kawata et al., 2013).

Timing of MAGE-A3/6 Activation in Cancer

While there are several possible pathways by which MAGE-A3/6 could be acting, I believe that data about the timing of MAGE-A3/6 expression may suggest that one of its oncogenic functions is to block autophagy. This is because, it is well documented that reduction of autophagy occurs early in the process of tumorigenesis and that induction of MAGE-A3/6 may be an easy way for a neoplastic cell to achieve this event. Matching this, there are several reports in the literature that suggest that early oncogenic insults have the ability to induce the expression of MAGE-A3/6. First, it is well known that smoking dramatically increases the likelihood that an individual will develop lung cancer and studies have probed what molecular features could be responsible for this predisposition. When patient brush border biopsies were taken from never smokers (less than 100 lifetime cigarettes) and compared to smokers who did not have signs cancer, analysis reveals that zero never smokers expressed MAGE-A3/6 but a significant portion of smokers demonstrated robust MAGE-A3/6 expression (Jang et al., 2001). In addition to smoking, several infections that are known to be predisposing factors in the development of cancer have been shown to induce MAGE-A3/6. One of these risk factors is infections by the bacteria *H. Pylori*. Infections by this bacterium are known to be a causative factor in the development of stomach ulcers and patients infected by *H. Pylori* has been shown to have a very high risk of gastric cancer (Parsonnet et al., 1991; Uemura et al., 2001). Additionally, it has been shown that even transient infection by *H. Pylori* is sufficient to induce the expression of MAGE-A3/6 (Fukuyama et al., 2012). Given this information, and the knowledge that TRIM28 is also associated with gastric cancer, it can be postulated that *H. pylori* infection induces MAGE-A3/6 expression, alters autophagy, and promotes tumorigenesis (Terebiznik et al., 2009).

TRIM28 Is an Autophagy Switch

While the ability of several oncogenic insults to induce MAGE-A3/6 is interesting alone, the fact that a pathogen has evolved to regulate autophagy in this manner is striking. This is because, I believe that expression of MAGE-A3/6 acts as a switch that is competent to alter TRIM28's role in the cell, flipping it from a pro-autophagy factor to a potent inhibitor of autophagy. Several previous studies have demonstrated in MAGE-negative cell lines that TRIM28 is able to promote autophagy. For example, one study has demonstrated the importance of TRIM28's SUMO ligase activity in promoting this process. The SUMO substrate critical to this function is the protein VPS34, a class III PI3-kinase, which in complex with Beclin 1 is essential for autophagosome formation (Tanida, 2011). In this process, TRIM28, together with hsp70, bind to the PI3K VPS34 and SUMOylate it (Yang et al., 2013). This SUMOylation increases the binding of VPS34 to Beclin1 and induces the formation of the autophagosome membrane (Yang et al., 2013). In addition to regulating the activity and localization of VPS34, TRIM28 also regulates autophagy at a transcriptional level. Several microRNAs have been shown to be regulated by TRIM28, and many of these increase the abundance of autophagy-related proteins such as Beclin 1, ULK1 and ATG12 (Barde et al., 2013). In contrast to this, when MAGE-A3/6 is expressed, TRIM28 clearly acts as an inhibitor of autophagy. Future studies could investigate if the presence of MAGE-A3/6 alters TRIM28's other autophagy signaling pathways. If MAGE-A3/6 has no effect on these pathways, it would suggest that degrading AMPK alone is sufficient to change the dominant effect of TRIM28, while a change in miRNAs or a decrease VPS34 SUMOylation could indicate that other MAGE-A3/6-TRIM28 substrates also play a role in regulating autophagy.

Molecular Drivers of MAGE-A3/6 Expression

While there are interesting implications from the timing and inducers of MAGE-A3/6 expression, additional information regarding what drives the expression of MAGEs at the

molecular level could also give key insight into how to combat MAGE-A3/6 in cancer and other diseases. Many studies have found that under normal conditions, MAGE expression is silenced by CpG methylation found in their promoters (Weber et al., 1994). It is also well known that these methylation marks are no longer present in cancer when MAGE-A3/6 is expressed, but this mechanism is insufficient to explain MAGE expression (Qiu et al., 2006). This is because, in experiments where the promoters of MAGEs are demethylated, they are not always expressed, suggesting that a specific transcription factor is required to drive the expression of MAGEs (Karpf et al., 2004; Suyama et al., 2002). While there could be several transcription factors able to drive MAGE-A3/6 expression in cancer, one factor has already been identified for its ability to drive its expression. Data suggest that the cancer-testis antigen and transcription factor BORIS is able to drive MAGE-A3/6 expression (Schwarzenbach et al., 2014; Vatolin et al., 2005). This finding is intriguing because it raises two distinct questions. First, if BORIS is a cancer-testis antigen and is able to promote the expression of the potent oncogene MAGE-A3/6, is it itself an oncogene? This question could easily be answered by repeating performing soft agar and mouse xenograft experiments using HCEC cells expressing BORIS.. The second question is what drives the expression of BORIS. Using one cancer specific gene to explain the expression of another simply extends the search for the causative agent in cancer-testis antigen expression and understanding BORIS expression could give great insight.

Physiological Role of MAGE-A3/6-TRIM28

One strategy to better understand the expression and role of MAGE-A3/6-TRIM28 in cancer is to investigate the normal role of MAGE-A3/6 in the testis. I believe that it is important to investigate if the functions of MAGE-A3/6 in degrading AMPK are a de novo function, only present when expressed in cancer or is the interaction between MAGE-A3/6-TRIM28 and

AMPK also related to their normal role within the testis. While there are few tools with which to investigate developing germ cells, there is limited evidence that MAGE-A3/6 may play some function in regulation of AMPK in the testis. This evidence begins with the fact that both TRIM28 and AMPK α 1, which are specifically regulated, are expressed in the testis at levels higher than the rest of the body (data not shown). Additionally, there are specific metabolic changes known to take place in the developing spermatogonia which could be dependent on the regulatory effects of MAGE-A3/6. It has previously been discovered that as the developing germ cells pass through the blood-testis barrier their exposure to nutrients is altered and they consequently change their energy and carbon sources (Nakamura et al., 1984). These cells transition from utilizing glucose supplied by the blood stream and instead they are forced to consume lactate produced by the surrounding Sertoli cells (Jutte et al., 1981; Jutte et al., 1982; Nakamura et al., 1984). Data produced in our lab suggest that this is also the stage in which MAGE-A3/6 is specifically expressed. One possible hypothesis is that MAGE-A3/6 allows the developing cells to adapt to this energy stress by modulating glucose metabolism. In HeLa cells, when MAGE-A3/6 is knocked down, glucose consumption and lactate production is increased. If the expression of MAGE-A3/6 had the reciprocal effect in the testis, reducing glucose usage and promoting lactate consumption, it would fit the proposed model.

TRIM/MAGE/AMPK Crosstalk

Finally, future studies should investigate the potential that the interplay between MAGE-A3/6, TRIM28, and AMPK may not be unique. This is because both MAGE-A3/6 and TRIM28 have closely related family members that could potentially share similar functions. For example, TRIM28 shares a common domain structure with three other ligases: TRIM24, TRIM33 and TRIM66 (TIF1 α , γ , δ), and they are all classified as type VI TRIMs (Hatakeyama, 2011). While

differing in size, each of these proteins contains a RBCC domain, TIF1 signature sequence (TSS), and adjacent PHD and Bromo domains (Hatakeyama, 2011). This family relation is particularly intriguing because TRIM24, the closest homologue, has already been identified as a substrate of AMPK phosphorylation (Hoppe et al., 2009). The possibility of feedback between these signaling pathways should be investigated.

Additionally, there are multiple additional MAGEs, such as MAGE-C2 and MAGE-A2, which are known to bind TRIM28. Currently, there seems to be no function for this redundancy and a scenario in which families of closely related MAGEs A2, A3, A6 and C2 are able to regulate TRIM24, 28 and 33, and thereby fine tune signaling presents an interesting and challenging problem to interrogate. Ultimately, my research has opened the door for studying MAGE-A3/6-TRIM28 and has the potential to generate a much deeper understanding of the role they are playing in cancer.

References

- Allouch, A., Di Primio, C., Alpi, E., Lusic, M., Arosio, D., Giacca, M., and Cereseto, A. (2011). The TRIM family protein KAP1 inhibits HIV-1 integration. *Cell host & microbe* *9*, 484-495.
- Bar-Peled, L., Schweitzer, L.D., Zoncu, R., and Sabatini, D.M. (2012). Ragulator is a GEF for the rag GTPases that signal amino acid levels to mTORC1. *Cell* *150*, 1196-1208.
- Barde, I., Laurenti, E., Verp, S., Groner, A.C., Towne, C., Padrun, V., Aebischer, P., Trumpp, A., and Trono, D. (2009). Regulation of episomal gene expression by KRAB/KAP1-mediated histone modifications. *Journal of virology* *83*, 5574-5580.
- Barde, I., Rauwel, B., Marin-Florez, R.M., Corsinotti, A., Laurenti, E., Verp, S., Offner, S., Marquis, J., Kapopoulou, A., Vanicek, J., *et al.* (2013). A KRAB/KAP1-miRNA cascade regulates erythropoiesis through stage-specific control of mitophagy. *Science* *340*, 350-353.
- Barnes, K., Ingram, J.C., Porras, O.H., Barros, L.F., Hudson, E.R., Fryer, L.G., Fougelle, F., Carling, D., Hardie, D.G., and Baldwin, S.A. (2002). Activation of GLUT1 by metabolic and osmotic stress: potential involvement of AMP-activated protein kinase (AMPK). *Journal of cell science* *115*, 2433-2442.
- Boccaccio, I., Glatt-Deeley, H., Watrin, F., Roeckel, N., Lalande, M., and Muscatelli, F. (1999). The human MAGEL2 gene and its mouse homologue are paternally expressed and mapped to the Prader-Willi region. *Human molecular genetics* *8*, 2497-2505.
- Bojkowska, K., Aloisio, F., Cassano, M., Kapopoulou, A., Santoni de Sio, F., Zangger, N., Offner, S., Cartoni, C., Thomas, C., Quenneville, S., *et al.* (2012). Liver-specific ablation of Kruppel-associated box-associated protein 1 in mice leads to male-predominant hepatosteatosis and development of liver adenoma. *Hepatology* *56*, 1279-1290.
- Buchheit, C.L., Weigel, K.J., and Schafer, Z.T. (2014). Cancer cell survival during detachment from the ECM: multiple barriers to tumour progression. *Nature reviews Cancer* *14*, 632-641.
- Cancer Genome Atlas Research, N. (2014). Comprehensive molecular profiling of lung adenocarcinoma. *Nature* *511*, 543-550.
- Carling, D., Clarke, P.R., Zammit, V.A., and Hardie, D.G. (1989). Purification and characterization of the AMP-activated protein kinase. Copurification of acetyl-CoA carboxylase kinase and 3-hydroxy-3-methylglutaryl-CoA reductase kinase activities. *European journal of biochemistry / FEBS* *186*, 129-136.
- Chen, L., Munoz-Antonia, T., and Cress, W.D. (2014). Trim28 contributes to EMT via regulation of E-cadherin and N-cadherin in lung cancer cell lines. *PLoS one* *9*, e101040.
- Choi, A.M., Ryter, S.W., and Levine, B. (2013). Autophagy in human health and disease. *N Engl J Med* *368*, 651-662.
- Chomez, P., De Backer, O., Bertrand, M., De Plaen, E., Boon, T., and Lucas, S. (2001). An overview of the MAGE gene family with the identification of all human members of the family. *Cancer research* *61*, 5544-5551.
- Chou, C.C., Lee, K.H., Lai, I.L., Wang, D., Mo, X., Kulp, S.K., Shapiro, C.L., and Chen, C.S. (2014). AMPK Reverses the Mesenchymal Phenotype of Cancer Cells by Targeting the Akt-MDM2-Foxo3a Signaling Axis. *Cancer research* *74*, 4783-4795.
- Clague, M.J., Heride, C., and Urbe, S. (2015). The demographics of the ubiquitin system. *Trends in cell biology* *25*, 417-426.
- Clarke, P.R., and Hardie, D.G. (1990). Regulation of HMG-CoA reductase: identification of the site phosphorylated by the AMP-activated protein kinase in vitro and in intact rat liver. *The EMBO journal* *9*, 2439-2446.
- Cui, Y., Yang, S., Fu, X., Feng, J., Xu, S., and Ying, G. (2015). High levels of KAP1 expression are associated with aggressive clinical features in ovarian cancer. *International journal of molecular sciences* *16*, 363-377.

- Dango, S., Wang, X.T., Gold, M., Cucuruz, B., Klein, C.A., Passlick, B., and Siemel, W. (2010). Expression of melanoma-antigen-A (MAGE-A) in disseminated tumor cells in regional lymph nodes of patients with operable non-small cell lung cancer. *Lung cancer* 67, 290-295.
- De Plaen, E., Arden, K., Traversari, C., Gaforio, J.J., Szikora, J.P., De Smet, C., Brasseur, F., van der Bruggen, P., Lethe, B., Lurquin, C., *et al.* (1994). Structure, chromosomal localization, and expression of 12 genes of the MAGE family. *Immunogenetics* 40, 360-369.
- Degenhardt, K., Mathew, R., Beaudoin, B., Bray, K., Anderson, D., Chen, G., Mukherjee, C., Shi, Y., Gelinas, C., Fan, Y., *et al.* (2006). Autophagy promotes tumor cell survival and restricts necrosis, inflammation, and tumorigenesis. *Cancer cell* 10, 51-64.
- Devos, J., Weselake, S.V., and Wevrick, R. (2011). Magel2, a Prader-Willi syndrome candidate gene, modulates the activities of circadian rhythm proteins in cultured cells. *Journal of circadian rhythms* 9, 12.
- Di Giacomo, A.M., and Margolin, K. (2015). Immune checkpoint blockade in patients with melanoma metastatic to the brain. *Seminars in oncology* 42, 459-465.
- Doyle, J.M., Gao, J., Wang, J., Yang, M., and Potts, P.R. (2010). MAGE-RING protein complexes comprise a family of E3 ubiquitin ligases. *Molecular cell* 39, 963-974.
- Dyck, J.R., Gao, G., Widmer, J., Stapleton, D., Fernandez, C.S., Kemp, B.E., and Witters, L.A. (1996). Regulation of 5'-AMP-activated protein kinase activity by the noncatalytic beta and gamma subunits. *The Journal of biological chemistry* 271, 17798-17803.
- Eskiocak, U., Kim, S.B., Ly, P., Roig, A.I., Biglione, S., Komurov, K., Cornelius, C., Wright, W.E., White, M.A., and Shay, J.W. (2011). Functional parsing of driver mutations in the colorectal cancer genome reveals numerous suppressors of anchorage-independent growth. *Cancer research* 71, 4359-4365.
- Esteve-Puig, R., Canals, F., Colome, N., Merlino, G., and Recio, J.A. (2009). Uncoupling of the LKB1-AMPKalpha energy sensor pathway by growth factors and oncogenic BRAF. *PloS one* 4, e4771.
- Fasching, L., Kapopoulou, A., Sachdeva, R., Petri, R., Jonsson, M.E., Manne, C., Turelli, P., Jern, P., Cammas, F., Trono, D., *et al.* (2015). TRIM28 represses transcription of endogenous retroviruses in neural progenitor cells. *Cell reports* 10, 20-28.
- Feng, Y., Gao, J., and Yang, M. (2011). When MAGE meets RING: insights into biological functions of MAGE proteins. *Protein Cell* 2, 7-12.
- Fukuyama, T., Yamazaki, T., Fujita, T., Uematsu, T., Ichiki, Y., Kaneko, H., Suzuki, T., and Kobayashi, N. (2012). *Helicobacter pylori*, a carcinogen, induces the expression of melanoma antigen-encoding gene (MAGE)-A3, a cancer/testis antigen. *Tumour Biol* 33, 1881-1887.
- Gaugler, B., Van den Eynde, B., van der Bruggen, P., Romero, P., Gaforio, J.J., De Plaen, E., Lethe, B., Brasseur, F., and Boon, T. (1994). Human gene MAGE-3 codes for an antigen recognized on a melanoma by autologous cytolytic T lymphocytes. *J Exp Med* 179, 921-930.
- Gerard, C., Baudson, N., Ory, T., and Louahed, J. (2014). Tumor mouse model confirms MAGE-A3 cancer immunotherapeutic as an efficient inducer of long-lasting anti-tumoral responses. *PloS one* 9, e94883.
- Guerineau, M., Kriz, Z., Kozakova, L., Bednarova, K., Janos, P., and Palecek, J. (2012). Analysis of the Nse3/MAGE-binding domain of the Nse4/EID family proteins. *PloS one* 7, e35813.
- Gwinn, D.M., Shackelford, D.B., Egan, D.F., Mihaylova, M.M., Mery, A., Vasquez, D.S., Turk, B.E., and Shaw, R.J. (2008). AMPK phosphorylation of raptor mediates a metabolic checkpoint. *Molecular cell* 30, 214-226.
- Hadad, S., Iwamoto, T., Jordan, L., Purdie, C., Bray, S., Baker, L., Jellema, G., Deharo, S., Hardie, D.G., Pusztai, L., *et al.* (2011). Evidence for biological effects of metformin in operable breast cancer: a pre-operative, window-of-opportunity, randomized trial. *Breast cancer research and treatment* 128, 783-794.
- Hanahan, D., and Weinberg, R.A. (2000). The hallmarks of cancer. *Cell* 100, 57-70.
- Hanahan, D., and Weinberg, R.A. (2011). Hallmarks of cancer: the next generation. *Cell* 144, 646-674.

- Hao, Y.H., Doyle, J.M., Ramanathan, S., Gomez, T.S., Jia, D., Xu, M., Chen, Z.J., Billadeau, D.D., Rosen, M.K., and Potts, P.R. (2013). Regulation of WASH-Dependent Actin Polymerization and Protein Trafficking by Ubiquitination. *Cell* 152, 1051-1064.
- Hardie, D.G. (2015). AMPK: positive and negative regulation, and its role in whole-body energy homeostasis. *Current opinion in cell biology* 33, 1-7.
- Hardie, D.G., and Alessi, D.R. (2013). LKB1 and AMPK and the cancer-metabolism link - ten years after. *BMC Biol* 11, 36.
- Hardie, D.G., Ross, F.A., and Hawley, S.A. (2012a). AMP-activated protein kinase: a target for drugs both ancient and modern. *Chemistry & biology* 19, 1222-1236.
- Hardie, D.G., Ross, F.A., and Hawley, S.A. (2012b). AMPK: a nutrient and energy sensor that maintains energy homeostasis. *Nature reviews Molecular cell biology* 13, 251-262.
- Hatakeyama, S. (2011). TRIM proteins and cancer. *Nature reviews Cancer* 11, 792-804.
- Hawley, S.A., Boudeau, J., Reid, J.L., Mustard, K.J., Udd, L., Makela, T.P., Alessi, D.R., and Hardie, D.G. (2003). Complexes between the LKB1 tumor suppressor, STRAD alpha/beta and MO25 alpha/beta are upstream kinases in the AMP-activated protein kinase cascade. *J Biol* 2, 28.
- Hawley, S.A., Pan, D.A., Mustard, K.J., Ross, L., Bain, J., Edelman, A.M., Frenguelli, B.G., and Hardie, D.G. (2005). Calmodulin-dependent protein kinase kinase-beta is an alternative upstream kinase for AMP-activated protein kinase. *Cell metabolism* 2, 9-19.
- Hedger, M.P. (2002). Macrophages and the immune responsiveness of the testis. *Journal of reproductive immunology* 57, 19-34.
- Herquel, B., Ouararhni, K., Khetchoumian, K., Ignat, M., Teletin, M., Mark, M., Bechade, G., Van Dorsseleer, A., Sanglier-Cianferani, S., Hamiche, A., *et al.* (2011). Transcription cofactors TRIM24, TRIM28, and TRIM33 associate to form regulatory complexes that suppress murine hepatocellular carcinoma. *Proceedings of the National Academy of Sciences of the United States of America* 108, 8212-8217.
- Herzog, M., Wendling, O., Guillou, F., Chambon, P., Mark, M., Losson, R., and Cammas, F. (2011). TIF1beta association with HP1 is essential for post-gastrulation development, but not for Sertoli cell functions during spermatogenesis. *Developmental biology* 350, 548-558.
- Ho, J., Kong, J.W., Choong, L.Y., Loh, M.C., Toy, W., Chong, P.K., Wong, C.H., Wong, C.Y., Shah, N., and Lim, Y.P. (2009). Novel breast cancer metastasis-associated proteins. *Journal of proteome research* 8, 583-594.
- Homet Moreno, B., Parisi, G., Robert, L., and Ribas, A. (2015). Anti-PD-1 therapy in melanoma. *Seminars in oncology* 42, 466-473.
- Hoppe, S., Bierhoff, H., Cado, I., Weber, A., Tiebe, M., Grummt, I., and Voit, R. (2009). AMP-activated protein kinase adapts rRNA synthesis to cellular energy supply. *Proceedings of the National Academy of Sciences of the United States of America* 106, 17781-17786.
- Hu, C., Zhang, S., Gao, X., Gao, X., Xu, X., Lv, Y., Zhang, Y., Zhu, Z., Zhang, C., Li, Q., *et al.* (2012). Roles of Kruppel-associated Box (KRAB)-associated Co-repressor KAP1 Ser-473 Phosphorylation in DNA Damage Response. *The Journal of biological chemistry* 287, 18937-18952.
- Hudson, J.J., Bednarova, K., Kozakova, L., Liao, C., Guerineau, M., Colnaghi, R., Vidot, S., Marek, J., Bathula, S.R., Lehmann, A.R., *et al.* (2011). Interactions between the Nse3 and Nse4 components of the SMC5-6 complex identify evolutionarily conserved interactions between MAGE and EID Families. *PLoS one* 6, e17270.
- Imamura, K., Ogura, T., Kishimoto, A., Kaminishi, M., and Esumi, H. (2001). Cell cycle regulation via p53 phosphorylation by a 5'-AMP activated protein kinase activator, 5-aminoimidazole-4-carboxamide-1-beta-D-ribofuranoside, in a human hepatocellular carcinoma cell line. *Biochemical and biophysical research communications* 287, 562-567.

- Inoki, K., Zhu, T., and Guan, K.L. (2003). TSC2 mediates cellular energy response to control cell growth and survival. *Cell* *115*, 577-590.
- Ivanov, A.V., Peng, H., Yurchenko, V., Yap, K.L., Negorev, D.G., Schultz, D.C., Psulkowski, E., Fredericks, W.J., White, D.E., Maul, G.G., *et al.* (2007). PHD domain-mediated E3 ligase activity directs intramolecular sumoylation of an adjacent bromodomain required for gene silencing. *Molecular cell* *28*, 823-837.
- Iyengar, S., and Farnham, P.J. (2011). KAP1 protein: an enigmatic master regulator of the genome. *The Journal of biological chemistry* *286*, 26267-26276.
- Iyengar, S., Ivanov, A.V., Jin, V.X., Rauscher, F.J., 3rd, and Farnham, P.J. (2011). Functional analysis of KAP1 genomic recruitment. *Molecular and cellular biology* *31*, 1833-1847.
- Jang, S.J., Soria, J.C., Wang, L., Hassan, K.A., Morice, R.C., Walsh, G.L., Hong, W.K., and Mao, L. (2001). Activation of melanoma antigen tumor antigens occurs early in lung carcinogenesis. *Cancer research* *61*, 7959-7963.
- Jones, R.G., Plas, D.R., Kubek, S., Buzzai, M., Mu, J., Xu, Y., Birnbaum, M.J., and Thompson, C.B. (2005). AMP-activated protein kinase induces a p53-dependent metabolic checkpoint. *Molecular cell* *18*, 283-293.
- Jutte, N.H., Grootegoed, J.A., Rommerts, F.F., and van der Molen, H.J. (1981). Exogenous lactate is essential for metabolic activities in isolated rat spermatocytes and spermatids. *J Reprod Fertil* *62*, 399-405.
- Jutte, N.H., Jansen, R., Grootegoed, J.A., Rommerts, F.F., Clausen, O.P., and van der Molen, H.J. (1982). Regulation of survival of rat pachytene spermatocytes by lactate supply from Sertoli cells. *J Reprod Fertil* *65*, 431-438.
- Karpf, A.R., Lasek, A.W., Ririe, T.O., Hanks, A.N., Grossman, D., and Jones, D.A. (2004). Limited gene activation in tumor and normal epithelial cells treated with the DNA methyltransferase inhibitor 5-aza-2'-deoxycytidine. *Molecular pharmacology* *65*, 18-27.
- Kim, J., Kundu, M., Viollet, B., and Guan, K.L. (2011). AMPK and mTOR regulate autophagy through direct phosphorylation of Ulk1. *Nature cell biology* *13*, 132-141.
- Klionsky, D.J., Baehrecke, E.H., Brumell, J.H., Chu, C.T., Codogno, P., Cuervo, A.M., Debnath, J., Deretic, V., Elazar, Z., Eskelinen, E.L., *et al.* (2011). A comprehensive glossary of autophagy-related molecules and processes (2nd edition). *Autophagy* *7*, 1273-1294.
- Komander, D., and Rape, M. (2012). The ubiquitin code. *Annual review of biochemistry* *81*, 203-229.
- Landgraf, R.R., Goswami, D., Rajamohan, F., Harris, M.S., Calabrese, M.F., Hoth, L.R., Magyar, R., Pascal, B.D., Chalmers, M.J., Busby, S.A., *et al.* (2013). Activation of AMP-activated protein kinase revealed by hydrogen/deuterium exchange mass spectrometry. *Structure* *21*, 1942-1953.
- Laplante, M., and Sabatini, D.M. (2012a). mTOR Signaling. *Cold Spring Harbor perspectives in biology* *4*.
- Laplante, M., and Sabatini, D.M. (2012b). mTOR signaling in growth control and disease. *Cell* *149*, 274-293.
- Li, J., Lu, Y., Akbani, R., Ju, Z., Roebuck, P.L., Liu, W., Yang, J.Y., Broom, B.M., Verhaak, R.G., Kane, D.W., *et al.* (2013). TCGA: a resource for cancer functional proteomics data. *Nature methods* *10*, 1046-1047.
- Li, X., Lin, H.H., Chen, H., Xu, X., Shih, H.M., and Ann, D.K. (2010). SUMOylation of the transcriptional co-repressor KAP1 is regulated by the serine and threonine phosphatase PP1. *Science signaling* *3*, ra32.
- Liang, J., Shao, S.H., Xu, Z.X., Hennessy, B., Ding, Z., Larrea, M., Kondo, S., Dumont, D.J., Gutterman, J.U., Walker, C.L., *et al.* (2007). The energy sensing LKB1-AMPK pathway regulates p27(kip1) phosphorylation mediating the decision to enter autophagy or apoptosis. *Nature cell biology* *9*, 218-224.
- Lin, L.F., Li, C.F., Wang, W.J., Yang, W.M., Wang, D.D., Chang, W.C., Lee, W.H., and Wang, J.M. (2013). Loss of ZBRK1 contributes to the increase of KAP1 and promotes KAP1-mediated metastasis and invasion in cervical cancer. *PloS one* *8*, e73033.

- Liu, W., Cheng, S., Asa, S.L., and Ezzat, S. (2008). The melanoma-associated antigen A3 mediates fibronectin-controlled cancer progression and metastasis. *Cancer research* 68, 8104-8112.
- Liu, X., Song, N., Liu, Y., Liu, Y., Li, J., Ding, J., and Tong, Z. (2015). Efficient induction of anti-tumor immune response in esophageal squamous cell carcinoma via dendritic cells expressing MAGE-A3 and CALR antigens. *Cellular immunology* 295, 77-82.
- Matsumoto, S., Iwakawa, R., Takahashi, K., Kohno, T., Nakanishi, Y., Matsuno, Y., Suzuki, K., Nakamoto, M., Shimizu, E., Minna, J.D., *et al.* (2007). Prevalence and specificity of LKB1 genetic alterations in lung cancers. *Oncogene* 26, 5911-5918.
- Meierhofer, D., Wang, X., Huang, L., and Kaiser, P. (2008). Quantitative analysis of global ubiquitination in HeLa cells by mass spectrometry. *Journal of proteome research* 7, 4566-4576.
- Meley, D., Bauvy, C., Houben-Weerts, J.H., Dubbelhuis, P.F., Helmond, M.T., Codogno, P., and Meijer, A.J. (2006). AMP-activated protein kinase and the regulation of autophagic proteolysis. *The Journal of biological chemistry* 281, 34870-34879.
- Mizushima, N., Yoshimori, T., and Levine, B. (2010). Methods in mammalian autophagy research. *Cell* 140, 313-326.
- Monte, M., Simonatto, M., Peche, L.Y., Bublik, D.R., Gobessi, S., Pierotti, M.A., Rodolfo, M., and Schneider, C. (2006). MAGE-A tumor antigens target p53 transactivation function through histone deacetylase recruitment and confer resistance to chemotherapeutic agents. *Proceedings of the National Academy of Sciences of the United States of America* 103, 11160-11165.
- Nakamura, M., Okinaga, S., and Arai, K. (1984). Metabolism of round spermatids: evidence that lactate is preferred substrate. *Am J Physiol* 247, E234-242.
- Nardiello, T., Jungbluth, A.A., Mei, A., Diliberto, M., Huang, X., Dabrowski, A., Andrade, V.C., Wasserstrum, R., Ely, S., Niesvizky, R., *et al.* (2011). MAGE-A inhibits apoptosis in proliferating myeloma cells through repression of Bax and maintenance of survivin. *Clinical cancer research : an official journal of the American Association for Cancer Research* 17, 4309-4319.
- Niraula, S., Dowling, R.J., Ennis, M., Chang, M.C., Done, S.J., Hood, N., Escallon, J., Leong, W.L., McCready, D.R., Reedijk, M., *et al.* (2012). Metformin in early breast cancer: a prospective window of opportunity neoadjuvant study. *Breast cancer research and treatment* 135, 821-830.
- Parsonnet, J., Friedman, G.D., Vandersteen, D.P., Chang, Y., Vogelman, J.H., Orentreich, N., and Sibley, R.K. (1991). *Helicobacter pylori* infection and the risk of gastric carcinoma. *N Engl J Med* 325, 1127-1131.
- Pebernard, S., McDonald, W.H., Pavlova, Y., Yates, J.R., 3rd, and Boddy, M.N. (2004). Nse1, Nse2, and a novel subunit of the Smc5-Smc6 complex, Nse3, play a crucial role in meiosis. *Molecular biology of the cell* 15, 4866-4876.
- Pernicova, I., and Korbonits, M. (2014). Metformin--mode of action and clinical implications for diabetes and cancer. *Nature reviews Endocrinology* 10, 143-156.
- Persaud, A., Alberts, P., Amsen, E.M., Xiong, X., Wasmuth, J., Saadon, Z., Fladd, C., Parkinson, J., and Rotin, D. (2009). Comparison of substrate specificity of the ubiquitin ligases Nedd4 and Nedd4-2 using proteome arrays. *Molecular systems biology* 5, 333.
- Persaud, A., and Rotin, D. (2011). Use of proteome arrays to globally identify substrates for E3 ubiquitin ligases. *Methods in molecular biology* 759, 215-224.
- Pon, J.R., and Marra, M.A. (2015). Driver and passenger mutations in cancer. *Annual review of pathology* 10, 25-50.
- Potts, M.B., Kim, H.S., Fisher, K.W., Hu, Y., Carrasco, Y.P., Bulut, G.B., Ou, Y.H., Herrera-Herrera, M.L., Cubillos, F., Mendiratta, S., *et al.* (2013). Using functional signature ontology (FUSION) to identify mechanisms of action for natural products. *Science signaling* 6, ra90.
- Qiu, G., Fang, J., and He, Y. (2006). 5' CpG island methylation analysis identifies the MAGE-A1 and MAGE-A3 genes as potential markers of HCC. *Clin Biochem* 39, 259-266.

- Qu, X., Yu, J., Bhagat, G., Furuya, N., Hibshoosh, H., Troxel, A., Rosen, J., Eskelinen, E.L., Mizushima, N., Ohsumi, Y., *et al.* (2003). Promotion of tumorigenesis by heterozygous disruption of the beclin 1 autophagy gene. *The Journal of clinical investigation* *112*, 1809-1820.
- Rabinowitz, J.D., and White, E. (2010). Autophagy and metabolism. *Science* *330*, 1344-1348.
- Ramirez, R.D., Sheridan, S., Girard, L., Sato, M., Kim, Y., Pollack, J., Peyton, M., Zou, Y., Kurie, J.M., Dimaio, J.M., *et al.* (2004). Immortalization of human bronchial epithelial cells in the absence of viral oncoproteins. *Cancer research* *64*, 9027-9034.
- Ramlogan-Steel, C.A., Steel, J.C., and Morris, J.C. (2014). Lung cancer vaccines: current status and future prospects. *Translational lung cancer research* *3*, 46-52.
- Roig, A.I., Eskiocak, U., Hight, S.K., Kim, S.B., Delgado, O., Souza, R.F., Spechler, S.J., Wright, W.E., and Shay, J.W. (2010). Immortalized epithelial cells derived from human colon biopsies express stem cell markers and differentiate in vitro. *Gastroenterology* *138*, 1012-1021 e1011-1015.
- Rowe, H.M., Friedli, M., Offner, S., Verp, S., Mesnard, D., Marquis, J., Aktas, T., and Trono, D. (2013a). De novo DNA methylation of endogenous retroviruses is shaped by KRAB-ZFPs/KAP1 and ESET. *Development* *140*, 519-529.
- Rowe, H.M., Jakobsson, J., Mesnard, D., Rougemont, J., Reynard, S., Aktas, T., Maillard, P.V., Layard-Liesching, H., Verp, S., Marquis, J., *et al.* (2010). KAP1 controls endogenous retroviruses in embryonic stem cells. *Nature* *463*, 237-240.
- Rowe, H.M., Kapopoulou, A., Corsinotti, A., Fasching, L., Macfarlan, T.S., Tarabay, Y., Viville, S., Jakobsson, J., Pfaff, S.L., and Trono, D. (2013b). TRIM28 repression of retrotransposon-based enhancers is necessary to preserve transcriptional dynamics in embryonic stem cells. *Genome research* *23*, 452-461.
- Sancak, Y., Bar-Peled, L., Zoncu, R., Markhard, A.L., Nada, S., and Sabatini, D.M. (2010). Regulator-Rag complex targets mTORC1 to the lysosomal surface and is necessary for its activation by amino acids. *Cell* *141*, 290-303.
- Sanchez-Cespedes, M., Parrella, P., Esteller, M., Nomoto, S., Trink, B., Engles, J.M., Westra, W.H., Herman, J.G., and Sidransky, D. (2002). Inactivation of LKB1/STK11 is a common event in adenocarcinomas of the lung. *Cancer research* *62*, 3659-3662.
- Sang, M., Lian, Y., Zhou, X., and Shan, B. (2011). MAGE-A family: attractive targets for cancer immunotherapy. *Vaccine* *29*, 8496-8500.
- Sato, M., Vaughan, M.B., Girard, L., Peyton, M., Lee, W., Shames, D.S., Ramirez, R.D., Sunaga, N., Gazdar, A.F., Shay, J.W., *et al.* (2006). Multiple oncogenic changes (K-RAS(V12), p53 knockdown, mutant EGFRs, p16 bypass, telomerase) are not sufficient to confer a full malignant phenotype on human bronchial epithelial cells. *Cancer research* *66*, 2116-2128.
- Schwarzenbach, H., Eichelser, C., Steinbach, B., Tadewaldt, J., Pantel, K., Lobanenkov, V., and Loukinov, D. (2014). Differential regulation of MAGE-A1 promoter activity by BORIS and Sp1, both interacting with the TATA binding protein. *BMC cancer* *14*, 796.
- Shackelford, D.B., and Shaw, R.J. (2009). The LKB1-AMPK pathway: metabolism and growth control in tumour suppression. *Nature reviews Cancer* *9*, 563-575.
- Shackelford, D.B., Vasquez, D.S., Corbeil, J., Wu, S., Leblanc, M., Wu, C.L., Vera, D.R., and Shaw, R.J. (2009). mTOR and HIF-1alpha-mediated tumor metabolism in an LKB1 mouse model of Peutz-Jeghers syndrome. *Proceedings of the National Academy of Sciences of the United States of America* *106*, 11137-11142.
- Shantha Kumara, H.M., Grieco, M.J., Caballero, O.L., Su, T., Ahmed, A., Ritter, E., Gnjjatic, S., Cekic, V., Old, L.J., Simpson, A.J., *et al.* (2012). MAGE-A3 is highly expressed in a subset of colorectal cancer patients. *Cancer Immun* *12*, 16.

- Shoji-Kawata, S., Sumpter, R., Leveno, M., Campbell, G.R., Zou, Z., Kinch, L., Wilkins, A.D., Sun, Q., Pallauf, K., MacDuff, D., *et al.* (2013). Identification of a candidate therapeutic autophagy-inducing peptide. *Nature* 494, 201-206.
- Sienel, W., Mecklenburg, I., Dango, S., Ehrhardt, P., Kirschbaum, A., Passlick, B., and Pantel, K. (2007). Detection of MAGE-A transcripts in bone marrow is an independent prognostic factor in operable non-small-cell lung cancer. *Clinical cancer research : an official journal of the American Association for Cancer Research* 13, 3840-3847.
- Simpson, A.J., Caballero, O.L., Jungbluth, A., Chen, Y.T., and Old, L.J. (2005). Cancer/testis antigens, gametogenesis and cancer. *Nature reviews Cancer* 5, 615-625.
- Smith, B.E., and Braun, R.E. (2012). Germ cell migration across Sertoli cell tight junctions. *Science* 338, 798-802.
- Society, A.C. (2015). *Cancer Facts and Figures 2015*.
- Suter, M., Riek, U., Tuerk, R., Schlattner, U., Wallimann, T., and Neumann, D. (2006). Dissecting the role of 5'-AMP for allosteric stimulation, activation, and deactivation of AMP-activated protein kinase. *The Journal of biological chemistry* 281, 32207-32216.
- Suyama, T., Ohashi, H., Nagai, H., Hatano, S., Asano, H., Murate, T., Saito, H., and Kinoshita, T. (2002). The MAGE-A1 gene expression is not determined solely by methylation status of the promoter region in hematological malignancies. *Leukemia research* 26, 1113-1118.
- Swaiika, A., Hammond, W.A., and Joseph, R.W. (2015). Current state of anti-PD-L1 and anti-PD-1 agents in cancer therapy. *Molecular immunology*.
- Tanida, I. (2011). Autophagy basics. *Microbiology and immunology* 55, 1-11.
- Terebiznik, M.R., Raju, D., Vazquez, C.L., Torbrick, K., Kulkarni, R., Blanke, S.R., Yoshimori, T., Colombo, M.I., and Jones, N.L. (2009). Effect of *Helicobacter pylori*'s vacuolating cytotoxin on the autophagy pathway in gastric epithelial cells. *Autophagy* 5, 370-379.
- Uemura, N., Okamoto, S., Yamamoto, S., Matsumura, N., Yamaguchi, S., Yamakido, M., Taniyama, K., Sasaki, N., and Schlemper, R.J. (2001). *Helicobacter pylori* infection and the development of gastric cancer. *N Engl J Med* 345, 784-789.
- Vatolin, S., Abdullaev, Z., Pack, S.D., Flanagan, P.T., Custer, M., Loukinov, D.I., Pugacheva, E., Hong, J.A., Morse, H., 3rd, Schrupp, D.S., *et al.* (2005). Conditional expression of the CTCF-paralogous transcriptional factor BORIS in normal cells results in demethylation and derepression of MAGE-A1 and reactivation of other cancer-testis genes. *Cancer research* 65, 7751-7762.
- Vittal, V., Stewart, M.D., Brzovic, P.S., and Klevit, R.E. (2015). Regulating the Regulators: Recent Revelations in the Control of E3 Ubiquitin Ligases. *The Journal of biological chemistry*.
- Wallrapp, C., Hahnel, S., Muller-Pillasch, F., Burghardt, B., Iwamura, T., Ruthenburger, M., Lerch, M.M., Adler, G., and Gress, T.M. (2000). A novel transmembrane serine protease (TMPRSS3) overexpressed in pancreatic cancer. *Cancer research* 60, 2602-2606.
- Wang, C., Ivanov, A., Chen, L., Fredericks, W.J., Seto, E., Rauscher, F.J., 3rd, and Chen, J. (2005). MDM2 interaction with nuclear corepressor KAP1 contributes to p53 inactivation. *The EMBO journal* 24, 3279-3290.
- Weber, J., Salgaller, M., Samid, D., Johnson, B., Herlyn, M., Lassam, N., Treisman, J., and Rosenberg, S.A. (1994). Expression of the MAGE-1 tumor antigen is up-regulated by the demethylating agent 5-aza-2'-deoxycytidine. *Cancer research* 54, 1766-1771.
- Weber, P., Cammas, F., Gerard, C., Metzger, D., Chambon, P., Losson, R., and Mark, M. (2002). Germ cell expression of the transcriptional co-repressor TIF1beta is required for the maintenance of spermatogenesis in the mouse. *Development* 129, 2329-2337.
- Weinstein, I.B. (2002). Cancer. Addiction to oncogenes--the Achilles heel of cancer. *Science* 297, 63-64.
- White, D., Rafalska-Metcalf, I.U., Ivanov, A.V., Corsinotti, A., Peng, H., Lee, S.C., Trono, D., Janicki, S.M., and Rauscher, F.J., 3rd (2012). The ATM substrate KAP1 controls DNA repair in heterochromatin:

- regulation by HP1 proteins and serine 473/824 phosphorylation. *Molecular cancer research : MCR* 10, 401-414.
- White, E. (2012). Deconvoluting the context-dependent role for autophagy in cancer. *Nature reviews Cancer* 12, 401-410.
- Wingo, S.N., Gallardo, T.D., Akbay, E.A., Liang, M.C., Contreras, C.M., Boren, T., Shimamura, T., Miller, D.S., Sharpless, N.E., Bardeesy, N., *et al.* (2009). Somatic LKB1 mutations promote cervical cancer progression. *PloS one* 4, e5137.
- Witek, M.E., Nielsen, K., Walters, R., Hyslop, T., Palazzo, J., Schulz, S., and Waldman, S.A. (2005). The putative tumor suppressor Cdx2 is overexpressed by human colorectal adenocarcinomas. *Clinical cancer research : an official journal of the American Association for Cancer Research* 11, 8549-8556.
- Wong, C.H., and Cheng, C.Y. (2005). The blood-testis barrier: its biology, regulation, and physiological role in spermatogenesis. *Curr Top Dev Biol* 71, 263-296.
- Yang, B., O'Herrin, S.M., Wu, J., Reagan-Shaw, S., Ma, Y., Bhat, K.M., Gravekamp, C., Setaluri, V., Peters, N., Hoffmann, F.M., *et al.* (2007). MAGE-A, mMage-b, and MAGE-C proteins form complexes with KAP1 and suppress p53-dependent apoptosis in MAGE-positive cell lines. *Cancer research* 67, 9954-9962.
- Yang, Y., Fiskus, W., Yong, B., Atadja, P., Takahashi, Y., Pandita, T.K., Wang, H.G., and Bhalla, K.N. (2013). Acetylated hsp70 and KAP1-mediated Vps34 SUMOylation is required for autophagosome creation in autophagy. *Proceedings of the National Academy of Sciences of the United States of America* 110, 6841-6846.
- Yee, J.B., and Hutson, J.C. (1985). Effects of testicular macrophage-conditioned medium on Leydig cells in culture. *Endocrinology* 116, 2682-2684.
- Yokoe, T., Toiyama, Y., Okugawa, Y., Tanaka, K., Ohi, M., Inoue, Y., Mohri, Y., Miki, C., and Kusunoki, M. (2010). KAP1 is associated with peritoneal carcinomatosis in gastric cancer. *Annals of surgical oncology* 17, 821-828.
- Yue, Z., Jin, S., Yang, C., Levine, A.J., and Heintz, N. (2003). Beclin 1, an autophagy gene essential for early embryonic development, is a haploinsufficient tumor suppressor. *Proceedings of the National Academy of Sciences of the United States of America* 100, 15077-15082.
- Zhao, S., Zhu, W., Xue, S., and Han, D. (2014). Testicular defense systems: immune privilege and innate immunity. *Cellular & molecular immunology* 11, 428-437.
- Zheng, B., Jeong, J.H., Asara, J.M., Yuan, Y.Y., Granter, S.R., Chin, L., and Cantley, L.C. (2009). Oncogenic B-RAF negatively regulates the tumor suppressor LKB1 to promote melanoma cell proliferation. *Molecular cell* 33, 237-247.
- Zheng, L., Yang, W., Wu, F., Wang, C., Yu, L., Tang, L., Qiu, B., Li, Y., Guo, L., Wu, M., *et al.* (2013). Prognostic significance of AMPK activation and therapeutic effects of metformin in hepatocellular carcinoma. *Clinical cancer research : an official journal of the American Association for Cancer Research* 19, 5372-5380.